Studies on the Mesophilic and Hyperthermostable Protein 8-Amino-7-oxononanoate Synthase: A Biotin Biosynthetic Enzyme

Lisa Mullan

Ph. D.

University of Edinburgh

December 2000

Declaration

I, Lisa Mullan, hereby certify that this thesis has been composed by myself, that it is a record of my work, and that it has not been accepted in partial or complete fulfilment of any other degree or professional qualification.

Lisa Mullan

University of Edinburgh

December 2000

Acknowledgements

I would like to thank Dr. Robert L. Baxter for giving me the opportunity to return to science in the pursuit of a Ph.D. and for all of his support and encouragement along the way. I am also extremely grateful to Dr. Dimitriy Alexeev for much help during the protein structural studies. Much of the initial calculation and processing of protein structural data was carried out by him at the Structural Biology Facility in Edinburgh. Thanks are also due to Dr. Scott Webster for his help and advice during the first two years of the course and to the rest of the Baxter group for their support.

I would like to thank the following who contributed to my work.....:

Dr. Scott Webster and Sally Shirran for mass spectrometry

Dr. Rory Watt and Mhairi Brunton for technical assistance in the preparation of pimeloyl-CoA and Kevin Shaw and Dr. Lu Jiang for assistance in its purification.

Nicola Preston, Helen Williams and Louise Levenden who carried out the DNA sequencing

Dr. Dominic Campopiano for the opportunity to attend the HGMP-RC Gene Identification course

..... and to my mental well-being:

Mum, Dad, Caz, Al, Rob & Laura, Liz, Angela & Steve, Gill & Col, Keith and most of all, Eunan.

Abstract

The biotin biosynthetic enzyme 8-amino-7-oxononanoate synthase (AONS) from *Escherichia coli* is an homodimeric enzyme and relies on a pyridoxal-5'-phosphate (PLP) cofactor for catalytic activity. Specific activity of the over-expressed enzyme is approximately 0.4U at 30°C. To investigate the role of residues at the active site on the catalytic mechanism of the enzyme, two separate mutants have been created by site directed mutagenesis. H133 lies in parallel with the pyridine ring of the cofactor, and was mutated to a phenylalanine residue, with subsequent loss of cofactor binding. Alteration of the lysine 236 residue crucial for forming an aldimine linkage with the cofactor, to alanine resulted in a reduction, but no loss, of cofactor binding. The specific activities of both mutants were reduced by approximately ten-fold.

The corresponding *bio*F gene from an hyperthermophilic bacterium, *Aquifex aeolicus*, was cloned and AONS over-expressed in an *E.coli* host. The enzyme was characterised by a number of biophysical techniques. It is a dimer in solution, with a monomeric mass of 42.3 kDa and one active site per subunit Specific activity of the purified enzyme was 0.7U at 30°C, and optimum activity occurred at 80°C. The heat stable enzyme displays a greater affinity for its PLP cofactor and the binding of the coenzyme on mutation of the active site histidine residue corresponding to H133 in *E.coli*, indicates that PLP is bound by a residue not involved in *E.coli* AONS-PLP binding. Orthorhombic crystals grew in wells containing 1.6M-2.5M ammonium sulphate at 60°C, which diffracted to 2.94Å. Analysis of the diffraction data suggested a space group of $P2_12_12$ and a large unit cell containing at least 6 subunits in the asymmetric unit. Phasing was achieved by molecular replacement using the structure of the *Bacillus sphaericus* AONS protein.

Abbreviations

Å - Angstrom (10^{-10} metres)

ADP - Adensosine diphosphate

AKB - 2-amino-3-oxobutyrate CoA ligase

ALAS - δ-aminolaevulinate synthase

amp - Ampicillin

AMP - Adenosine monophosphate

AON - 8-amino-7-oxononanoate

AONS - 8-amino-7-oxononanoate synthase

ATP - Adenosine 5'- triphosphate

BCCP - biotin carboxyl carrier protein

bp -base pair

BES – (N,N-bis[2-Hydroxyethyl]-2-aminoethane-sulfonic acid)

Ca^{2+} - Calcium ion

CaCl - Calcium Chloride

CAPS – (3-[Cyclohexyamino]-2-aminoethane-sulfonic acid)

CO_2 - carbon dioxide

CoA - Coenzyme A

CoASH - unbound Coenzyme A

Cs^{+} - Caesium

CsCl - Caesium chloride

Da - Daltons

DAN - 7,8-diaminononanoate

DANS - 7,8-diaminononanoate synthase

DNA - deoxyribonucleic acid

DTB - Dethiobiotin

DTBS - Dethiobiotin synthase

EDTA - ethylene diaminetetraacetic acid

IPTG - Isopropl β,D-thiogalatopyranoside

HEPES – (N-[2-Hydroxyethyl]-piperazine-N'-[2'-ethansulfonic acid])

HPLC - High pressure liquid chromatography

K - Kelvin (-273°C)

K^+ - Potassium ion

KCl - Potassium chloride

K_2HPO_4 - Dipotassium phosphate

KH_2PO_4 - Potassium diphosphate

Kb - kilobases

kDa - kilodaltons

LB - Luria Bertani medium

M - molar

µl - microlitres (10^{-6})

ml - millilitres (10^{-3})

µM - micromolar (10^{-6})

mM - millimolar (10^{-3})

mol - moles

Mg^{2+} - Magnesium ion

$MgCl_2$ - Magnesium chloride

Na^+ - Sodium ion

NaCl - sodium chloride

NAD^+ - Nicotinamide adenine dinuclotide

NADH - reduced form of Nicotinamide adenine dinuclotide

NADP+ - Nicotinamide adenine dinuclotide phosphate

NADPG - reduced form of Nicotinamide adenine dinuclotide phosphate

$NaBH_4$ – Sodium borohydride

NCS – Non-crystallographic symmetry

NTP - Nucleotide triphosphate

ng - nanograms (10^{-9})

$(NH_4)_2SO_4$ - Ammonium sulphate

nm - nanometres (10^{-9})

OD - Optical density

PCR - Polymerase Chain Reaction

PEG - Polyethylene glycol

PLP - Pyridoxal-5'-phosphate

rpm - revolutions per minute

RNA - ribonucleic acid

RT - Room temperature

S-AdoMet - S-adenosyl methionine

SDS PAGE - Sodium dodecyl sulphate polyacrylamide gel electrophoresis

SPT - Serine palmitoyl transferase

TAE - Tris acetate EDTA

TCA - Trichloroacetic acid

TFA - Trifluoroacetic acid

Tris - Tris [hydroxymethyl] aminomethane

UV/vis - Ultraviolet/visible

wt - wild type

Table of Contents

Tables and Figures

List of Tables:

Chapter 1: Introduction to Biotin

Chapter 3: Characterisation of *E.coli* AONS

Chapter 4: Introduction to Thermophiles

Chapter 5: Characterisation of AONS from *Aquifex aeolicus*

List of Figures:

Chapter 1: Introduction to Biotin

Chapter 3: Characterisation of *E.coli* AONS

Appendix III: Purification of *E.coli* AONS

Chapter 1
Introduction to Biotin Biosynthesis

1.1 Biotin

Biotin, a water-soluble vitamin, is an essential cofactor for the transportation of an activated carboxyl (CO_2) group in biological carboxylase, decarboxylase and transcarboxylase reactions (1-3). The three different reactions are classified into classes I, II and III.

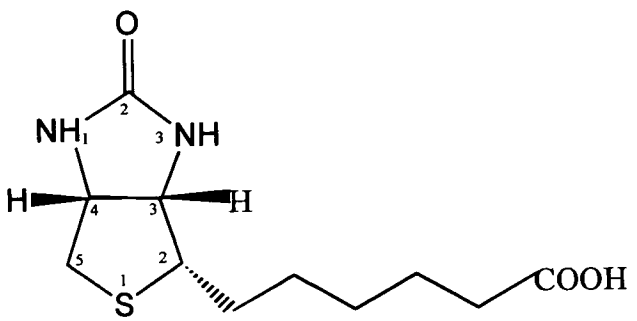

Figure 1.1.1

The absolute configuration of biotin was elucidated in 1966 (4) using x-ray crystallography. An imidazolone (*ureido*) ring is *cis* fused to a tetrahydrothiophene ring, substituted at position 2 by a valeric acid moiety.

Carboxylase reactions, termed class I reactions, require ATP and use bicarbonate as the carboxyl source (1) Possibly the best studied of this group is acetyl-CoA carboxylase (EC 6.4.1.2), an enzyme involved in fatty acid synthesis with an essential requirement for biotin. In *E.coli*, the formation of malonyl-CoA from acetyl-CoA is catalysed by three protein components of this enzyme. Biotin is anchored via its valeric acid side chain to the ε amino group of a lysine residue of the Biotin Carboxyl Carrier Protein (BCCP). The length of the linkage allows rotational freedom for the cofactor. Biotin is carboxylated at the imidazolone (*ureido*)-N^1 in two steps. First, carboxybiotin is formed at the expense of ATP at the active site of biotin carboxylase. The activated carboxybiotin group is then transferred to the active site of the carboxytransferase component and proton abstraction occurs at imidazolone-N^3 (5) The resulting intermediate reacts with acetyl-CoA, causing transfer of the carboxyl group to produce malonyl-CoA. Class II reactions are catalysed by decarboxylases and are not ATP dependent. They occur in anaerobic prokaryotes and include sodium transport channels The third class of biotin-dependent reactions, class III, are catalysed by

transcarboxylases. This type of reaction does not require ATP is unique and proceeds on two separate subunits of the same enzyme, catalysing fermentation of propionic acid in propionii-bacteria (see table I) (6)

Animals are unable to produce biotin themselves, and must rely on either dietary sources, such as liver, kidneys, legumes and nuts, or microorganisms within the gut flora. Biotin deficiency in animals can cause intra-muscular and immune disorders and signs include alopecia, dermatitis and pernicious anaemia (7). Should such a deficiency be diagnosed, biotin is also commercially available as vitamin H (or B_8) (6) which is especially important as an additive to animal foodstuffs (8).

Biotin is also useful as a biotechnology probe (9). One of the strongest protein-ligand interactions known ($K_d=10^{-15}M$) is that of biotin with the tetrameric 70kDa egg white protein avidin (10-11). Each subunit is folded into an 8-stranded β-barrel and biotin binds at one end of this barrel, in a pocket between two tryptophan (12). This phenomenon has been harnessed and used as a tool for biochemical research. The interaction is also being used as a model for investigating macromolecule-ligand binding.

Although biotin is commercially significant, the shortest synthetic route for vitamin production consists of 12 chemical steps (Hoffmann-La Roche synthesis). In contrast, the natural enzymes of the biotin operon in *Escherichia coli* achieve this conversion in only four steps from pimeloyl-CoA *via* proteins encoded by the genes *bio*F, *bio*A, *bio*D and *bio*B. An attractive aim would be to produce this molecule biologically, but if future commercial production is to be directed by microbial fermentation, the biosynthesis of biotin must be fully understood and characterised.

Class	Enzyme	Physiological role
Class I: Carboxylases	Acetyl-CoA carboxylase	Gluconeogenesis, lipogenesis
	Pyruvate carboxylase	Fatty acid biosynthesis
Enz-biotin + ATP + HCO_3^- $\overset{Mg^{2+}}{\leftrightarrow}$ Enz-biotin-CO_2^- + ADP + P_i + H^+	Propionyl-CoA carboxylase	Catabolism of odd numbered fatty acids and amino acids Ile; Thr; Met; Val
Enz-biotin-CO_2^- + R-H $\leftrightarrow$ Enz-biotin + R-CO_2^-	3-Methylcrotonyl-CoA carboxylase	Leucine catabolism
	Geranyl-CoA carboxylase	Isoprenoid catabolism in bacteria
	Urea carboxylase	Urea catabolism in *urease*$^+$ urea autotrophs
Class II: Decarboxylases	Methylmalonyl-CoA decarboxylase	Final step in anaerobic lactate fementation
Enz-biotin + R-CO_2^- $\leftrightarrow$ Enz-biotin-CO_2^- + R-H	Oxaloacetate decarboxylase	Inducible enzyme in certain citrate autotrophs
Enz-biotin-CO2- + $2(Na^+)_{in}$ $\leftrightarrow$ Enz-biotin + HCO_3^- + $2(Na^+)_{out}$		
Class III: Transcarboxylases	Methylmalonyl-CoA carboxyltransferase	Fermentation of propionic acid in Propioniibacteria
Enz-biotin + oxaloacetate $\leftrightarrow$ Enz-biotin-CO_2^- + pyruvate		
Enz-biotin-CO_2^- + propionyl-CoA $\leftrightarrow$ Enz-biotin + methylmalonyl-CoA		

Table 1.1

Biotin dependent enzymes

1.2 Biotin Biosynthetic Pathway

Biotin is produced in minute quantities in nature and the biosynthetic pathway consists of similar enzymes in fungi (13), bacteria (14-15) and higher plants (6) (16-17). It is thought that a maximum of only 1000 molecules of biotin is present at any one time in the cells of *E.coli* (18) and concentrations do not generally exceed nanomolar quantities in bacteria (6). In contrast, biotin in concentrations up to 11μM may be found in the cytosol of plant mesophyll cells (19).

Discovered as the result of cross-feeding and deletion mapping experiments (14) (18) the four step synthesis in *E.coli* involves enzymes encoded by the genes *bio*F, *bio*A, *bio*D and *bio*B found on the *bio* operon at 17 min, lying between the attachment site of the λ phage (*λatt*) and the *uvr* gene, on the bacterial genome (20-21).

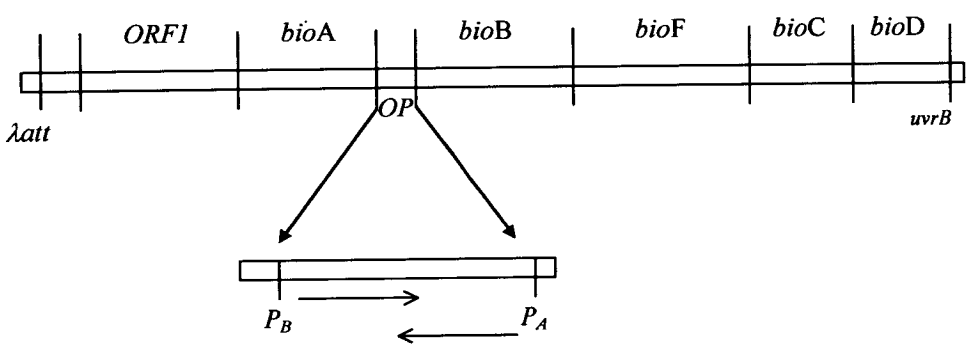

Figure 1.2.1

The biotin operon found at 17 min on the *E.coli* genome. Transcription of *bio*BFCD is promoted to the right while *bio*A transcription takes place on the complementary DNA strand. Partially overlapped face-to-face promotors initiate this divergent transcription. This is a cartoon representation and gene sizes are not drawn to scale.

Two further genes, *bio*C, also found on the operon, and *bio*H, a separate gene at 74min (22) encode enzymes, which have been implicated in the synthesis of pimeloyl-CoA. The sequences of the genes of the biotin operon were determined by Otsuka and co-workers in 1988 (23), and the stop codons and initiators of each gene on the operon were found to overlap. The biotin operon, *bio*ABFCD, is

divergently transcribed (24) with the promotor and operator sites OP_A and OP_B contained in a 40 nucleotide imperfect palindrome between *bio*A and *bio*B (25). There is also an open reading frame downstream of *bio*A, ORF1, the function of which remains unknown.

A biotin operon, similar to that which exists in *E.coli*, is also found in other gram negative facultative anaerobes such as *Erwinia herbicola* (26), *Serratia marcescens* (27), *Citrobacter freundii* and *Salmonella typhumurium* (28). In a further gram negative bacterium, *Xylella furiosa*, however, the biotin genes are scattered throughout the genome (29). Gram positive bacteria, of which *Bacillus sp.* is the most widely studied, display a different clustering of these enzymes. *Bacillus subtillis* also has a single biotin operon. This is transcribed in one direction only and contains the genes *bio*WAFDBI and an ORF2 downstream of *bio*I, which appears to encode a P450-like enzyme not apparently essential for biotin synthesis (30). There are, however, two *bio* gene clusters contained on the *Bacillus sphaericus* genome (31). The first operon, *bio*DAYB contains the genes encoding the enzymes for the final steps in biotin biosynthesis and a gene, *bio*Y, coding for a protein of unknown function. The second cluster contains three biotin genes, *bio*XWF. The first, *bio*X, encodes a protein of unknown function, whilst the bioW and bioF proteins together can complement an *E.coli* strain deficient in bioC and bioH on addition of pimelate, suggesting bioW is involved in the synthesis of pimeloyl-CoA. In *Brevibacterium flavium,* there is no *bio*F gene and *bio*A and *bio*D are situated on unlinked chromosomes (32). *Saccharomyces cerevisiae* also has biotin synthetic genes located on different chromosomes. The extremely thermostable bacteria *Aquifex aeolicus* has biotin genes similar to *Bacillus sp.* They are not, however, clustered in an operon, but are found scattered throughout the genome (33).

Synthesis of pimeloyl-CoA varies within different bacterial and plant hosts, and different species have various clustering of the genes. *B.sphaericus* and *A.aeolicus* catalyse the synthesis of this chemical by expressing *bio*W which converts pimelic acid into pimeloyl-CoA. This protein is not present in *E.coli* and current consensus is that the BioC and BioH proteins are involved in pimeloyl-CoA synthesis. Pimeloyl-CoA is also synthesised in plants from pimelic acid (16). Experiments

conducted with biotin genes in an *E.coli* host suggest that it is this step which may prove limiting to biotin production (34). The four main steps of biotin biosynthesis and the method of biotin repression, however, are generally conserved across the organisms synthesising this chemical. They have been best characterised in *E.coli*.

1.2.1 8-Amino-7-oxononanoate Synthase (AONS)

The first committed enzyme in the biosynthetic pathway of *E.coli*, 8-amino-7-oxononoate synthase (EC 2.3.1.47) is the product of the *bio*F gene. It has an essential requirement for the versatile cofactor pyridoxal-5'-phosphate (PLP), and catalyses the decarboxylative condensation of L-alanine and pimeloyl-CoA to yield 8-amino-7-oxononanoate (AON). Only L-alanine may act as a substrate for AONS (35) and its stereoisomer, D-alanine, is an inhibitor (36).

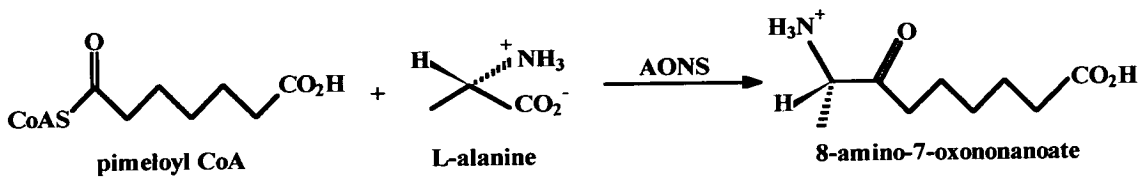

Figure 1.2.2

The stereospecific carboxylative condensation of L-alanine and pimeloyl-CoA

Although the enzyme was initially purified by Eisenberg and co-workers in the 1970's (14), the exact sequence of the *E.coli bio*F gene was only elucidated more than a decade later (23). More recent research into the mechanism of AONS from *E.coli* (36-37) and *B.sphaericus* (38-39), has shown that the holoenzyme is formed by attachment of the PLP cofactor C_4 group *via* a Schiff base linkage to the side chain of a lysine residue in the AONS active site. On addition of L-alanine, an external substrate aldimine is formed with PLP. Abstraction of the substrate C_α proton results in formation of the first quinonoid of the reaction. Rotation around the C_α proton (36) confers the correct orientation of the intermediate for nucleophillic attack upon the thioester bond of the pimeloyl CoA, releasing CoASH

and forming a β-ketoacid intermediate. Subsequent decarboxylation results in a second quinonoid intermediate. A proton derived from the solvent attacks at C_8 of the α-oxoamine quinonoid (39) prior to formation of the external product aldimine. The product is displaced from the cofactor by the initial lysine residue and 8-amino-7-oxononanoate is released (see fig 1.2.3).

This mechanistic route places AONS as a member of the family of α-oxoamine synthases (40). The three other enzymes of this family are: δ-aminolaevulinate synthase (ALAS: EC 2.3.1.37), a protein catalysing the initial step of haem biosynthesis (41-42); serine palmitoyl transferase (SPT: EC 2.3.1.50), a membrane bound protein involved in the initial stage of sphingolipid biosynthesis (43) and 2-amino-3-oxobutyrate CoA ligase (AKB: EC 2.3.1.29), an enzyme involved in the threonine biosynthetic pathway (44). ALAS is found in non-plant eukaryotes and is encoded by two separate genes. Both proteins function as homodimers and one is a housekeeping, hepatic form, whilst the other is an erythoid-specific form. It is mutations in this latter form that have been implicated in causing sideroblastic anaemia in humans and the mechanism of this enzyme has been extensively studied (42) (45-52) but no structure is currently available. SPT is also a eukaryotic enzyme and it is suggested that the two separate proteins LCB1 and LCB2 interact to form a heterodimer. A third protein, Tsc3 (53) appears to enhance catalytic activity. All four enzymes catalyse the decarboxylative condensation of an amino acid and an acyl-CoA.

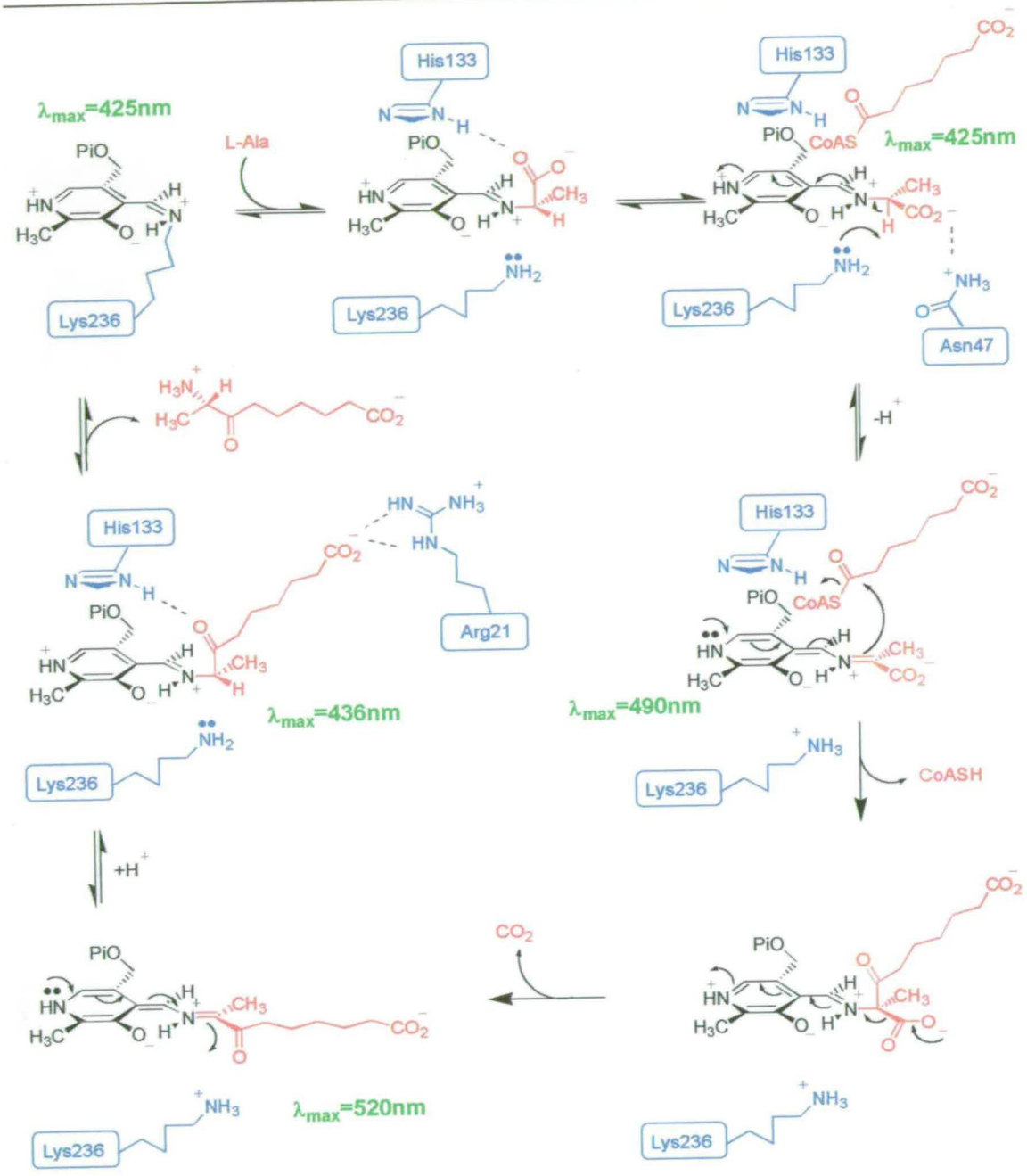

Figure 1.2.3

Proposed mechanism for the reaction (red) catalysed by AONS. Residues thought to be involved in catalysis are coloured blue (36). UV/visible wavelengths of the various intermediates are shown in green.

The structure of this protein in *E.coli* (37) confirms that AONS functions as a homodimer, each monomer of which has a mass of 41,464 Da and is composed of three distinct domains. The active sites are found in deep clefts within the central, major domain and utilise residues from both monomers.

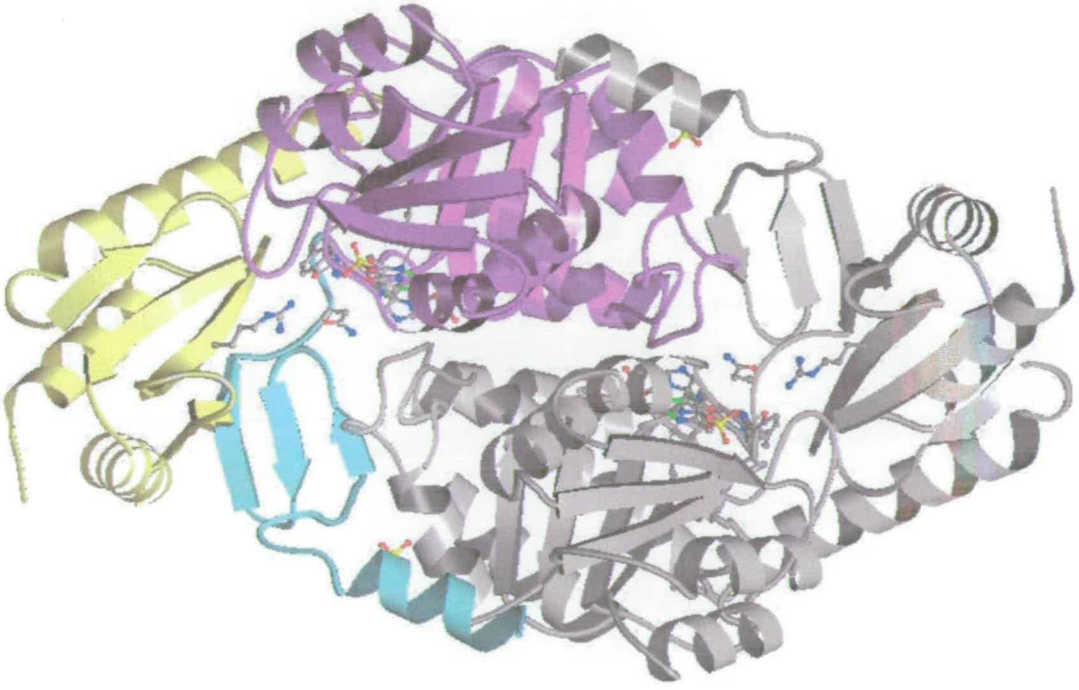

Figure 1.2.4

The crystal structure of AONS (PDB: 1BS0) from *E.coli* was resolved to 1.65Å. (37) with a space group $P3_112$. The small N-terminus (blue) attaches close to the active site *via* a loop to the major domain (red). The C-terminal domain is shown in yellow.

The AONS enzyme houses the PLP binding lysine (K236) within a deep cleft, which allows space for the pantothenic arm of the pimeloyl-CoA substrate to be admitted. A small N-terminal domain is linked to a larger central (major) domain which is composed of a seven-stranded β-sheet, of which one sheet is antiparellel to the others - a motif common to all PLP dependent enzymes (111). The sheet is flanked by two α-helices, and curved about two more. The C-terminal domain is approximately 100 residues in size. The structure of the holoenzyme shows that there is a conformational change upon PLP binding, evidence that is supported by the observation that AONS slowly loses its cofactor over time. An active site histidine residue (H133) moves to lie in a parallel stacked system with the pyridine ring of the cofactor.

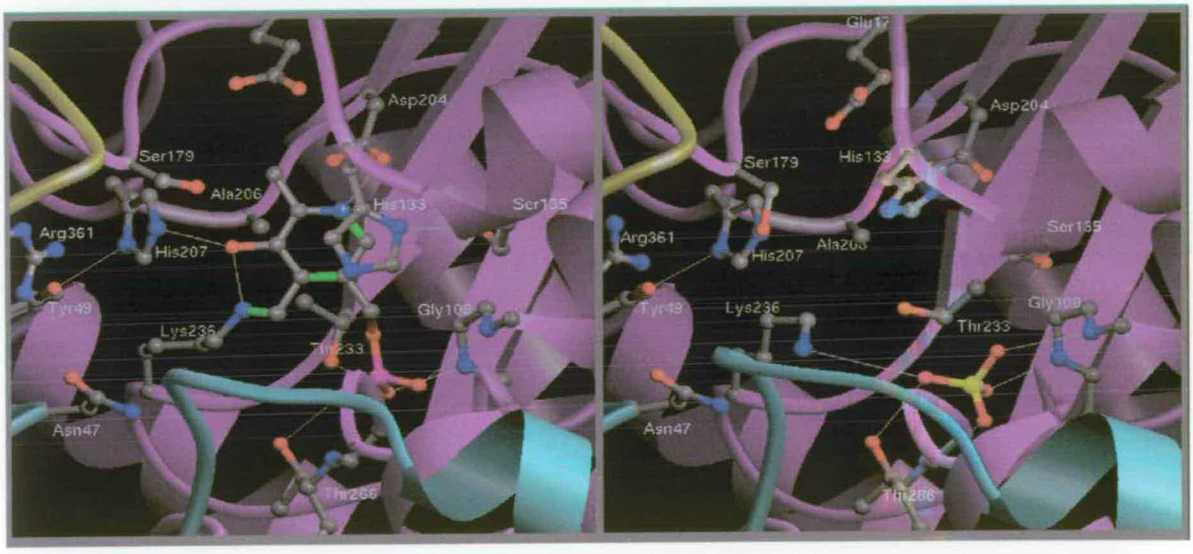

Figure1.2.5

Active site of *E.coli* AONS. The apoenzyme is represented in the right hand image and the H133 residue is located away from the centre of the site. H133 swings through 180° on binding of the PLP cofactor (left hand image) to lie in parallel with the pyridine ring. The image was created in Molscript.

This cofactor is stabilised by hydrophobic interactions with His133 and co-ordinated further by main chain nitrogen atoms of Gly108, Ser107, which are hydrogen bonded to the phosphate tail of PLP. The hydroxyl groups of Thr233 and a threonine (Thr266) residue in the opposite monomer are also

co-ordinated to the pyridine ring and phosphate tail of the cofactor. Studies of the product (AON) bound protein at 2Å reveal that there is a rotation of the pyridine ring of approximately 15° with respect to that for the internal aldimine. There is significant conformational change of the C-terminal domain of the protein on binding the product. The final turn of the helix is unwound and the tip of this flexible domain moves a maximum of 5.5Å to emulate a lid closure on the external product aldimine (36).

The motif GXGXGG has been suggested as a putative phosphate binding site (45). Structural studies of *E.coli* AONS have shown that this motif is located too distant from the phosphate tail of the PLP cofactor to act in this manner. Instead, the motif appears to stabilise dimer interactions and the loop on which the crucial Lys236 cofactor binding residue is found.

The fold of this enzyme is related to both subgroups I and II (54) aminotransferases (see section 1.3.2), however, it shares highest fold homology with dialkylglycine decarboxylase (55), a protein belonging to subgroup II. Another member of this structural subgroup is 7,8-diaminonanoate synthase, which catalyses the second reaction of the biotin biosynthetic pathway (see section 1.2.2). A recent re-classification by Grishin (56) places AONS and the α-oxoamine synthase family in fold type I, aminotransferase class II.

1.2.2 7,8-Diaminononanoate Synthase (DANS)

The *bio*A gene encodes the protein 7,8-diaminononanoate synthase (EC 2.6.1.62) which catalyses the second step of biotin biosynthesis. Like AONS, it has an essential requirement for the vitamin B_6 derived cofactor, PLP. The reaction utilises the product of the AONS catalysis, 8-amino-7-oxononanoate, and involves transamination of an amino group from an S-adenosyl methionine (S-AdoMet) donor, an as yet unique role for this molecule. The reaction is thought to occur via a ping-pong mechanism (23), (57) and S-AdoMet binding is competitively inhibited by the AON substrate. Although the initial step of the reaction involves the formation of an AdoMet-PLP imine followed by

the transfer of the amino group to AON, little is known about subsequent intermediates of the reaction and the breakdown product of S-AdoMet.

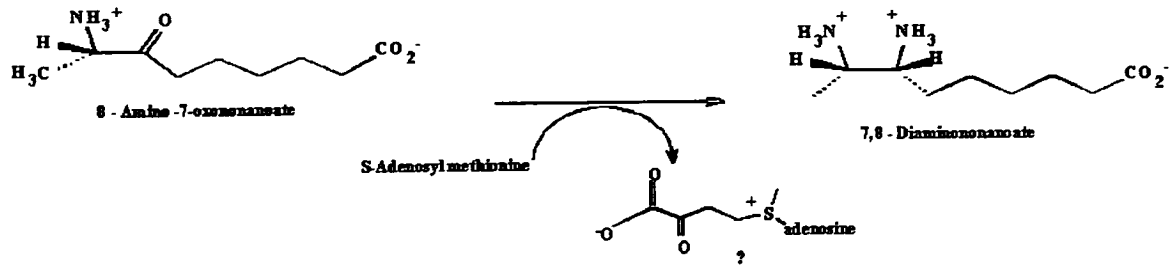

Figure 1.2.6

The conversion of 8-amino-7-oxononanoate to 7,8 diaminononanoate.

First purified by Izumi and colleagues in 1972 (35) and subsequently by Stoner and Eisenberg three years later (14), initial studies suggested that DANS was dimeric with an essential requirement for S-AdoMet as the amino donor, since analogues of this compound proved inactive (58). The homodimeric nature of this enzyme was proved two decades later when Käck and co-workers crystallised and then solved the structure of DANS (59).

Each monomer of DANS has a mass of 47,000 Da and is composed of two domains. The large domain consists of the central residues of the polypeptide and as a 7 stranded, predominately parallel β-sheet, surrounded by α-helices. The small domain is split into two, one moiety lying either side of the large domain.

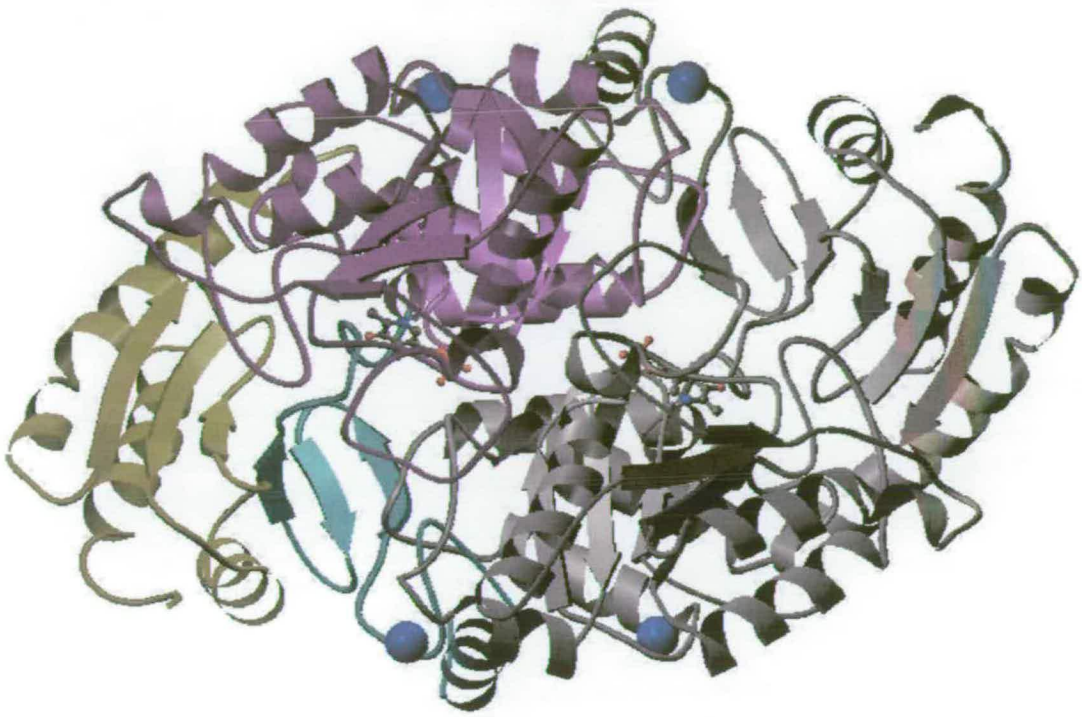

Figure 1.2.7

The structure of DANS (PDB: 1DTY) was resolved to 1.8Å (59). This structure was also been solved by Alexeev *et al*, 1999 (unpublished). With a fold similar to the previous enzyme in the pathway, the small N-terminal region is shown in blue, the major domain in red and the carboxy terminus in yellow.

The active site is located in a cleft formed by both domains of one monomer, and residues from the large domain of the opposite subunit. The PLP cofactor is located at the bottom of the cleft, and the phosphate group interacts with several residues, including a serine group, anchoring a phosphate oxygen to both main and side chain atoms. AON is bound with its polar head group towards the cofactor, and the carboxyl tail close to the entrance of the active site cleft. This orientation prevents AON itself acting as an amino donor.

The fold of this PLP dependent aminotransferase is similar to that first observed in aspartate aminotransferase (EC 2.6.1.1) (60) and places it in the group of Type I aminotransferases (61). DANS belongs to subgroup II together with ornithine aminotransferase (EC 4.1.1.17) (62), with which it shares highest sequence homology, and dialkylglycine decarboxylase (EC 4.1.1.64) (55), an enzyme which also shares high structural similarity with AONS.

It has been suggested that the *bio*A gene is evolutionarily related to the *bio*F gene (23) as the two biotin enzymes are of comparable molecular weight, share a requirement for PLP as the cofactor and the product of one is the substrate for the other. Both enzymes bind adenosyl derivatives and the divergent transcription relation in facultative anaerobes led to the postulation that *bio*A was maybe the result of duplication and transposition of the *bio*F gene (57).

1.2.3 Dethiobiotin Synthase (DTBS)

The conversion of 7,8-diaminononanoate to dethiobiotin proceeds through three stages and is catalysed by a 47,600 Da homodimer.

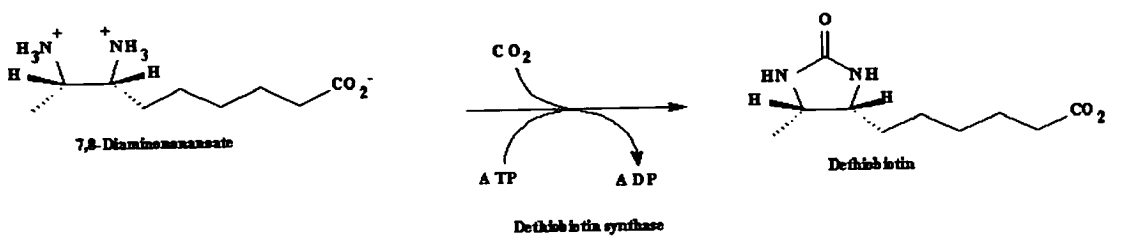

Figure 1.2.8

The conversion of 7,8-diaminononanoate to dethiobiotin

The protein dethiobiotin synthase (EC 6.3.3.3), encoded by the *bio*D gene, is a carboxylase (63). Distinct from others in its class, DTBS utilises CO_2 directly, and does not require biotin as a cofactor (64-65). DTBS also has a requirement for Mg^{2+}.

Originally discovered by Rolfe and Eisenberg (20) as a result of cross-feeding experiments, DTBS requires 1 mole each of its ATP and CO_2 substrates, producing 1 mole of ADP as release product (66). The active site stretches across the interface of the two monomers with the 7,8-diaminononanoate substrate bound to one monomer, and the ATP substrate bound to the other (64). On binding, 7,8-diaminononononoate reacts with CO_2 to produce an 8-amino carbamate, the first intermediate (67). Although this reaction can proceed without catalysis, DTBS confers regiospecificity on the reaction, producing the N7 carbamate (68-70). Nucleophillic attack of this carbamate on the ATP substrate cleaves off an inorganic phosphate, resulting in the second intermediate - a phosphoric carbamate mixed anhydride (67). Closure of the imidazolone (*ureido*) ring through a tetrahedral intermediate forms the product dethiobiotin (DTB) (71-72), and in plants, a second intermediate 9-mercaptodethiobiotin, has been isolated (16)

Although ATP is necessary as a substrate, the enzyme seems to lack the consensus ATP binding site GXGXXG (23) (73). It does, however, possess the P-loop sequence GTDTEVGKT[1] - one residue longer than that of the consensus (64) - a mononucleotide binding motif.

DTBS has very little sequence similarity with any other proteins currently in the database, but the crystal structure of this enzyme, determined both by Alexeev *et al* (64) and Lindqvuist *et al* (74), display an overall resemblance of fold to adenylosuccinate synthase (PurA) and nitrogenase iron protein (NIP). All three are homodimers, but have little similarity in dimer organisation.

[1] Underlined residues are conserved

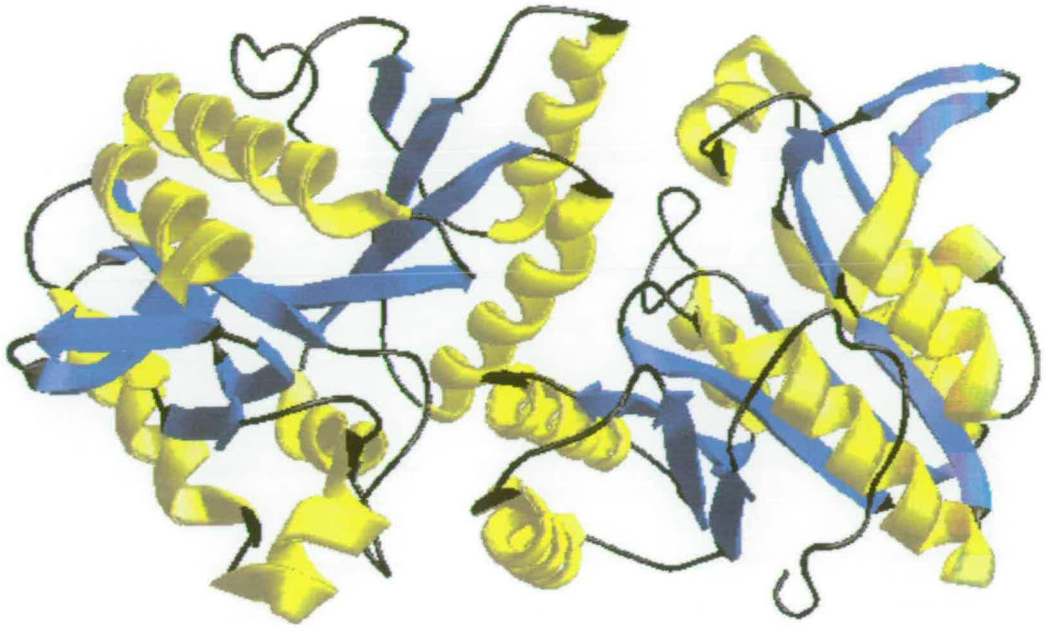

Figure 1.2.9

The structure of DTBS (PDB: 1BS1) was resolved to 1.65Å (74)and 1.8Å (Alexeev *et al*, 1994) with space group C2. The active site is once again at the interface between the two subunits.

The DTBS monomer is folded as a single α/β globular domain (64) and the protein topology is similar to the oncoprotein Ha-*ras*-p21. Other topological similarities are found between DTBS and other ATP dependent proteins.

1.2.4 Biotin Synthase

The *bio*B gene is located adjacent to the promoter palindrome sequence of the biotin operon in *E.coli* and encodes the 38kDa protein biotin synthase (EC 2.8.1.6), responsible for the insertion of a sulphur atom and subsequent closure of, the tetrahydrothiophene ring of the biotin molecule. This transformation involves the cleavage of two C-H bonds (75) of an inert methyl and methylene group (15) and ring closure proceeds *via* a thiol intermediate (76).

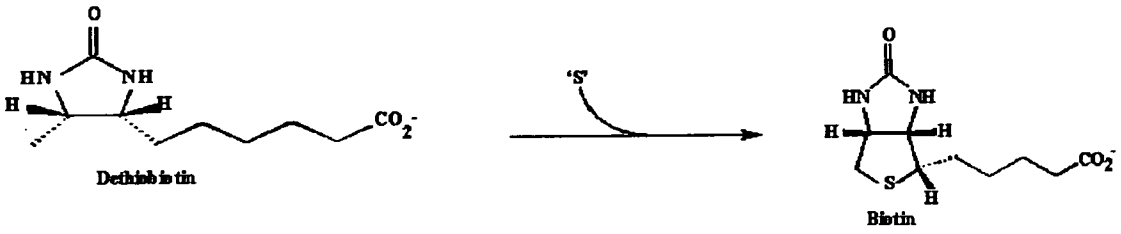

Figure 1.2.10

The conversion of dethiobiotin to biotin

Investigation of the mechanism of this enzyme has led to the conclusion that several cofactors are also required for full catalysis: fructose-1,6-biphosphate, S-AdoMet, Fe^{2+}, NADPH, KCl, cysteine (77-78) In plants, this enzyme has been, linked to a cellular organelle, possibly the mitochondria (17) (79). The enzymes flavodoxin (PDB: 1AG9) and flavodoxin $NADP^+$ reductase (PDB: 1FDR) are also necessary and participate in the electron cycling reactions (18). A third electron transport protein, MioC has also recently been discovered and is involved in FMN binding (80). The involvement of a low molecular weight product, thought to be derived from S-AdoMet and a breakdown product from the reaction catalysed by 7,8-diaminononaoate synthase, has also been suggested, but there is currently no firm evidence of the identity of this chemical (77) (L.A. McIver *pers. commun.*).

Biotin Synthase appears to act as a homodimer, with each monomer containing one $[2Fe\text{-}2S]^{2+}$ cluster with incomplete cysteinyl-S co-ordination. This cluster has been shown in the biotin synthase of *E.coli* (81) and *B.sphaericus* (82) to be reduced under anaerobic conditions to a $[4Fe\text{-}4S]^{4+}$ cluster with complete cysteinyl-S co-ordination, a process which is reversible under aerobic conditions. There are three other enzymes in the family of iron-sulphur cluster proteins. Anaerobic ribonucleotide reductase (83), lysine 2,3-aminomutase (84) and pyruvate formate lyase (85) also require S-AdoMet, Fe^{2+} and the flavodoxin reduction system. Like biotin synthase, they catalyse reactions which involve proton abstraction from an activated carbon atom, achieved by free radical chemistry, using S-AdoMet as radical donor. This was investigated for biotin synthase in 1997 by Guianvarc'h and co-workers (86) and it was shown that a deoxyadenosyl radical was generated

together with methionine in equimolar amounts. Deuterium labelling studies suggest that one molecule of S-AdoMet is required for each C-H cleavage step.

The sulphur, which is inserted into the tetrahydrothiophene ring has been shown to come from the iron-sulphur cluster of the protein itself (87). Thus regeneration of the cluster is necessary after each catalysis and it has recently been suggested that this is mediated by a NifS type protein (88-89) which mobilises sulphur from cysteine (and thiosulphate) for the formation of $[2Fe\text{-}2S]^{2+}$ clusters (90). Cysteine itself has been shown to donate a sulphur atom (78), (91).

All four enzymes of the iron-sulphur cluster family have a conserved cysteine triad CX_3CX_2C. Mutation of these residues in *E.coli* biotin synthase to alanine (92) or serine (93) inactivated the enzyme. Some $[2Fe\text{-}2S]^{2+}$ cluster formation was still apparent for the alanine mutations, but no evidence of this was seen on mutation of the residues to serine.

1.2.5 Repression of Biotin Biosynthesis

The production of biotin in *E.coli* is repressed as the result of negative feedback inhibition by the repressor protein product, BirA (EC 6.3.4.15), although it has been shown that repression of BioH in *E.coli* does not occur (94). The gene, *bir*A, originally named *bio*R, was found together with the permeability protein encoded by *bio*P at 85 min on the *E.coli* genome (14). BirA is a 33,500 Da monomeric protein and functions in conjunction with the allosteric effector biotinyl-5'-adenylate (bio-5'-AMP) (95), formed on reaction of free biotin with ATP and catalysed by BirA (96). It was recognised early on that the protein product of this gene had dual functionality (97-98).

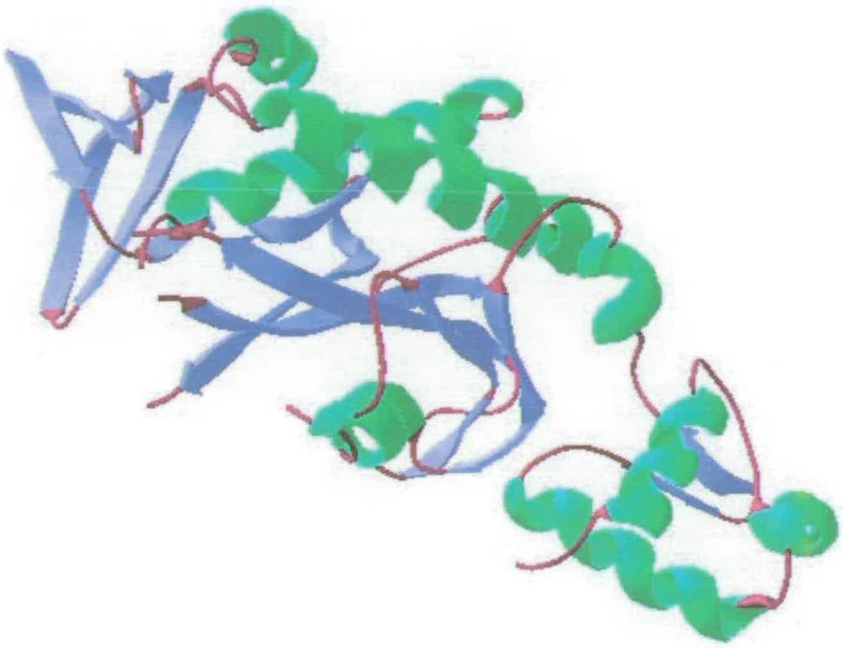

Figure 1.2.11

The structure of BirA from *Ecoli* (PDB: 1BIA) was solved to 2.3Å.(Wilson, 1992) with a space group $P4_32_12$. α-helices are shown in green, β sheets in blue. The putative DNA binding domain is bound loosely to the central domain.

In the absence of maximal concentrations of biotin, the protein is constitutively expressed and BirA displays biotin-protein ligase activity in attaching the vitamin onto the BCCP subunit of a biotin-requiring enzyme. In the presence of excess biotin in the cell (see section 1.2), BirA switches function and two monomers bind co-operatively to the two operator half sites of the biotin operon, thus repressing expression of the biotin at the genetic level (99-100). As levels of apo-BCCP rise once again in the cell, this enzyme competes with *bio*O for interaction with holo-BirA. In *E.coli* *bir*A$^-$ cells transformed with a multicopy plasmid containing the *bio*ABFCD operon produced biotin at levels 10,000 fold greater than wild type cells (34).

The enzyme consists of three domains. The N-terminal domain contains the helix-turn-helix DNA binding motif, suggesting operator repression occurs at the amino terminal. This is loosely associated with the central domain, one side of which is solvent exposed. Biotin binds at a site in this domain, and it is suggested that ATP binds to the protein at a nearby site. The C-terminal domain is composed of several anti-parallel β sheets and is not implicated in immediate substrate binding.

Studies of the regulation of biotin in species of *Bacillus* conclude that inhibition is similar to that studied in *E.coli* and other bacteria (8) (30) (31) (101) but not in plants. Studies of *Arabidopsis thaliana* have revealed that the biotin ligase function of BirA is performed by biotin holo-carboxylase synthetase (HCS) (6). This enzyme is found in three locations in the cell, the cytosol, the mitochondria and the chloroplast, where it has an apparently high affinity for biotin (K_m = 28nM) (102). The protein does not, however contain the helix-turn-helix DNA binding motif, and does not repress biotin production, a process that remains to be understood in plants.

1.3 Pyridoxal -5'- Phosphate

1.3.1 Mechanism of PLP catalysis

The 5'-phosphate ester of pyridoxal (vitamin B_6) is a versatile cofactor (103) in the enzymatic catalysis of reactions as diverse as: transamination; racemisation; α-decarboxylation; aldol cleavage and β- and γ-eliminations. Pyridoxal-5'-phosphate (PLP) effectively acts as an electron sink, in these reactions (104). Electrophilic reactivity is enhanced by the pyridine ring nitrogen of the coenzyme. This group reacts readily and reversibly with a lysine residue in the apoenzyme to form an imine linkage. The adjacent hydroxyl group (deprotonated at position 3 in figure 1.3.1) of the coenzyme enhances reactivity of the cofactor. As a free molecule, in the absence of an enzyme, PLP itself may undergo transaminations with amino acids (105).

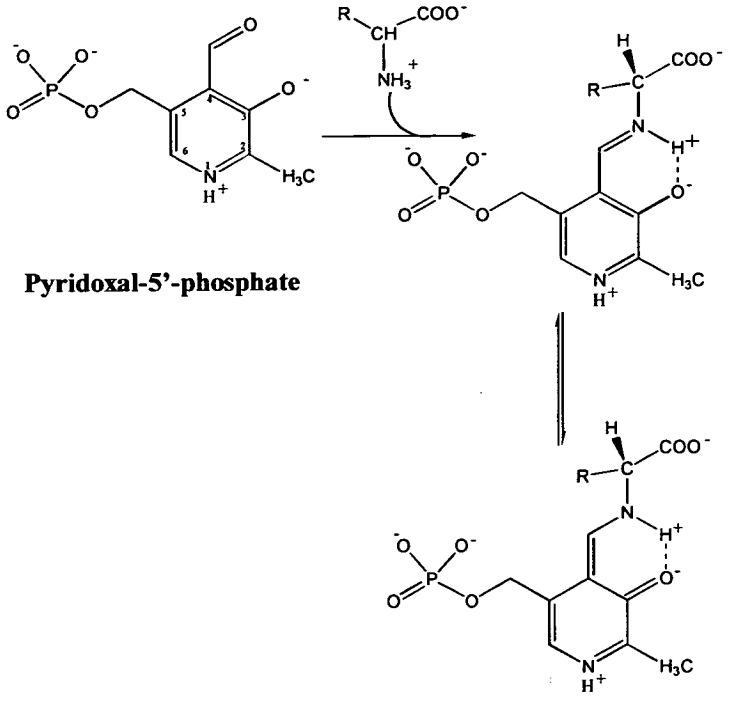

Figure 1.3.1

Reaction of PLP with an amino acid. The incoming amino acid displaces the oxygen of PLP to form an imine bond.

Characterisation of PLP dependent enzymes has shown that in the absence of substrate, the C_4 aldehyde group of PLP is bound within the enzyme by a Schiff base linkage to the amino group of an active site lysine residue as an internal aldimine. However, in the presence of a substrate, transimination occurs and an external aldimine is formed between the PLP cofactor and the substrate. There is evidence that the enzymes also change conformation from 'open' to 'closed' where access of the solvent to the coenzyme and bound substrate is prevented (60) (106). Both aldimines display planar geometry but the intermediate in these two steps, a geminal diamine, formed with both enzyme and substrate bound to the C_4 of PLP, displays tetrahedral geometry (107).

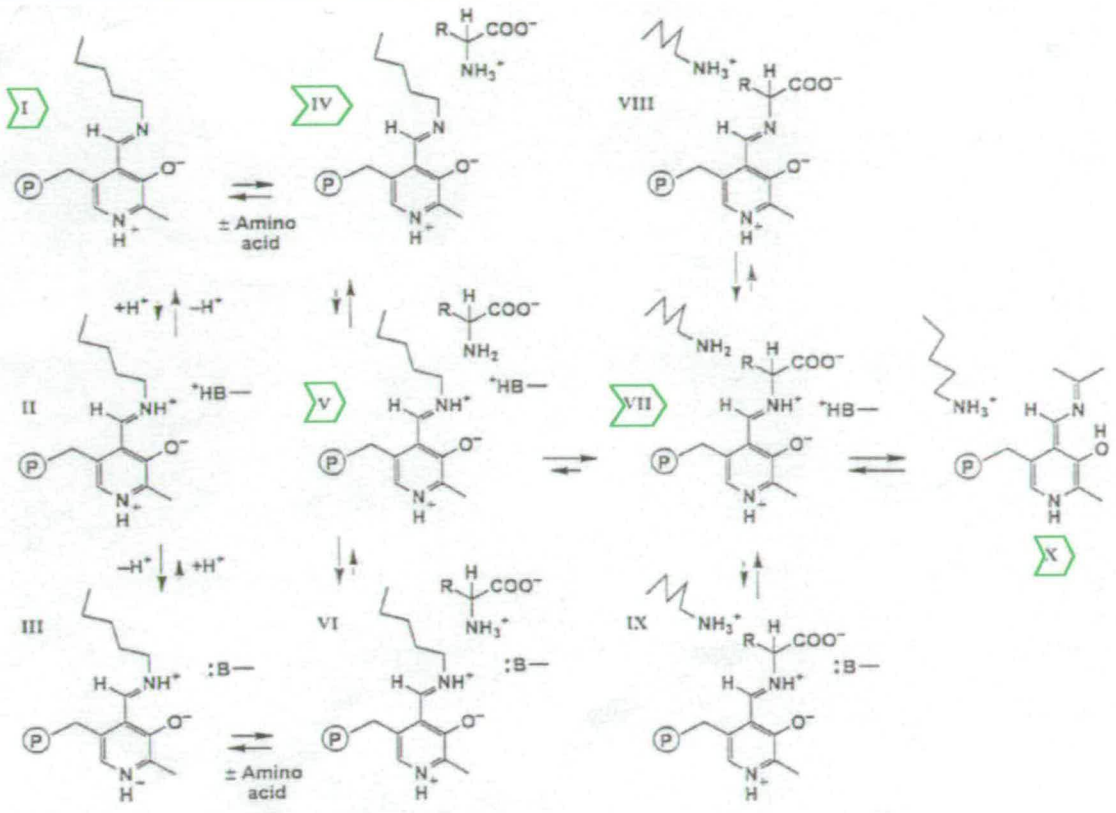

Figure 1.3.2

The proposed intermediates between the holoenzyme and the first quinonoid intermediate (104). The green arrows show progress of the reaction. Active site residues in the enzyme govern the stability and thermodynamic potential of the intermediates.

Upon formation of the PLP external aldimine, the reaction proceeds *via* a resonance stabilised quinonoid intermediate (104) achieved by α-proton loss; decarboxylation, or side chain cleavage at the C_α atom of the substrate (fig 1.3.3). The type of reaction which precedes the initial quinonoid intemediate confers the specificity of the enzyme and is determined by the orientation of the bond to be cleaved, which must be perpendicular to the pyridine ring (108-109). It is this orientation which offers optimal overlap of the σ and π electron orbitals of the substrate bond, thus labilising the π system of the ring most effectively (104). The quinonoid itself is stabilised relative to the external aldimine by the cofactor binding lysine and enhances reactivity within the active site. This is known

as the Circe effect (110). After cleavage at C_α, the mechanism can take one of several routes, resulting in radically different reactions.

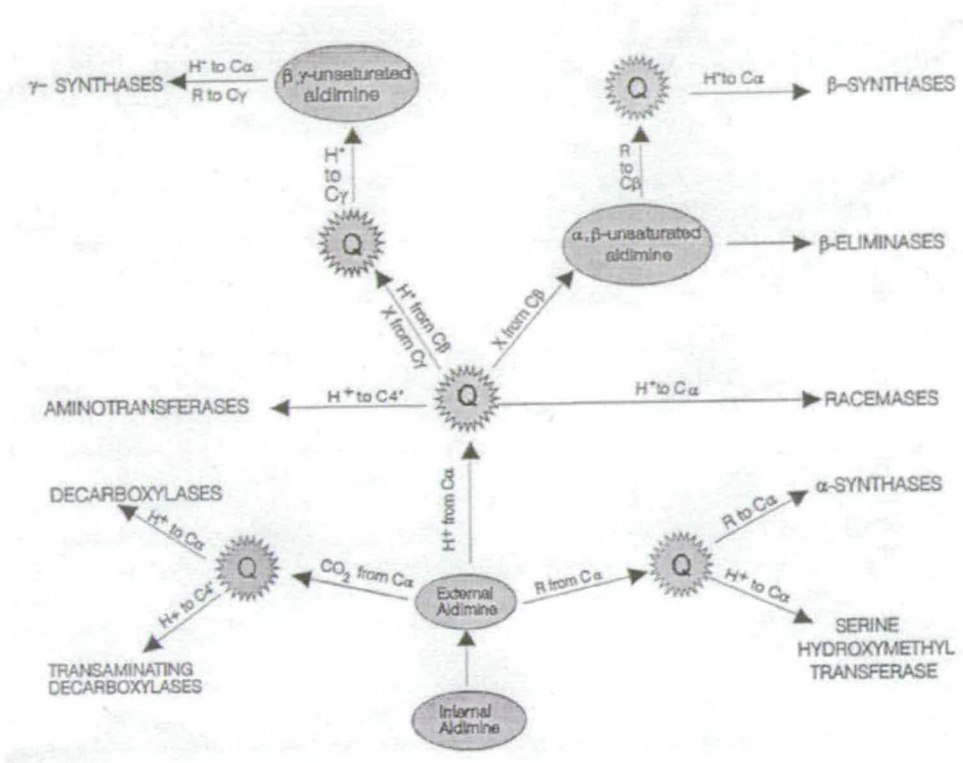

Figure 1.3.3

Versatility of PLP enzymes (107). The three possible routes of a PLP catalysed reaction all proceed through a quinonoid intermediate.

1.3.2 Folding of PLP dependent enzymes

Aminotransferases constitute the largest group in the α family of PLP dependent enzymes. Alexander and co-workers in 1994 (40) expanded the homology relationship of this superfamily during an investigation into the sequence homology of a large cross section of PLP dependent enzymes, defining four fold type subclasses by their differences in structural architecture. They defined three families of enzymes, α; β and γ which correlated in the majority of cases with their mechanistic regio-specificity. The largest group of PLP dependent enzymes is represented by the α-family which include the α-oxoamine synthase family (see section 1.2.1), all aminotransferases and

many amino acid decarboxylases. There are two amino acids, which are completely conserved throughout this family. The lysine which forms an imine linkage with the cofactor, and the aspartate residue which makes a salt bridge with the pyridine ring nitrogen (107). All aminotransferases were also found to contain a 7-stranded β sheet, a feature common to most PLP dependent enzymes in the cofactor binding domain (111-112), and sequence homology shows similarities in the hydrophobic and hydrophilic areas in this region. The structure of 8-amino-7-oxononanoate synthase has also been shown to contain the 7-stranded β sheet (see section 1.2.1), suggesting its presence elsewhere amongst members of the α family of PLP dependent enzymes. Grishin and co-workers reclassified the Alexander groupings in 1995 (56) after observing that members of the α- and γ-families displayed the same fold. They also restructured the subclasses of aminotransferases and assigned four principal fold types to describe the majority of PLP dependent enzymes for which secondary structures were available. A fifth was assigned to the fold type of glycogen phosphorylase, which uses the phosphate tail of PLP for catalysis, and two further folds, VI and VII, were tentatively introduced for enzymes of unknown structure.

Fold type I is typified by aspartate aminotransferase (see section 1.3.2) and includes subgroups I, II and IV as defined by Mehta *et al* (61) and members of the α and γ families. Many of the residues interacting with the coenzyme are conserved. All monomer subunits are similar in size and contain a small amino terminal region, a large, central domain, and a smaller domain at the C-terminal. The large domain consists of several α helices packed around a 7-stranded β sheet. All strands except one run parallel to each other and the majority of cofactor binding residues arise from their carboxy-termini. Other coenzyme - protein interactions are *via* residues from the opposite monomer. The small domain also has α/β architecture. The core is a three or four stranded anitparallel β sheet. Differences between proteins are found between the N-terminal regions and in the position of the protein domains relative to each other. It is into this group that 8-amino-7-oxononanoate synthase has been classified.

Fold type II is best represented by the tryptophan synthase β subunit. It is a complex dimer of two fold β/α pairs with the β subunits lying back-to-back. They each act independently, but are allosterically affected by one another.

The structure of fold type III proteins differs from the general αβ fold of PLP dependent enzymes. A typical example of this fold type is alanine racemase, the structure of which is a TIM barrel ($(\beta/\alpha)_8$). The PLP cofactor is bound with the A face exposed to the solvent and initial mechanistic studies suggest that initial catalysation is achieved by a two base mechanism involving tyrosine as well as the critical cofactor binding lysine residue (113).

D-amino acid aminotransferase is a good example of fold type IV. This enzyme is a member of the aminotransferase subgroup III and the active site serves to orientate the cofactor so that the A face of PLP is solvent exposed. This is in direct contrast to the B face exposed in enzymes of fold types I and II, but similar to fold type III.

Aims of this Project

The AONS protein from *E.coli* has been structurally and biochemically characterised (36-37). It is present in solution as a homodimer of 83 kDa and catalyses the decarboxylative condensation of L-alanine and pimeloyl-CoA to form 8-amino-7-oxononanoate synthase.

Studies of the active site have revealed certain crucial residues. Lysine 236 forms a Schiff base linkage to the C4' of the PLP cofactor and is also believed to be the general base for proton abstraction prior to the formation of the first quinonoid intermediate in the reaction pathway. Histidine 133 lies in parallel with the pyridine ring of the cofactor and participates in the π electron system to stabilise the PLP molecule within the active site. In order to discover the exact nature of activity of these residues, point mutations have been made, and the mutated proteins purified and characterised using a number of biophysical techniques.

Chapter 2
Materials and Methods

Equipment used has been cited where appropriate. Reagents were purchased from Sigma, Gibco BRL, Fisher Scientific, Pharmacia, Difco, Acros and were of suitable grade for research purposes.

2.1 Microbiology

2.1.1 Cell Lines and Plasmid Vectors

All cell lines were derived from *Escherichia coli* and stored at -20°C or -80°C in 10% glycerol until required. Commercially competent cells were purchased in batches and stored in 10µl or 25µl aliquots at -80°C.

Table 2.1

Escherichia coli strains used throughout the project

Cell Line	Genotype	Description of use
Escherichia coli JM101 (114)	F'; *tra*D36; *lacI*^{q}; Δ (*lacZ*); M15; *proA*$^+$B$^+$/*sup*E *thi*; Δ (*lac-pro*AB)	Storage of DNA as glycerol stocks at -80°C
Escherichia coli JM109 (114)	F'; *tra*D36; *lacI*^{q}; Δ (*lacZ*); M15; *proA*$^+$B$^+$/e14- (*mcr*A-); Δ (*lac-pro*AB); *thi gyr*A96 (Nal^r); *end*A1; *hsd*R17 ($r_k^-m_k^-$); *rel*A1; *sup*E44; *rec*A1	A *recA*$^-$ cell line to obtain stocks of plasmid DNA from overnight cultures.
Top10 One Shot™ competent cells (Invitrogen) (115)	F$^-$; *mcr*A; Δ(*mrr-hsd*RMS-*mcr*BC) Φ80*lacZ*ΔM15; Δ*lac*X74; *deo*R; *rec*A1; *ara*D139; Δ(*ara-leu*)7697; *gal*U; *gal*K; *rps*L; *end*A1; *nup*G	*recA*$^-$ cell line from *E.coli* to obtain stocks of plasmid DNA from overnight cultures. They replaced the JM109 strain.
Escherichia coli HMS 174 (DE3 lysogen) (Novagen) (116)	F$^-$; *rec*A1; *hsd*R(r_{k12}^- m_{k12}^+); Rif^r (DE3)	Constructed with a DE3 lysogenic region, which acts upon the *lac* promoter present in pET plasmids, this strain was used for expression of protein.

High copy number plasmid vectors were used to obtain and amplify DNA. Low copy number plasmids were used for protein over-expression, where they were placed under the control of a bacterial host repressor.

Table 2.2

Bacterial vectors. pDC13 was constructed by Dr. Dominic Campopiano (University of Edinburgh) and consists of the insertion of a ribosome binding site into a pUC18 vector. Use of this plasmid was by kind permission.

Plasmid	Phenotype	Copy Number	Description of use
pUC18 (Novagen)	amp^r; *lacZ'*	~ 500	This vector was used to obtain DNA stocks, as the copy number is uncontrolled
pDC13* (pUC18/RBS)	amp^r; *lacZ'*	~ 500	Designed for protein expression, this plasmid was used for mutated proteins.
pET16b (Novagen)	amp^r; T7 promotor; Xa protease cleavage site	~ 50	Derived from pBR322 and T7*lac* promotor control of gene expression. Use in HMS174 (DE3) cell line for protein expression
pET6H (pET11d derivative created at Edinburgh)	amp^r; T7 promotor; Xa protease cleavage site; N-terminal 6 Histidine sequence	~ 50	Derived from pBR322 and T7*lac* promotor control of gene expression. Use in HMS174 (DE3) cell line for protein expression

All microbiology work was carried out using asceptic techniques. Broths and containers were all autoclaved (121°C for 20 min at 15 psi). Sterile 20ml universal tubes (Invitrogen) were utilised for small overnight cultures and larger bacterial cultures were grown up in 500ml shake flasks (Sigma) or a glass 10 litre fermentor (New Brunswick Scientific). All cultures were cultivated in 2YT (16g/l Bactotryptone, 10g/l Yeast Extract, 5g/l NaCl, pH 7.5) or Luria Bertani (10g/l Bactotryptone, 10g/l NaCl, 5g/l Yeast Extract, pH 7.5) broth by agitation (250rpm) at 37°C. Commercial competent cells were initially grown and plated out in SOC (20g/l Bactotryptone, 5g/l yeast extract, 0.5g/l NaCl, 5g/l $MgSO_4$, 3.2g/l glucose, pH 7.5) media. Unless otherwise stated, transformant cells containing vectors pUC18, pET16b and pET6H were spread onto agar plates (15g/l bacto-agar in LB broth) containing 100μg/ml ampicillin and also grown in the presence of 100μg/ml ampicillin.

Aliquots of 1ml of each transformant were frozen with 10% glycerol at -20°C over 48 hours and then transferred to -80°C for storage. These represented the glycerol stocks used for storage of all clones.

2.1.2 Preparation of Competent Cells

A 20μl aliquot of the desired strain of *E. coli* was used to innoculate 10ml LB (Luria Bertani) broth The culture was grown up overnight. A 200μl aliquot of this overnight culture was then transferred into 9.8ml LB broth solution containing 20mM $MgCl_2$ and grown for a further 50 minutes until OD_{600nm} = 0.2 (Unicam UV/vis spectrophotometer UV4). The cells were harvested (Denley BR401 3,000 rpm, 15min, 4°C) and the supernatant discarded.

The pellet was re-suspended in 4ml transformation buffer (10mM Tris, pH 8.0, 50mM $CaCl_2$) and stored on ice for 30 minutes before further centrifugation of the cells (Denley BR401 3,000 rpm, 15min, 4°C). The supernatant was discarded and the pellet re-suspended in 400μl transformation buffer and stored on ice for 12-24 hours (117).

This process was employed for the first 12 months of research. During this period, transformation efficiency became increasingly lower, resulting in the subsequent purchase and employment of competent cells from a commercial origin for the remaining period of research. The initial pellet was stored on ice for 2 hours in 4 ml transformation buffer to increase final transformation efficiency and, after the final incubation period, frozen in 100µl aliquots at -80°C.

2.1.3 Transformation

Non-commercial origin:

1-15µl of the desired DNA (up to 100ng) was added to 100µl competent cells, gently mixed and placed on ice for 30 minutes. The cells were subjected to a heat shock (37°C, 5 min) and 1ml warmed (37°C) 2YT broth was added. The cells were left for 1 hour at 37°. Cells were then pelleted (MSE microfuge 13,000rpm, 5 min, RT) and the supernatant discarded. The pellet was re-suspended in 50µl 2YT broth and spread to dryness on 2YT/amp (100µg/ml) agar plates. The plate was incubated overnight at 37°C.

Commercial Top 10 One Shot™ cells:

1-5µl (up to 40ng) DNA was added to 25µl Top 10 One Shot™ cells, gently mixed and stored on ice for 30 minutes. The solution was then heated (42°C) for exactly 30 seconds and returned to ice for a further 2 minutes. 200µl SOC medium was added and the cells agitated (250rpm, 37°C) for one hour before a 40µl aliquot was plated to dryness on a 2YT/amp agar plate. This was incubated overnight at 37°C.

Commercial HMS174 (DE3) cells:

1-5µl DNA (up to 40ng) was added to 10µl competent HMS 174 (DE3) cells, gently mixed and stored on ice for 30 minutes. The solution was then heated (42°C) for exactly 30 seconds and returned to ice for a further 2 minutes. 80µl SOC medium was added and a 40µl aliquot plated to dryness on a 2YT/amp agar plate which was incubated overnight at 37°C.

1, Unicam UV.vis spec. UV4), the cells were induced with IPTG to a final concentration of 1mM and allowed to grow for a further period of three hours.

The cells were harvested (Sorvall SLA 1500 rotor 7,000 rpm, 10 min, 4°C) and the final pellet washed with 20mM potassium phosphate buffer (20mM K_2HPO_4, 20mM KH_2PO_4, pH 7.5; 2mM EDTA).

At this point, the pellet could be frozen at -20°C and the purification process continued at a later date if necessary. A frozen cell pellet was thawed on ice before re-suspending it in buffer for further purification.

The washed pellet was re-suspended in 20mM potassium phosphate buffer (4ml buffer/1g pellet) and the cells disrupted by sonication (MSE Soniprep 15 x 30 sec bursts at 14 amplitude microns). The resulting cell suspension was centrifuged (Sorvall SS-34 rotor 10,000 rpm, 30 min, 4°C) and the pellet containing the cell debris discarded. If the cell pellet was tinged with yellow, it was re-sonicated to extract any remaining protein.

The supernatant represented the cell free extract to be consecutively fractionated with ammonium sulphate; heated; or loaded straight onto an affinity column.

2.2.3 Ammonium Sulphate Fractionation

Due to the heat sensitive nature of *E.coli* AONS proteins, the following steps were carried out on ice or at 4°C.

For wild type and mutant AONS proteins from *E. coli*, the crude extract was initially cut by slow addition of 35% ammonium sulphate (19.7g $(NH_4)_2SO_4$ /100ml protein solution) with gentle

agitation and subsequent centrifugation (Sorvall SS-34 rotor 10,000 rpm, 30 min, 4°C). The white pellet was discarded.

E.coli AONS was then precipitated by increasing the ammonium sulphate content of the supernatant to 65% (18.7g $(NH_4)_2SO_4$ /100ml protein solution). After slow addition of ammonium sulphate, the solution was left to stir gently overnight at 4°C.

The precipitant mixture was subsequently centrifuged (Sorvall SS-34 rotor 10,000rpm, 30 min, 4°C) and the supernatant discarded. The pellet was re-suspended in an arbitrary amount of 20mM potassium phosphate buffer (supplemented with 20% (10.7g $(NH_4)_2SO_4$ /100ml buffer) and syringe filtered (0.45μm) in preparation for chromatographic purification.

2.2.4 Consecutive heat treatment

After obtaining the crude extract, initial purification of AONS from *Aquifex aeolicus* was commenced by heating. In order to avoid rapid precipitation of cellular proteins, which may have resulted in the removal of AONS from the solution, the crude extract was heated first at 60°C for 10 minutes. The solution was centrifuged (Sorvall SS-34 rotor 10,000rpm, 30 min, 4°C), the pellet discarded, and the supernatant heated to 80°C for a further 10 minutes. After centrifugation as above, the pellet was discarded and the supernatant filtered (0.45μm) in preparation for chromatographic purification.

2.2.5 Hydrophobic Interaction Chromatography

A HiLoad 16/10 Phenyl Sepharose column (Pharmacia Biotech) - column volume 25ml - was calibrated with 20mM phosphate buffer containing 20% ammonium sulphate. The protein extract was run on a linear ammonium sulphate gradient decreasing over 10 (or 20) column volumes from 20-0%. This technique was used for the initial chromatographic purification of *E.coli* AONS.

2.3.2 DNA Isolation from Agarose

DNA fragments were excised from the agarose gel with a sharp blade and transferred into an Eppendorf tube. They were then purified using the Prep-a-Gene® kit (Bio Rad) or QIAquick (QIAGEN). DNA was eluted in a volume of 40µl.

2.3.3 DNA Restriction Digests

A volume of 1µl restriction endonuclease was used for each digest. This was added to the DNA solution along with an appropriate buffer. Incubation of the digests was at 37°C.

For analysis purposes, one hour digests of 5-10µl *bio*F DNA with the appropriate enzymes and corresponding buffers were run on 1% agarose gel.

For ligation purposes, 10-20µl plasmid DNA was restricted overnight Each digest was run on a 1% agarose gel to verify size and then retrieved from the gel as described above (see section 2.3.2).

2.3.4 Ligation of DNA

Digested DNA (section 2.3.3) retrieved from agarose gel by the Prep-a-Gene® kit was ligated together at room temperature over 48 hours. A typical ligation involved: 13µl *bio*F DNA; 3µl plasmid DNA; 2µl T4 ligase (New England Biolabs); 2µl T4 ligase buffer (New England Biolabs). A control reaction was run alongside the ligation, replacing the 13µl insert DNA by H_2O.

Complete ligations were then transformed into Top10 One Shot™ competent cells and the new construct retrieved from overnight cultures by the Wizard Mini-Prep® (Promega) or QIAprep (QIAGEN).

2.2.6 Anion Exchange Chromatography

For the final stage of purification, wild type and mutant AONS from *E.coli*, were loaded onto a HiLoad 16/10 Q-sepharose 50ml column (Pharmacia Biotech). Protein from desirable fractions collected after hydrophobic interaction chromatography was pooled and dialysed against 20mM potassium phosphate buffer to remove excess $(NH_4)_2SO_4$ and syringe filtered (0.45μm). The protein was eluted over 20 column volumes using a linear NaCl (0-1M) gradient. This method was also employed for the separation of *A.aeolicus* AONS.

Fractions showing protein impurities were further purified using a Resource Q 1ml column (Pharmacia Biotech) run as above.

2.2.7 Nickel Affinity Chromatography

This column was used for the preparation of His_6-tagged AONS from *E.coli*.

A HiTrap® 5ml chelating column (Pharmacia-Biotech) was first charged with 50mM $NiSO_4$ to produce the nickel chelation resin of the column.

The filtered crude extract was loaded onto the column in binding buffer (5mM Imidazole; 0.5M NaCl; 20mM Tris-HCl, pH 7.9). The column was washed with 5 column volumes of wash buffer (60mM Imidazole; 0.5M NaCl; 20mM Tris-HCl, pH 7.9) and protein eluted with 5 column volumes of elution buffer (1M Imidazole; 0.5M NaCl; 20mM Tris-HCl, pH 7.9. 5ml fractions were collected in 20ml 20mM potassium phosphate buffer, pH 7.5 for an initial dilution of imidazole. Protein fractions were pooled and dialysed exhaustively against 20mM potassium phosphate buffer to remove the imidazole.

2.2.8 SDS Polyacrylamide Gel Electrophoresis (SDS PAGE)

The contents of chromatographic fractions were analysed by SDS PAGE (118).

SDS sample buffer (100mM tris.HCl, pH 6.8, 20% (w/v) glycerol, 15% (v/v) β-mercaptoethanol, 3% (w/v) SDS, 0.25% (w/v) bromophenol blue) was added to each protein fraction (v/v) and then boiled for five minutes. A 15µl volume of each sample was loaded onto a 4% stacking gel and run through a 15% separating gel at 200V for approximately 45 minutes (Bio Rad Protean II discontinuous buffer minigel system), in SDS running buffer (180mM Glycine, 25mM Tris, 0.1% w/v SDS).

The size of proteins was gauged using a low molecular weight standard (Pharmacia, 14.4 - 94 kDa). Gels were stained with Coomassie Blue R250 (40% Methanol, 10% Acetic acid, 0.1%w/v Coomassie Blue - R250), de-stained (40% Methanol, 10% Acetic acid) and visualised under white light.

Completed gels were incubated overnight at 37°C in a water bath containing 1% glycerol and dried using Gel Drying Film (Promega).

2.2.9 Determination of protein concentration

An approximate estimate of the concentration of a protein solution was used to gauge the amount of protein to be loaded onto a purification column and was obtained by measuring the optical density of the sample (Unicam UV/vis spectrophotometer UV4). An OD_{280nm} value of 1 is approximately equal to 1mg/ml protein concentration (119).

Accurate concentrations were measured using the Bradford Assay (120) or the BCA Protein Assay Reagent (Pierce) as per manufacturer's instructions. In both cases, Bovine Serum Albumin was used as a reference.

Pure protein was frozen at -20°C with 10% glycerol (v/v).

2.2.10 Protein Mass Spectrometry

Protein samples (0.5μM) were separated from the salt in the buffer on a 5μg C-4 300A column (Jupiter) at constant 0.01% acetonitrile concentration and a 10-100% linear gradient acetonitrile in water (Waters 2690 HPLC unit) over 40min at a flow rate of 0.05ml/min. Separation was monitored at 280nm (Waters 486 Tunable Absorbance Detector) and on removal of the salt, the HPLC was connected to a Platform II quadrupole mass spectrometer (Micromass) equipped with an negative electrospray ion source. The cone voltage was set to 70V and the source temperature to 65°C. Scanning at intervals of 0.1sec, the scans were accumulated, the spectra combined and the average molecular mass determined using the MaxEnt and Transform algorithms of MassLynx software Version 2.3 (Micromass).

2.3 Molecular Biology

2.3.1 Agarose Gel Electrophoresis

DNA samples were mixed with 6x loading dye (blue/orange, Promega) and run on a 1% agarose (Gibco BRL) gel containing 5μl (10mg/ml) Ethidium Bromide for analysis. The samples were run (Gibco BRL H5 system) in TAE buffer (40mM Tris-acetate, 1mM EDTA) for approximately 45 minutes at 100V. DNA fragments were visualised under ultraviolet light.

Fragment size was gauged using λHindIII standard (23kb-0.5kb) and/or PCR standard (1Kb - 50bp) (Sigma). Subsequently, these standards were replaced by Hyperladder I (100bp - 10Kb) and Hyperladder IV (50bp - 1Kb) (Promega).

2.3.5 DNA Mutagenesis

Site directed mutagenesis was conducted by the Polymerase Chain Reaction megaprimer method (121) to specifically mutate certain DNA bases corresponding to amino acids present within the active site of AONS. All primer oligonucleotides for mutagenesis were used at a concentration of 10μM. The underlined codons represent the mutated residues. Restriction sites are highlighted in bold.

		EcoRI BspHI
FEcoBsp primer	5'- CGC	**GAA TTC GTC ATG** AGC TGG CAG GAA AAA - 3'
M13 reverse pUC18 primer	5'- CGC CAG GGT TTT CCC AGT CAC - 3'	
K236A forward mutant primer	5'- ACT TTT GGC GCA GGA TTT GGC - 3'	
H133F forward mutant primer	5'- CGG CTT AGC TTC GCC TCA TTG - 3'	
		*Nco*I
AQF Forward primer	5'-CAT ACT GGG AAT T**CC ATG** GGT TGG ATT GAG GAG GAA-3'	
AQF Reverse primer	5'-GGC GGA TCC TAA GCC CTT CCT TT-3'	
AQF H118F forward mutant primer	5'-GAC GAA TTA AAT TTC GCA TCT ATA ATA-3'	

FEcoBsp and M13 primers were used as the forward and reverse primers respectively for mutations within *E.coli bio*F and the AQF forward and reverse primers for *A.aeolicus bio*F.

2.3.5.1 Production of Megaprimers

The following were combined in a 0.5ml PCR tube: 1μl template DNA (pUC18/*bio*F); 10μl 5x PCR buffer (335mM Tris, pH 8.8, 83mM $(NH_4)_2SO_4$, 33.5mM $MgCl_2$, 50mM 2-Mercaptoethanol, 33.5μM

EDTA, 0.82mg/ml Bovine Serum Albumin, 7.5mM dNTPs); 5µl M13 primer (10µM); 5µl mutant primer (10µM); 28µl H_2O; 1µl Deep Vent Polymerase (New England Biolabs) and gently mixed. The solution was covered with a layer of liquid paraffin and placed in the Perkin Elmer 480 Thermal Cycler. PCR was conducted over 30 cycles (95°C, 1 min; 54°C, 1 min; 72°C, 2min). A final 5 minute extension at 72°C encouraged final coupling of DNA bases and the reaction was analysed by 1% agarose gel electrophoresis.

2.3.5.2 Mutant Extension

Megaprimers were isolated from the agarose gel and used as the reverse primer for the mutant extension reaction. The M13 reverse primer was replaced by the FEcoBsp primer. The following were combined in a 0.5ml PCR tube: 1µl template DNA (pUC18/*bio*F); 10µl mutant megaprimer; 5µl FEcoBsp primer (10µM); 34µl H_2O; 2 Ready-to-go® PCR beads (Pharmacia Biotech) and cycled as above.

2.3.5.3 Mutant Amplification

Mutant extensions were isolated from the agarose gel and used as the template for the final amplification reaction. The forward and reverse primers were FEcoBsp and M13 respectively. Components were combined in a 0.5ml PCR tube and cycled as above.

Amplified *Eco*RI/*Bam*HI restricted mutants were ligated into a *Eco*RI/*Bam*HI restricted pUC18 vector respectively and verified by agarose gel electrophoresis and dRhodamine sequencing. Correct constructs were then digested *Eco*RI/*Bam*HI, and subsequently *Bsp*HI/*Bam*HI and ligated into *Nco*I/*Bam*HI restricted pET16b vectors.

2.3.6 DNA sequencing

Mutants ligated into pUC18 vectors were sequenced to ensure that the construct was correct. An 8µl volume of sequencing premix (PE Applied Biosystems) was combined in an 0.5ml PCR tube with 10µl mutant DNA, 1µl M13 reverse primer and 1µl H_2O for the reverse reaction, replacing the M13 primer with 1µl NR (NEW REV) pUC18 forward primer (5'-GTT GTG TGG AAT TGT GAG CGG-3') (Gibco BRL) for the forward reaction. A layer of paraffin oil was added and the reactions thermally cycled (96°C, 30 sec; 45°C, 15 sec; 60°C, 4 min) for 30 cycles.

The oil was removed, the PCR reaction transferred to an Eppendorf tube and 7µl ammonium acetate (1/3 vol) added. 2.5 volumes of 95% ethanol was then introduced and the entire mix stored at -20°C for 2 hours.

The solutions were centrifuged (MSE microfuge, 13,000rpm, 15 minutes, RT) and the supernatant discarded. The pellet was repeatedly washed with 500µl 70% ethanol and centrifuged as above. The pellet was dried under a vacuum for 10 minutes (Gyrovap). Sequencing was carried out by Sanger dideoxy chain termination (122) on an ABI Prism 377 DNA sequencer. Results were analysed using ABI Prism editview software for the Apple Macintosh, and subsequently Vector Nti5 software (InforMax Inc.)

2.4 Enzymology

2.4.1 Steady State Kinetics

Frozen aliquots of AONS protein solution were thawed on ice and dialysed in 20mM potassium phosphate buffer containing 100µM PLP (pyridoxal-5'-phosphate, Sigma) for one hour.

Enzymatic activity of AONS and consequent production of Coenzyme A was coupled to CoA consumption of a second enzyme α-ketoglutarate dehydrogenase (36) (47). All assays were carried out at 30°C unless otherwise specified in the text.

A typical assay contained: 20mM potassium phosphate buffer, pH 7.5; 10 x assay buffer[2]; varying L-alanine; varying Pimeloyl CoA; 0.01U α-ketoglutarate dehydrodgenase (Sigma); 1μM AONS made up to a final volume of 1ml with H_2O

The reference cell contained all components with the exception of AONS. The progress of the assay was recorded on a Hewlett Packard 8452A Diode Array Spectrophotometer at a wavelength of 340nm using Multicell Kinetics software. The assay proceeded for 10 minutes and was monitored at 10 second intervals. The data were fitted to Michaelis-Menton saturation curves according to equation 1.

$$V_0 = \frac{V_{max}[S]}{[S] + K_s} \quad \text{.....Equation 1}$$

This assay was developed by Dr Scott Webster from an assay for ALAS (47). Pimeloyl CoA is not commercially available, thus it was synthesised in the laboratory according to (38), using 7-(phenylthiocarbonyl) heptanoic acid and Coenzyme A (Sigma) as starting materials.

2.4.2 UV Spectral Analysis

Frozen aliquots of AONS protein solution were thawed on ice and dialysed in 20mM potassium phosphate buffer containing 100μM pyridoxal-5'-phosphate (Sigma) for one hour. Non-enzyme bound PLP was removed by multiple washes with 20mM potassium phosphate buffer through a Centrex UF2 concentrator (Schleicher & Schuell). Complete removal of free PLP was monitored by a decrease in absorbance at 390nm and subsequent shift to 410nm-430nm (Hewlett Packard 8452A

Diode Array Spectrophotometer). The protein in its washed state was used initially to calculate the absorbance coefficient of the enzyme-cofactor complex chromophore.

2.4.2.1 pH stability

The prepared enzyme (8-10μM) was incubated with 1M HEPES buffer, adjusted to a pH value in the range pH 6 - pH 9, for 20 minutes at 30°C. For AONS protein from *A.aeolicus*, this incubation was also conducted at 60°C. The resulting spectra were measured against a reference of 1M HEPES buffer at the relevant pH (Hewlett Packard 8452A Diode Array Spectrophotometer) using General Scanning (DOS based) software.

2.4.2.2 Temperature stability

The prepared enzyme (10μM) was heated at various temperatures between 0-100°C for 10 minutes. A 50μl aliquot of the heated protein solution was then assayed (see section 2.5.1) at 30°C.

An additional experiment for the stability of AONS from *A.aeolicus* was to ascertain the activity profile in relation to temperature. A 50μl aliquot of dialysed enzyme (10μM) was incubated with 10mM potassium phosphate buffer; 55mM L-alanine and 150μM Pimeloyl CoA for 10 minutes at specific temperatures between 0-100°C. Reactions were then quenched with tricarboxylic acid (Sigma) to a final concentration of 1% and centrifuged to pellet the denatured protein (MSE microfuge 13,000rpm, 5 min, RT). A 50μl volume of the supernatant was then assayed with 20mM potassium phosphate buffer, 10x assay buffer, 0.01U α-ketoglutarate dehydrogenase, made up to 1ml with H_2O at 30°C.

[2] 10x assay buffer contains: 10mM NAD^+; 30mM $MgCl_2$; 2.5mM thiamine pyrophosphate; 10mM α-ketoglutarate

initial screens using Structure Screen I and II (Molecular Dimensions Ltd) and an ammonium sulphate screen. A 100µl volume of screening solution was introduced into the plate well. Protein solution and well solution (v/v) were combined in a droplet, which was placed on the platform. Wells were covered with polythene tape and incubated at the desired temperature.

2.5.3 X-ray diffraction

Crystals varying in size from 100-600nm were mounted in Cryoloops (Hampton Research) and frozen in liquid nitrogen, using Paraton N oil as the cryoprotectant. X-ray diffraction was carried out at 100K at SRS, CLRC Daresbury Laboratory on Station 7.2 using a MarResearch 345mm image plate and wavelength λ=1.488Å.

The data was processed using DENZO (123) and scaled with the SCALEPACK software (124).

2.5.4 Crystal structure solution

Diffraction data parameters were obtained using the Computational Crystallography Project 4 (CCP4) suite of programs software (125), (www.dl.ac.uk/CCP/CCP4/main.html).

Phasing was solved by molecular replacement(126), using the structures of both *E.coli* (37) and *Bacillus sphaericus* (Cambillau & Ploux, 2000, unpublished) AONS as search models. An electron density map was created using CCP4 software and the structure was refined manually in O (127), (http://xray.bmc.uu.se) and computationally in CNS XPLOR (128).

2.5.5 Polymer formation

A Superose 200 column (Amersham Pharmacia) of volume 360ml was equilibrated with 20mM potassium phosphate buffer, pH 7.5 and 100mM NaCl and calibrated with 1ml protein solution containing 1mg each of: Bovine serum albumin (66kDa); Ovalbumin (45kDa); Carbonic anhydrase (29kDa); Cytochrome C (12.5kDa) and blue dextran (1,000kDa). Blue dextran eluted at 110ml, which was termed the void volume. Elution volumes of the standard proteins were then calculated by subtraction of the void volume from the elution volume. The ration of elution volume to void volume was plotted against the logarithm^{10} of the molecular weight of each standard to obtain a standard curve. One millilitre protein solution containing 2mg *A.aeolicus* AONS and 1mg blue dextran was then loaded onto the column and allowed to elute. The molecular weight of AONS in its native form was read from the standard curve.

2.6 Bioinformatics

All programs were accessed either on their original server, or through the database service provided by the Human Genome Mapping Project (www.hgmp.mrc.ac.uk).

2.6.1 DNA Sequence Retrieval

DNA sequences were retrieved from the European Molecular Biology Laborotory (EMBL) database, held at the European Bioinformatics Institute (EBI) (www.ebi.ac.uk) or from the Genome Representative Organisation sector of Genbank (www.ncbi.nlm.nih.gov/Entrez/Genome/org.html).

Protein sequences were retrieved using the SWISSPROT and TrEMBL databases accessed through the Swiss ExPASY[3] server (www.expasy.ch/) of the Swiss Institute of Bioinformatics. Alternatively, sequences were directly retrieved from the Sequence Retrieval System (www.srs.ac.uk) supported by EBI.

2.6.2 Protein Sequence Alignment

Protein sequences were accessed (see above section) and converted into PIR format. This data was pasted into the EMBL based alignment engine CLUSTALW that is found on the sites of the EBI and several mirror sites and alignment carried out with the default scoring matrix algorithm (BLOSUM 62). The resulting alignment was adjusted in Align X (InforMax Inc.). Secondary structure alignment was computed *via* the DSSP program. Several protein sequences were aligned and an evolutionary dendrogram created using Vector Nti5 software.

2.6.3 Protein Structure Retrieval

Released protein structures were accessed from the Brookhaven Protein Databank (PDB) (www.rcsb.org) using a four digit identification code. The downloaded data was manipulated in Swiss-3D, a shareware program offered by the Swiss Institute of Bioinformatics.

[3] Expert Protein Analysis System

Chapter 3
Characterisation of *E.coli* AONS

3.1 Isolation and Purification of wild type and His_6-tagged AONS

3.1.1 Purification of wild type AONS

The *bio*F gene was initially cloned from pBO3O 15/9, a plasmid containing the whole *E.coli bio* operon fragment, into pUC18 as an *Eco*RI/*Bam*HI fragment. *Bsp*HI/*Bam*HI fragment containing the gene was subsequently sub-cloned into the *Nco*I/*Bam*HI site of the over-expression vector pET16b, destroying both the *Bsp*HI and *Nco*I site (36).

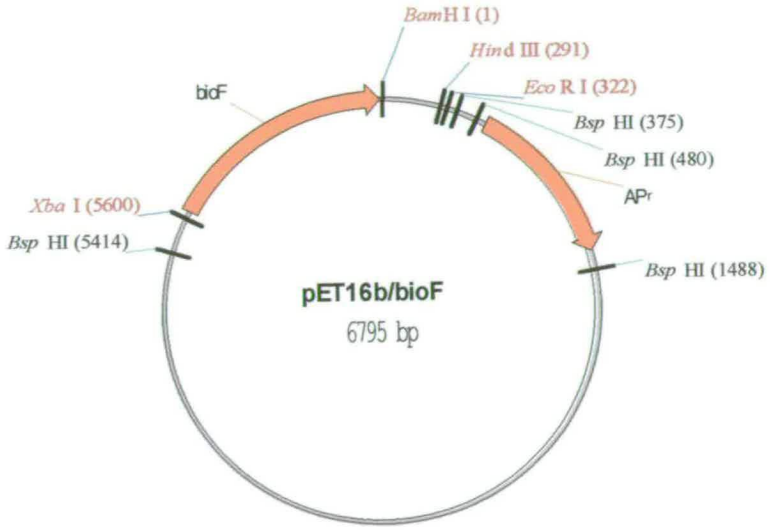

Figure 3.1.1

The vector pET16b containing the *bio*F gene from *E.coli*. The gene was sub-cloned as a *Bsp*HI/*Bam*HI fragment into a *Nco*I/*Bam*HI digest of pET16b where it was placed under the control of a powerful T7 inducible promotor.

AONS was over-expressed in HMS 174 (DE3) cells which were induced with a final concentration of 1mM IPTG for three hours before harvesting. The protein was purified by sequential ammonium sulphate fractionation and hydrophobic interaction chromatography followed by anion exchange chromatography (see section 2.2).

The approximate yield was 10mg/litre of protein of 95% purity as estimated by SDS PAGE. Initially, the protein displayed the characteristic yellow colour of its PLP cofactor, but the majority of this colour disappeared on purification, dialysis or freezing. Details of activity at each purification step are shown in table 3.1

Table 3.1

Purification table of *E.coli* AONS from expression of HMS 174 (DE3). Protein concentration was measured using the method of Bradford (120) and specific activity was measured in a coupled assay using 50mM L-alanine and 200μM pimeloyl-CoA. 1U AONS represents the transformation of 1μmol pimeloyl-CoA per minute at 30°C

Purification Step	Volume (ml)	Protein (mg/ml)	Specific activity (U/mg)	Total activity (U)	Yield (%)	Purification fold
Crude extract	50	55	--	--	--	--
65% ammonium sulphate	45	50	0.02	45	100	1
Hydrophobic interaction	104	1.8	0.2	37.4	83	10
Anion exchange	44	2.1	0.4	37	82	20

3.1.2 Purification of His_6-tagged AONS

The addition of an N-terminal tag consisting of 6 histidines was designed to allow for a faster purification of both wild type and mutant AONS proteins. The *bio*F gene was sub-cloned from pUC18 by excision of the *Eco*RI/*Bam*HI fragment and subsequent digestion to obtain the *Bsp*HI/*Bam*HI fragment. This was directionally ligated into the tagged over-expression vector pET6H at the *Nco*I/*Bam*HI regions

of the polycloning site, eliminating both the *Bsp*HI site and the *Nco*I site, as before. The T7 inducible promotor of the vector was located upstream of the 6-histidine sequence (MHHHHHHA), so induction with IPTG resulted in production of the tagged protein.

The resulting cell free extract was loaded directly onto a nickel affinity chromatography column and His_6-tagged AONS eluted at the second column volume of elution buffer.

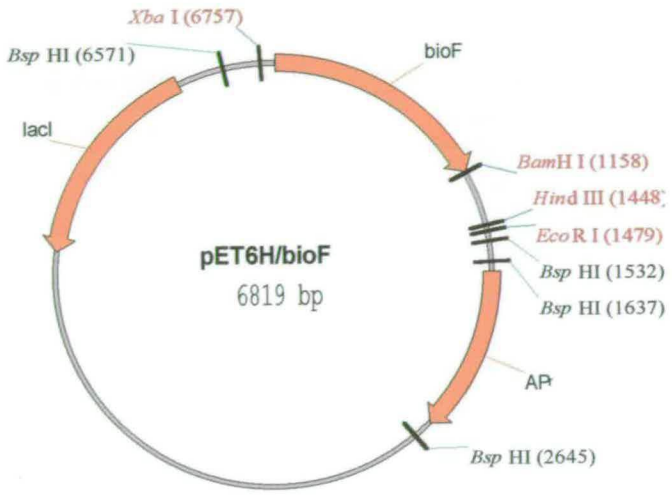

Figure 3.1.2

The pET6H vector containing the *bio*F gene. Transcription of the gene results in a protein with a N-terminal 6 histidine tag. Expression is controlled by the T7 IPTG-inducible promotor.

Protein fractions were collected in tubes containing 20mM potassium phosphate buffer, pH 7.5 in a fraction : buffer ratio of 1:3. The elution buffer contained an elevated concentration (1M) of imidazole, and collection of the fractions in this manner prevented precipitation of the eluted protein. Exhaustive dialysis of the protein removed the imidazole and 6His-tagged AONS was frozen at -20°C. A typical preparation yielded 15mg/l His_6-tagged AONS of 95% purity as estimated by SDS PAGE. Specific activity of the purified protein was 0.4U.

3.2 Physical characterisation of His_6-tagged AONS

3.2.1 Cofactor Binding

The absorption coefficient (ε) of the enzyme-cofactor imine linkage was measured as 7,752 l mol^{-1} cm^{-1}, a value corresponding to that of the unmodified wild type (see section 5.2.1). Thus there was no significant difference in measured affinity of the His_6-tagged protein for its cofactor and loss of colour on freezing and dialysis of the unmodified enzyme.

3.2.2 Mass spectrometry

ESI mass spectrometry was performed on His_6-tagged AONS and the spectrum can be seen in fig 3.3.1. The measured molecular weight value of the apo-enzyme indicates a mass corresponding to the post-translational cleavage of the formyl methionine residue from the tag. This is the same as the post-translational modification procedure observed on the unmodified wild type enzyme (36). The measure mass of 42,627 Da was 8 Daltons greater than the predicted value of 42,619 Da, an error of 0.02%.

3.3 Absorbance spectra of wild type and His_6-tagged AONS

3.3.1 Absorbance spectra of wild type AONS

Monitoring of the UV/visible spectra of both enzymes with their substrates and products was conducted between 300nm-600nm. Characteristic peaks for wild type AONS were seen at 334nm and 425nm. These correspond to the protonated and non-protonated forms of the lysine bound PLP internal imine respectively. To investigate this, the imine bond was reduced by incubation of the enzyme with 2mM $NaBH_4$ (sodium borohydride) for twenty minutes at 30°C.

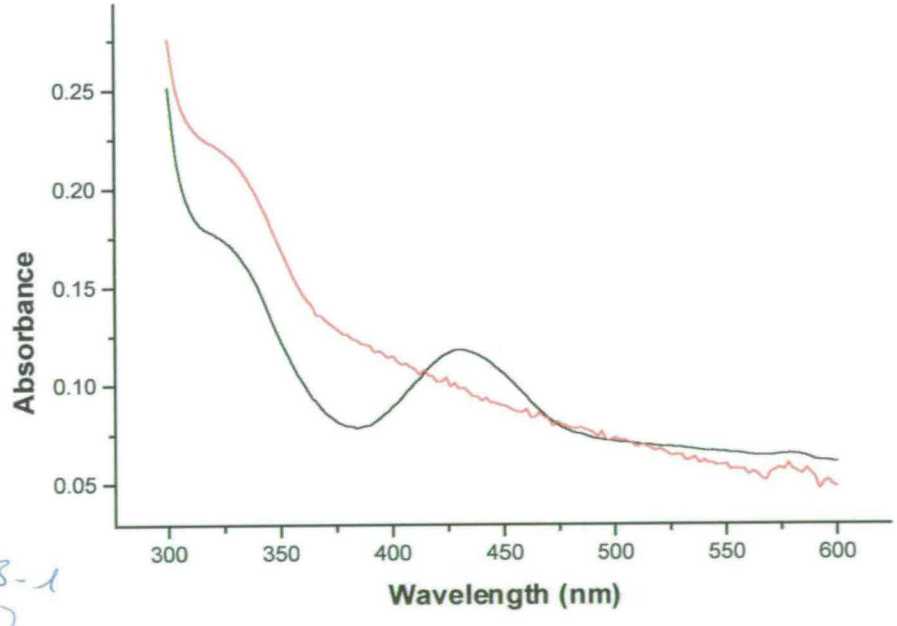

3.3-1

Figure 3.3.2

Spectra of $NaBH_4$ reduced and wild type spectra. *Wt* AONS (12μM) was incubated for 20 minutes with 2mM $NaBH_4$ at 30°C. The native spectrum is represented by the black line and the reduced spectrum is seen in red.

The maximum of the imine bound cofactor at 425nm disappears, but the maximum at 334nm increases visibly. This maximum is the probable result of reduction of the Schiff base linkage to a single bond between the PLP cofactor and the lysine residue of the enzyme.

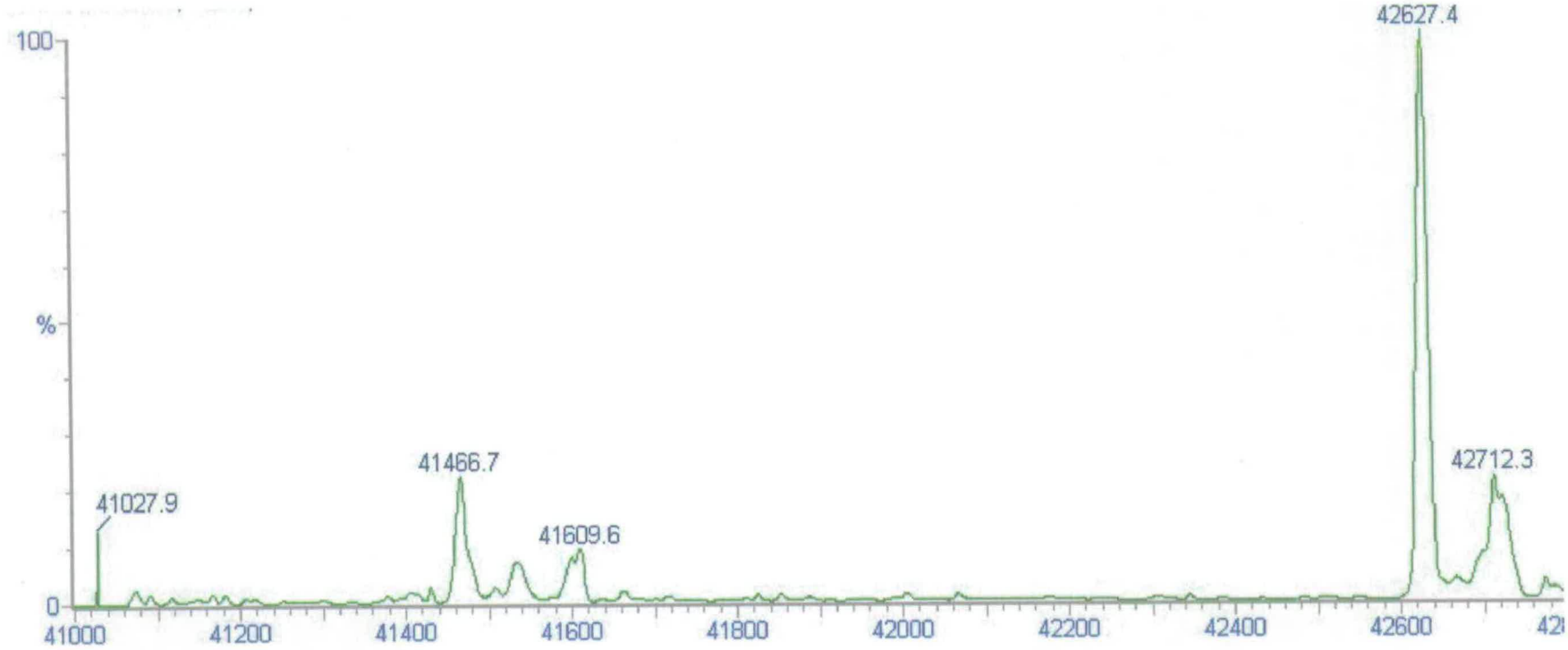

Figure 3.3.1

ESI Mass spectrometry of His_6-tagged AONS. The protein was separated from salts in the buffer by HPLC purification with H_2O/Acetonitrile containing 0.01% Trifluoroacetic acid on a C5 column. The predicted mass of the protein was 42,619 Da.

On addition of L-alanine to the native spectrum, the peak at 425nm becomes less well-defined, and on addition of the second substrate, pimeloyl-CoA, to the complex, a maximum at 486nm becomes visible (fig 3.3.3). At the same time, a reduction in the absorbance at 425nm suggests conversion of bound L-alanine into the product. Very little reduction of the L-alanine external aldimine is observed on addition of $NaBH_4$, suggesting the enzyme forms a closed complex on substrate binding, reducing access of the reagent.

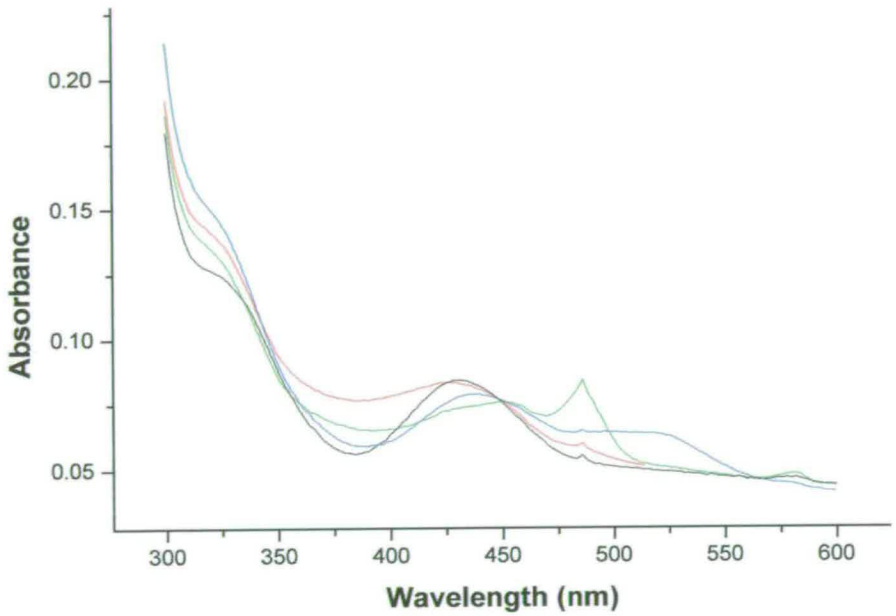

Figure 3.3.3

Change in the cofactor absorption spectra of *E.coli* AONS on addition of substrates and product. Spectra were acquired at 30°C and pH 7.5. The AONS-PLP complex can be seen in black (10μM); in the presence of: 10mM L-alanine (red); 10mM L-alanine and 100μM pimeloyl-CoA (green); 2mM AONS (blue).

On addition of the product, AON, to the native enzyme, a clear shoulder can be observed at 520nm suggesting the formation of the enzyme-product aldimine. The longer wavelength is predictable on the basis of the addition of a ketone function to the chromophore.

3.3.2 Absorbance spectra of His_6-tagged AONS

To establish whether there were any differences between the His_6-tagged protein and its wild type equivalent, the same UV/visible spectrophotometric characterisation was carried out on the His_6-tagged protein.. The native spectrum of its holoenzyme also displays characteristic peaks at 334nm and 425nm indicating the presence of the imine bound form of the cofactor as before. A series of experiments similar to those conducted for wild type enzyme was carried out. They included addition of substrates and product to the protein.

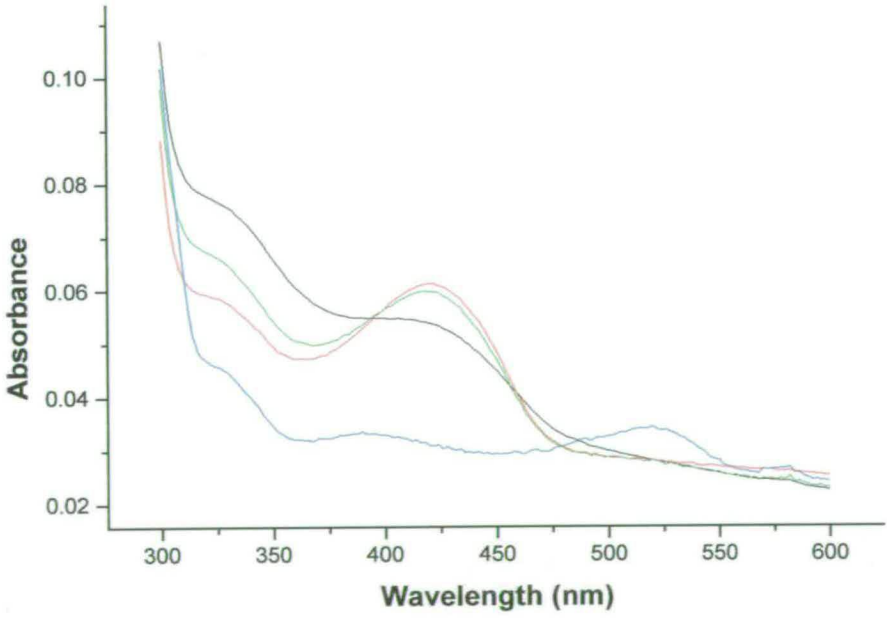

Figure 3.3.4

Change in the cofactor absorption spectra of *E.coli* His_6-tagged AONS on addition of substrates and product. Spectra were acquired at 30°C and pH 7.5. His_6-tagged AONS-PLP complex (6μM); in the

presence of: 10mM L-alanine (red); 10mM L-alanine and 100μM pimeloyl-CoA (green); 2mM AONS (blue).

In fig 3.3.4, the black line represents the native spectrum, which indicates a slightly higher absorbance of the band at 425nm relative to the concentration of protein compared with *wt* AONS. This band is enhanced on addition of L-alanine, but relatively little change is seen in the spectrum of addition of pimeloyl-CoA. There is no visible evidence of a quinonoid peak at 486nm on addition of the second substrate which contrasts to the behaviour of the wild type enzyme. On incubation of the His_6-tagged enzyme with the product, AON, there is a noticeable decrease in absorbance at 425nm and a large band appears as a shoulder at 520nm. This is comparable to results obtained with the *wt* enzyme. Coupled with the increase in the product band, there is a decrease in absorbance at 425nm, suggesting depletion of the residual enzyme-cofactor complex. Both wild type and His_6-tagged proteins were incubated at different pH values. Neither enzyme showed any pH dependency between pH 6.5 - pH 9, suggesting that the pK_a of the active site lies outside this range.

3.3.3 Dissociation constant of L-alanine

The maximum increase at 425nm of the external substrate aldimine was used to determine the dissociation constant of the first substrate for His_6-tagged AONS. L-alanine was titrated into the complex and the resulting absorbance increase at 425nm was plotted against the substrate concentration in a Michaelis-Menton saturation curve according to equation 2.

$$\Delta A_{max} = \frac{\Delta A_{max}[L-alanine]}{K_{\bar{d}} + [L-alanine]} \quad \text{.....Equation 2}$$

This revealed a dissociation constant of 160mM for L-alanine which is lower than the constant obtained for wild type AONS where K_d = 900mM (36)

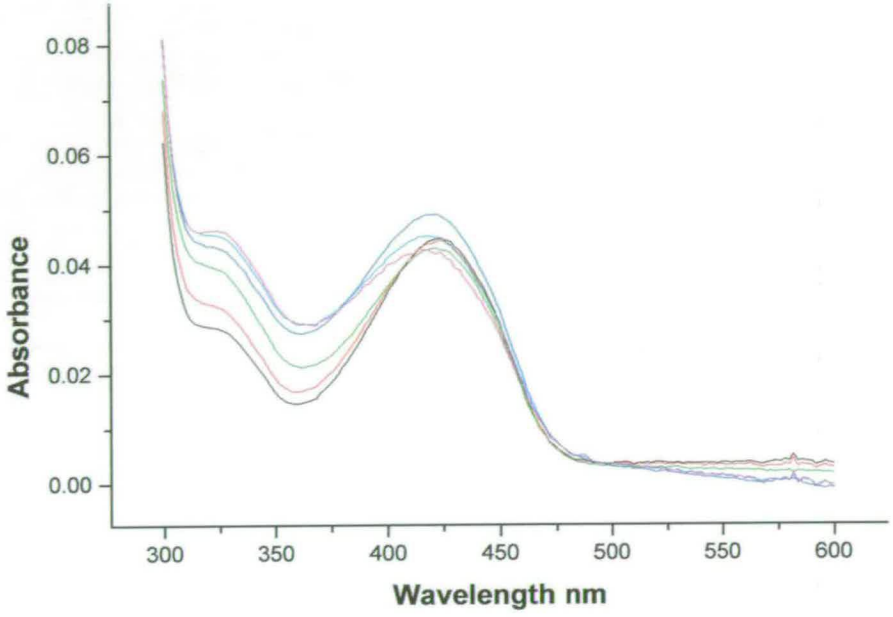

Figure 3.3.5

Titration of 10μM His_6-tagged AONS with L-alanine. AONS was mixed with the substrate in 200mM potassium phosphate buffer, pH 7.5, and left to equilibrate for 30 minutes at 30°C. Acquisition of the spectra was at 30°C and pH 7.5. Titration of AONS with L-alanine. Concentrations are 100μM (pink); 500μM (cyan); 1mM (blue); 11mM (green); 22mM (red); 55mM (black).

3.4 Steady state kinetics of wild type and His_6-tagged AONS

Steady state kinetic assays were performed by means of the coupled assay adapted by Webster *et al* (36) from the assay to determine kinetic activity of ALAS by Hunter & Ferreira (47). Assays were performed at 30°C and data were fitted to Michaelis-Menton saturation curves according to equation 1 (see section 2.4.1). The steady state rate constants for both wild type and His_6-tagged AONS are summarised in table 3.1. The turnover of the wild type protein was approximately three fold faster than that for the His_6-tagged protein, suggesting that the His_6 tag has some effect on the geometry of the active site.

The binding specificity of His_6-tagged AONS for pimeloyl-CoA is comparable with that for the wild type enzyme, as evinced from the K_m data. However, the K_m of His_6-tagged AONS for L-alanine is approximately half that of the wild type. This contrasts to the results of L-alanine titration of the modified protein.

Table 3.2

Steady state kinetic parameters of *E.coli* wild type and His_6-tagged AONS. Kinetics measurements were performed at 30°C, pH 7.5 using the coupled assay. Errors are given in parentheses

		pimeloyl-CoA		L-alanine	
AONS	k_{cat} (s^{-1})	K_m (μM)	k_{cat}/K_m ($s^{-1}M^{-1}$)	K_m (mM)	k_{cat}/K_m ($s^{-1}M^{-1}$)
Wild type	0.06(0.01)	25(2)	2400(430)	0.50(0.04)	120(21)
His_6-tagged	0.02(0.003)	22(2)	909(114)	1(0.2)	20(3.5)

An approximate five-fold enhancement in L-alanine binding for the His_6-tagged enzyme, coupled with a higher K_m value for this first substrate, may suggest that formation of the external substrate aldimine in the tagged protein is more favourable than external aldimine formation in the wild type enzyme. Orientation of this aldimine in the His_6-tagged protein, however, may be such that abstraction of the Cα proton is hindered.

The differences in L-alanine binding between the two enzymes, coupled with changes in the steady state kinetics; the higher absorption coefficient for the PLP-substrate external aldimine and the absence of a visible quinonoid peak on addition of pimeloyl-CoA, suggests that the N-terminal tag may alter the functionality of the enzyme. In view of the differences between the wild type and the modified proteins, the method of tagging the AONS enzyme for the purposes of mutant purification was discarded.

3.5 Mutagenesis of wild type AONS

Several conserved residues in the active site of AONS have been identified (see section 1.2.1). The lysine 236 residue of the *E.coli* AONS enzyme forms the internal aldimine Schiff base linkage with the PLP cofactor. A lysine residue is crucial in all PLP dependent enzymes thus far investigated (for reviews see: (104); (107); (111)). This basic residue was altered by site directed mutagenesis to an alanine residue. An oligonucleotide containing 21 bases was designed as the forward primer and incorporated the mutated codon with several correct codons either side to allow annealing onto the pUC18/*bio*F template. The reverse primer was M13, which anneals to a site on the pUC18 vector approximately 100bp downstream of the gene. The megaprimer was approximately 500bp and this was subsequently used as the reverse primer to produce the complete gene fragment from the original template, pUC18/*bio*F, and a forward primer, FEcoBsp, designed to incorporate an *Eco*RI and a *Bsp*HI restriction site upstream of the gene.

Directional ligation of the amplified gene into an *Eco*RI/*Bam*HI digest of pUC18/RBS and subsequent transformation of this plasmid into Top 10 One Shot competent cells allowed low-level over-expression of the mutant gene. Sub-cloning the gene into the over-expression vector pET16b was carried out as for wild type (see section 3.1.1). Using a similar procedure and a megaprimer of 750bp, a second active site residue, histidine 133, was mutated to a phenylalanine residue.

3.6 Isolation and purification of mutants

The K236A and H133F mutants were over-expressed and purified according to the original protocol developed for wild type AONS. The initial cell pellet was the creamy beige colour of harvested cells and not the yellow which can be seen on over-expression of wild type or His_6-tagged AONS. The cell free extract containing the mutant enzymes displayed a hint of yellow, but the protein solution did not turn a deep yellow until after fractionation with 35% ammonium sulphate. Due to the less basic nature of the mutant enzymes, and thus reduced hydrophobicity, they eluted from the first chromatographic column with 15% ammonium sulphate. This contrasts to the behaviour of the wild type enzyme, which elutes in the latter stages of the gradient at 3% ammonium sulphate. The mutant proteins eluted from the anion exchange chromatographic column at 180mM NaCl, in contrast to the wild type which elutes at 260mM NaCl. It seemed unlikely, therefore, that the characterisation results of mutant enzymes purified in this manner could be affected by any residual wild type enzyme activity.

Table 3.3

Purification table of **K236A** mutant *E.coli* AONS. Protein concentration was measured using the method of Bradford and specific activity was measured in a coupled assay using 50mM L-alanine and 200μM pimeloyl-CoA. 1U AONS represents the transformation of 1μmol pimeloyl-CoA by 1mg enzyme per minute at 30°C

Purification Step	Volume (ml)	Protein (mg/ml)	Specific activity (U)	Yield (%)	Purification fold
Crude extract	60	49	--	--	--
35% ammonium sulphate	62	39	0.01	82	1
65% ammonium sulphate	35	39	0.013	46	1.3
Hydrophobic interaction	150	3.3	0.017	17	1.7
Anion exchange	50	2.4	0.035	4	3.5

Yield is approximately 15mg/l of K236A of ≥ 95% purity as estimated by SDS PAGE. The specific activity of the purified mutant protein was approximately one tenth of that observed for wild type AONS.

Yield was approximately 11mg/ml and the purification factor was similar to that obtained for the wild type enzyme. Protein purity was 90% as judged by SDS PAGE and specific activity was one fifth of that observed for the wild type enzyme.

On the basis of visible spectroscopy, it appeared that a small amount of PLP cofactor remained bound to the K236A mutant throughout the purification and freezing process. However, the H133F mutant lost all of its PLP cofactor during anion exchange chromatography and subsequent concentration of the enzyme.

Table 3.4

Purification table of **H133F** mutant *E.coli* AONS from expression in an *E.coli* host. Protein concentration was measured using the method of Bradford and specific activity was measured in a coupled assay using 50mM L-alanine and 200μM pimeloyl-CoA. 1U AONS represents the transformation of 1μmol pimeloyl-CoA per minute at 30°C

Purification Step	Volume (ml)	Protein (mg/ml)	Specific activity (U/mg)	Total activity (U)	Yield (%)	Purification fold
Crude extract	45	47	--	--	--	--
35% ammonium sulphate	45	35.5	0.012	19.2	100	1
65% ammonium sulphate	25	13	0.047	15.3	80	3.9
Hydrophobic interaction	100	1.7	0.06	10.2	53	5
Anion exchange	45	2	0.075	6.75	35	6.25

3.7 Physical Characterisation of the K236A and H133F mutants

Attempts to dialyse PLP into both mutant proteins were successful, and a maximum could be seen at 425nm for K236A. Upon washing of the protein with potassium phosphate buffer, pH 7.5 and no additional PLP, the aldimine linkage was lost in the H133F protein, suggesting that the imine bond is not stable in the absence of the basic histidine residue.

The absorption coefficient of the PLP bound form of K236A was measured at ε=1856 l mol^{-1} cm^{-1}, a figure four fold lower than the corresponding coefficient for wild type AONS (see section 5.2). This suggests that cofactor binding has been considerably reduced by the removal of the lysine residue, but may also indicate that the cofactor may be held in the active site by other residues.

An approximate size was estimated for the mutant proteins by SDS PAGE analysis using wild type AONS as a reference and was necessary during the purification process. The mass of the K236A and H133F proteins was identified with ESI mass spectrometry (table 3.6).

Table 3.5

ESI Mass spectroscopy of K236A and H133F mutant AONS. The protein was separated from salts in the buffer by HPLC purification with H_2O/Acetonitrile containing 0.01% Trifluoroacetic acid.

Mutant AONS	Predicted (Da)	Measured (Da)
K236A	41,407.15	41,413.2
H133F	41,474.3	41,478.6

3.8 UV/visible Characterisation of pyridoxal-5'-phosphate

As has been noted above, the two AONS mutants lose much of their ability to bind the cofactor PLP. For this reason, UV/visible spectroscopy was carried out on a 100μM PLP solution to establish the nature of binding by the free molecule. The results of this characterisation were then used to assess whether the changes in absorbance observed on the visible spectra of the mutant enzymes is due to the protein active site residues, or behaviour of the free PLP aldehyde.

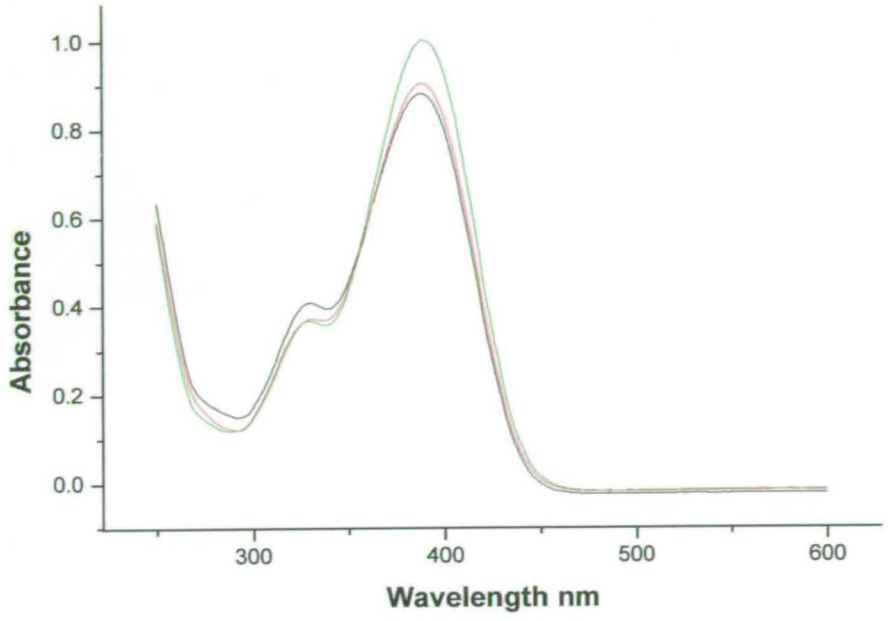

Figure 3.8.1

Titration of 100μM PLP with potassium phosphate The PLP aldehyde was incubated for 20 minutes at 30°C and pH 7.5. Ionic strengths: 5mM potassium phosphate (black); 200mM (red); 1M (green)

The spectrum of PLP displays characteristic peaks of the aldehyde at 390nmn and the protonated form of this bond at $C_{4'}$ at 330nm (129). As the ionic concentration of the potassium phosphate buffer increases, the absorbance maxima of the PLP solution can be seen to change. The absorbance at 390nm increases with increasing ionic strength, with a corresponding decrease in absorbance at 330nm. An isosbestic point can be seen at 360nm, indicating an equivalence point between the protonated and deprotonated forms of the aldehyde.

A solution containing free PLP was also titrated against L-alanine in order to establish the behaviour of the free molecule with the first substrate of the AONS catalysed reaction. The salt concentration was held constant at 160mM for each titration. The imine bond formed between PLP and L-alanine is visible as an absorbance at wavelength 425nm. The absorbance maximum at 340nm corresponds to the form of the molecule protonated at C_4· and decreases as the imine bond is formed. The dissociation constant (K_d) of L-alanine from the free cofactor molecule is 9mM. This is a ten-fold increase on the dissociation constant measured in the native enzyme (36), indicating that the active site presents a more favourable environment for formation of the external aldimine than does the free molecule aldehyde.

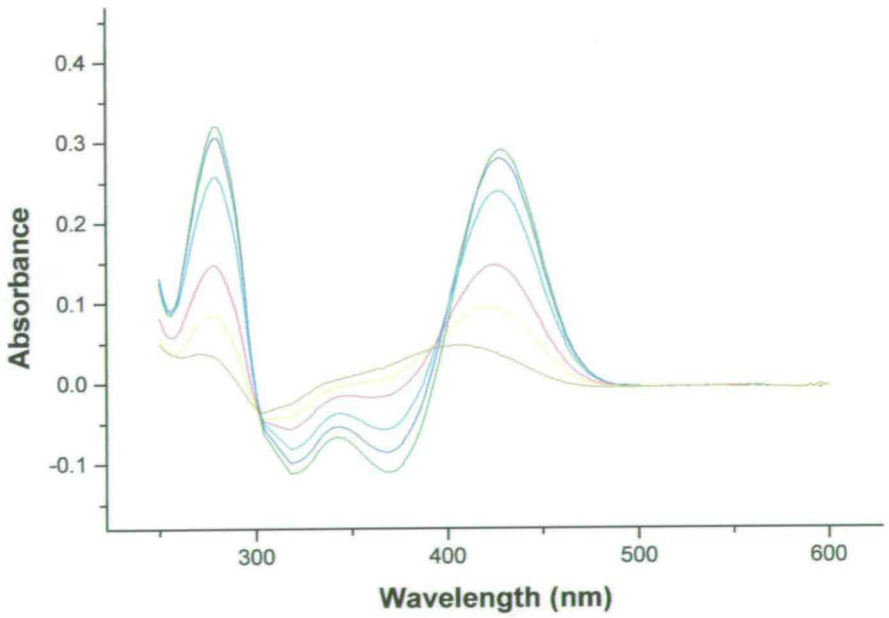

Figure 3.8.2

Titration of 100μM PLP against L-alanine. The cofactor molecule was incubated with the amino acid for 20 minutes at 30°C and pH 7.5. L-alanine concentrations 100mM (green); 50mM (blue); 25mM (cyan); 10mM (pink); 5mM (yellow); 1mM (brown)

Finally, in order to establish the characteristic spectra of PLP under various acidic or basic conditions, the free molecule was titrated against pH.

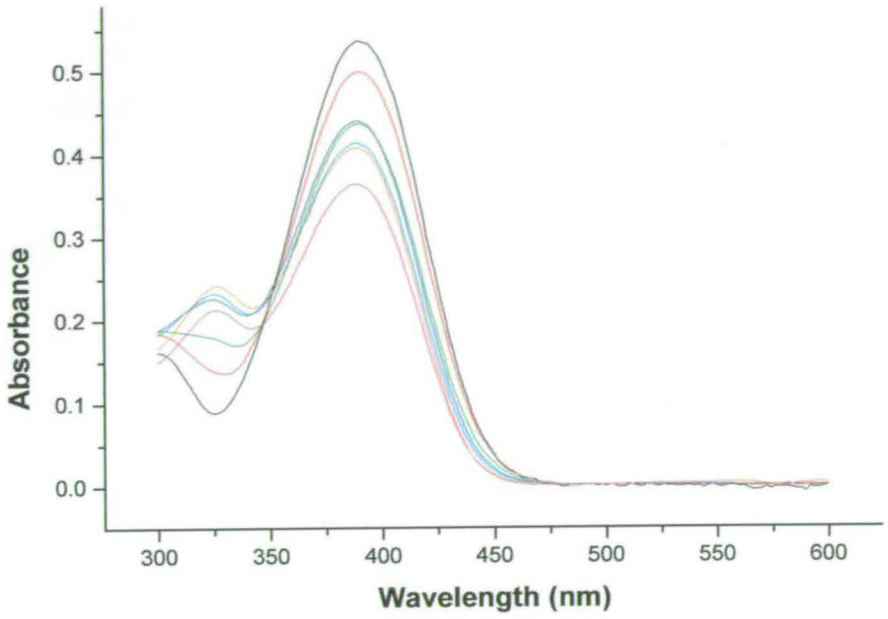

Figure 3.8.3

pH titration of 100μM PLP at 30°C. Free PLP was incubated in 1M HEPES at the relevant pH value for 30 minutes and the spectrum recorded. pH 9 (black); pH 8.4 (red); pH 8.1 (green), pH 7.8 (blue); pH 7.6 (cyan); pH 7.3 (orange); pH 6.9 (pink)

The absorbance of the aldehyde bond at 390nm is maximised as the solution becomes more basic. There is also a decrease in absorbance at 330nm in this environment. As the solution changes slowly towards a more acidic pH value, a decrease in absorbance at 390nm can be observed. There is, however, no definite trend detected at 330nm. These results suggest that the basic environment allows for maximum aldehyde concentration at $C_{4'}$ and an alteration in these conditions slowly reduces this band as electrophilic attack

by the solvent occurs at this position. This spectral change is not observed in the native enzyme, suggesting a constant pH value is retained in the active site.

3.9 UV/visible Characterisation of K236A and H133F mutants

All UV/visible spectroscopy characterisations of mutant and wild type proteins were carried out at a maximum salt concentration of 200mM.

3.9.1 Absorbance spectra of K236A AONS

Prior to spectroscopic analysis, the protein was dialysed against 20mM potassium phosphate buffer, pH 7.5 containing 100μM PLP and the excess PLP was subsequently removed by exhaustive washing with 20mM potassium phosphate buffer. Cofactor absorption peaks are visible at 330nm and 425nm respectively for the holoenzyme. On addition of the first substrate, there is a shift in the chromophore absorbance to the slightly shorter wavelength of 420nm, and the peak at 330nm disappears entirely. Thus, the UV/visible spectrum of the K236A AONS mutant shares all the characteristic peaks seen in the spectrum of wild type AONS.

The visibility of a peak at 425nm in K236A suggests the presence of an imine bond within the active site. Since the free PLP molecule aldehyde has an absorbance at 390nm, an absorbance at a longer wavelength suggests either a possible condensation reaction with another basic residue within the active site as the lysine is no longer available for such binding and alanine lacks the amino group found as part of the lysine residue and thus cannot form an imine bond with PLP; or a shift caused by some other environmental factor.

The spectrum of the K236A-L-alanine bound form does not change on addition of up to 300μM pimeloyl-CoA and no intermediate at 486nm is seen.

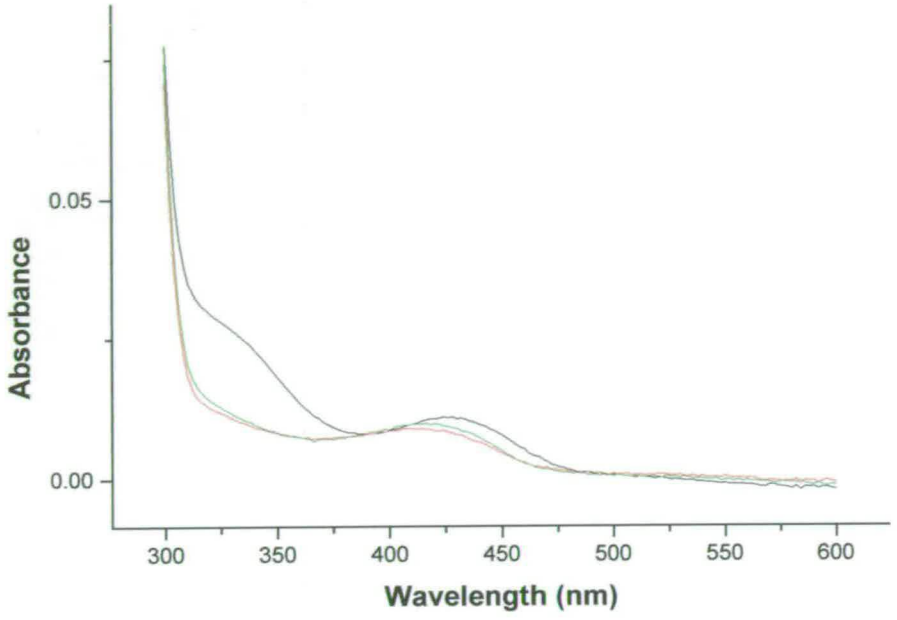

Figure 3.9.1

Absorbance spectra of 8μM K236A holoenzyme and on incubation with L-alanine at 30°C for 20 minutes. Spectra were acquired at 30°C and pH 7.5. K236A holoenzyme (black); in the presence of 1mM L-alanine (red); in the presence of 100mM L-alanine (green)

As has already been observed, the 330nm absorbance peak disappears from the K236A spectrum on addition of L-alanine. Titration of the mutant protein confirms this, as larger concentrations of the amino acid substrate do not affect this result and neither do they produce a change in the absorbance at 420nm, suggesting that this absorbance may not be due to the external aldimine linkage, but rather a shift in alignment of the linkage observed in the absence of L-alanine.

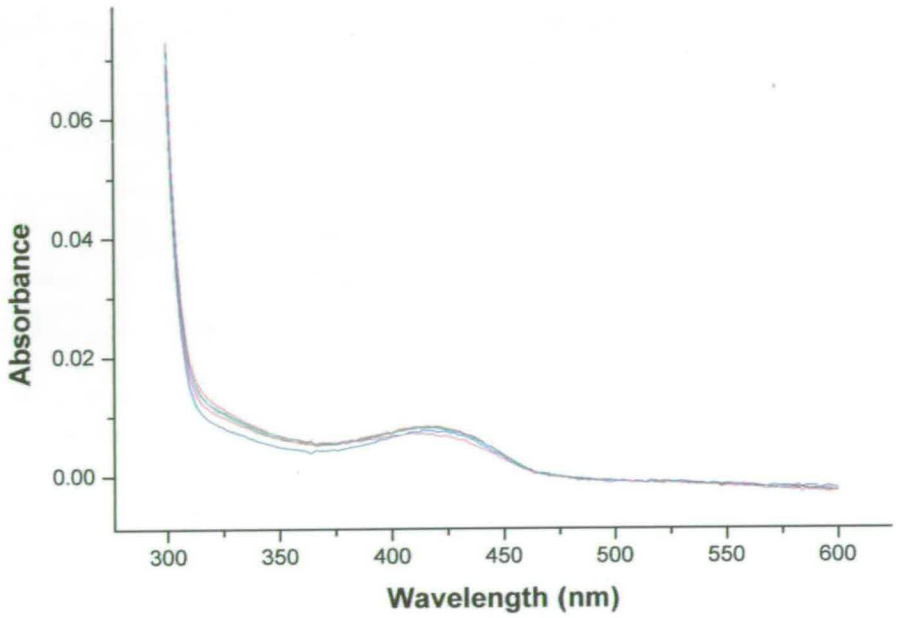

Figure 3.9.2

Titration of 10μM K236A with L-alanine at 30°C and pH 7.5. The protein was incubated for 20 minutes at 30°C. L-alanine concentrations: 200mM (red); 100mM (green); 50mM (blue); 10mM (cyan); 1mM (pink)

The protein was titrated with concentrations of L-alanine up to 1M without any noticeable changes in the spectrum. Thus it was impossible to calculate a dissociation constant for L-alanine-PLP complex of this mutant and the first substrate, but negative results would suggest the absence of the lysine residue renders the active site incapable of binding of L-alanine alone. However, identical spectra were obtained on repetition of this titration in the presence of 200μM pimeloyl-CoA, suggesting that addition of the second substrate into the active site does not alter the configuration of the bound cofactor.

3.9.2 Absorbance spectra of H133F AONS

The H133F mutant protein was prepared in the same way as K236A AONS. The UV/visible spectrum of the washed protein displays no absorbance maxima between 330nm - 430nm, suggesting that there is no imine binding of the cofactor within the active site. The absence of a maximum at 390nm also indicates that the aldehyde form of the cofactor is not present.

In order to assess the changes on addition of substrates, 2μM PLP was added to the 10μM protein solution.

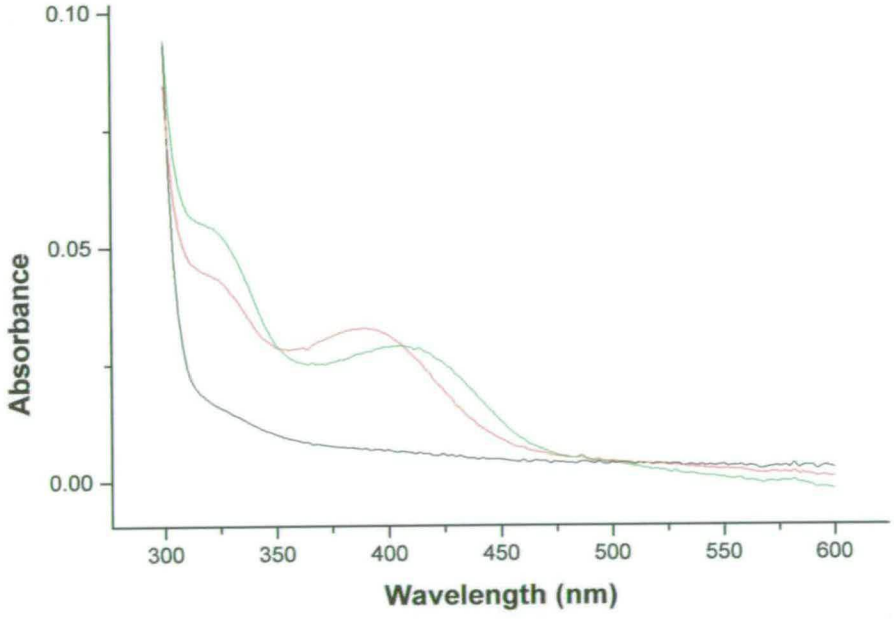

Figure 3.9.3

Absorbance spectra of 10μM H133F apoenzyme and on incubation with L-alanine at 30°C for 20 minutes. Spectra were acquired at 30°C and pH 7.5. H133F apoenzyme (black); in the presence of 2μM PLP and 1mM L-alanine (red); in the presence of 2μM PLP and 100mM L-alanine (green)

On addition of 2μM PLP, a characteristic peak at 390nm was visible. This did not shift on addition of L-alanine concentrations below 8mM, suggesting dissociation of the amino acid substrate from PLP was not affected by the mutated enzyme. At elevated L-alanine concentrations, there was a red shift in the absorption peak to a more characteristic 420nm wavelength. Addition of pimeloyl-CoA did not affect the spectrum at concentrations of up to 300μM and, as with the K236A mutant, no peak was visible at 486nm.

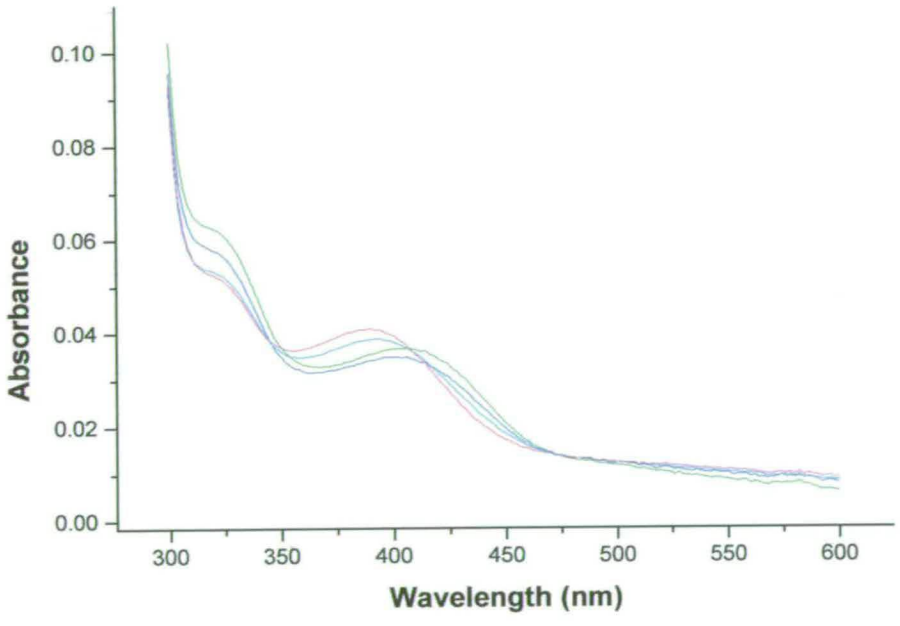

Figure 3.9.4

Titration of 10μM H133F with L-alanine at 30°C and pH 7.5. The protein was incubated for 20 minutes at 30°C with 2μM PLP and various L-alanine concentrations: 100mM (red); 50mM (green); 10mM (blue); 5mM (cyan); 1mM (pink)

The absorbance peak shifts from 390nm to 420nm on addition of L-alanine concentrations exceeding 10mM, but subsequent titration increases absorbance at the longer wavelength. The peak at 330nm is visible at all concentrations of L-alanine, but is only enhanced on addition of larger quantities of the amino acid. At lower concentrations, results would suggest titration of the PLP cofactor as if it were a free molecule. However, enhanced concentration of the substrate seems to induce a change in the active site, and subsequently the external aldimine bond.

3.9.3 pH studies on K236A and H133F AONS

Studies into the pH of the active site of the mutants proved inconclusive as both proteins were unstable in low salt buffers of 50mM HEPES; 50mM CAPS; 50mM CHAPS and 10mM Bis-Tris-Propane. This may suggest that a metal ion may be required for mutant protein stability, however, addition of monovalent cations (Na^+, K^+) as sodium and potassium chloride salts, did not reverse this instability, even at very low concentrations.

3.10 Steady State Kinetic Characterisation of K236A and H133F mutants

The coupled assay was used to test the activity of PLP alone and indicated that the cofactor was unable to catalyse the thioester bond cleavage in the absence of the enzyme.

3.10.1 Steady state characterisation of K236A AONS

The Michaelis constants for the steady state kinetics of K236A were calculated for pimeloyl-CoA using the coupled assay in the presence of 200mM L-alanine. Constants for the amino acid substrate could not

be obtained as the enzyme displayed no significant difference in activity at any concentration, suggesting an alteration in binding of L-alanine. In fact, the enzyme displayed residual activity in the absence of L-alanine suggesting it may be possible that the K236A-L-alanine complex is acting as a hydrolase on the pimeloyl-CoA substrate.

Table 3.6

Steady state kinetic constants for K236A AONS *E.coli.* Constants were measured at 30°C and pH 7.5 and fitted to a Michaelis-Menton saturation curve.

		pimeloyl-CoA		L-alanine	
AONS	k_{cat} (s^{-1})	K_m (μM)	k_{cat}/K_m ($s^{-1}M^{-1}$)	K_m (mM)	k_{cat}/K_m ($s^{-1}M^{-1}$)
wild type	0.06(0.01)	25(2)	2400(430)	0.50(0.04)	120(21)
K236A	0.001($7E^{-5}$)	45(11)	22(3)	--	--

There is a significant decrease in the turnover of the lysine mutant enzyme. This sixty-fold reduction in catalytic activity suggests that cleavage of the thioester bond of the pimeloyl-CoA substrate does not occur in an efficient manner. Binding of this substrate is not significantly different to wild type binding of pimeloyl-CoA, suggesting that access for this molecule is unhindered. The inability to obtain constants for the binding of L-alanine may indicate inaccurate or inefficient binding of the substrate with the cofactor.

3.10.2 Steady state characterisation of H133F AONS

The PLP loaded form of the H133F AONS mutant was prepared by dialysing the protein for one hour in 20mM potassium phosphate buffer, pH 7.5 containing 100μM PLP. Assays were carried out using the coupled assay protocol developed for wild type *E.coli* AONS.

Table 3.7

Steady state kinetic constants for H133F AONS *E.coli*. Constants were measured at 30°C and pH 7.5 and fitted to a Michaelis-Menton saturation curve.

		pimeloyl-CoA		L-alanine	
AONS	k_{cat} (s^{-1})	K_m (μM)	k_{cat}/K_m ($s^{-1}M^{-1}$)	K_m (mM)	k_{cat}/K_m ($s^{-1}M^{-1}$)
wild type	0.06(0.01)	25(2)	2400(430)	0.50(0.04)	120(21)
H133F	0.001($6E^{-5}$)	46(3)	22(1)	15(3)	0.06(0.009)

There is a clear reduction in catalytic binding and efficiency observed in the H133F mutant. The turnover of pimeloyl-CoA, as evinced from the k_{cat} values, suggests that activity of the enzyme has been reduced significantly by sixty-fold. This reduction results from a vast, two thousand-fold decrease in binding specificity of the enzyme for L-alanine. Binding efficiency of the amino acid is also much reduced, a thirty-fold decrease, which compares with a K_m constant for pimeloyl-CoA barely twice that of the wild type enzyme, suggesting that binding of the second substrate remains relatively unaffected by the mutation. This results in a binding specificity for the second substrate of only one hundred fold lower than observed for the wild type enzyme.

Discussion

A His_6-tagged fusion of *E.coli* AONS was constructed and over-expressed. It displays similar activity to the *wt* enzyme but the absence of a visible quinonoid peak on incubation of the external substrate aldimine complex with pimeloyl-CoA suggests differences in stability of this intermediate. This difference in quinonoid formation is also reflected by the decrease in catalytic activity of the His_6-tagged protein. The lower specificity seen in His_6-tagged AONS for its substrates may be a result of decreased access to the active site of the enzyme caused by the polyhistidine adduct at the N-terminal of the protein.

Structural studies (37) show that the N-terminal region is characterised by an α-helix motif in close proximity to the C-terminus responsible for closure of the active site on addition of the product, AON (36), and possibly on addition of the substrates (37) as has been noted for several other enzymes (see reviews 107; 111 and references therein). The presence of a long polyhistidine tag in this region may sterically hinder the substrates as they enter the active site, thus reducing binding efficiency of the enzyme. The absence of a pH dependency within the active site of the His_6-tagged enzyme suggests that closure may well occur on binding of the substrates.

While the polyhistidine fusion was chosen to enable simple and accurate purification of the mutant proteins without contamination of the wild type enzyme, the results of kinetic studies make it obvious that this strategy had to be discarded.

Both mutants involved replacing a basic residue with a uncharged amino acid and this altered the pI of the enzyme. This was evident on purification of the mutant proteins by FPLC. The mutant enzymes elute from the initial hydrophobic interaction columns at a significant fraction interval from where the wild

type enzyme is seen to elute. This is repeated for the anion exchange column, thus ensuring that any residual wild type enzyme is not included in the final protein solution.

Whilst characterisation of the PLP spectra has already been described (129) it was necessary in this study to show the activity of the free PLP molecule under the conditions required for assay of the mutant AONS proteins. These were especially important when considering the activity of the histidine mutant. The relative lack of effect of the ionic concentration at 200mM and below indicated that the cofactor was not altered at different concentrations of buffer. Although the lower concentration favours a possible protonated aldehyde form, seen at 340nm, there is no evidence to suggest that this alters the species bound within the active site. There is also no evidence to indicate that the species in the active site are pH dependent, unlike the free PLP molecule. This is further evidence to suggest that there is closure of the protein molecule to the surrounding solvent.

There is a ten-fold increase in L-alanine dissociation constant for the free PLP imine compared to that found in the wild type *E.coli* AONS enzyme. This is a significant difference, and indicates that the residues involved in the active site of the enzyme contribute to lowering this constant and thus enhancing catalytic activity. This is an example of the Circe effect described by Cordes and Jencks (110) which suggests that the intrinsic affinity of an enzyme for its substrates can be increased in comparison to the free molecule. The lysine mutant of aspartate aminotransferase is a good example of this (130). K258A is active on addition of primary amines and lowers the activation energy of external aldimine formation by reducing the binding energy of the cofactor and the amino acid substrate.

There is much evidence to suggest that the lysine residue involved in cofactor binding is critical for catalytic activity in PLP enzymes as it is involved in cofactor binding and general base catalysis of C_α proton abstraction (48); (50); (130-134). Mutation of this residue to alanine results in an enzyme with little or no activity. The lysine to alanine mutation of the corresponding residue in *E.coli* AONS results

in a protein with reduced activity. Turnover is reduced sixty-fold on comparison with wild type AONS and binding of substrates is inefficient. On purification, the enzyme appears to display the internal cofactor aldimine, although the lysine residue is absent. This could be a result of binding of the cofactor to another basic residue within the active site. Alternatively, PLP may be bound to an amino group taken up by the protein during the purification process in a similar manner to that observed for O-acetylserine sulfhydrylase from *Salmonella typhimurium* (135). Structural studies have shown that the cofactor is covalently bound to a methionine residue in the active site and stabilised by an "asparagine loop" which moves 7Å to make this bond. This loop corresponds to the "glycine rich loop" (45) observed in the ALAS sequence and alignment of the asparagine loop with the **GIGSGGSG** region in *E.coli* AONS suggests it is the same motif. The cofactor within this enzyme tilts so that the $C_{4'}$ atom is directed towards the entrance to the active site. A similar configuration in the K236A *E.coli* AONS mutant may suggest an explanation for the apparent absence of an absorbance maximum corresponding to a quinonoid intermediate. Observed catalytic activity, however, suggests that such an intermediate must be created in order to cleave the thioester bond of the pimeloyl-CoA. The formation of this intermediate therefore indicates that a proton is abstracted from C_{α}. Residual activity of this enzyme on the absence of L-alanine suggests confirmation of this theory. The absence of a significant change in K_d of L-alanine from this mutant indicates that concentration is not necessarily relevant to L-alanine binding within the active site. The disappearance of the peak at 330nm on addition of this substrate, however, suggests that it becomes chemically involved in the interaction already present in the active site of the protein, and its addition results in a thermodynamic unfavourability for the protonated form of an imine bond.

Studies into the structural conformation of murine cytoplasmic serine hydroxymethyltransferase have already shown intermediate states in the chemical pathway of its catalysis (136). The complexity of the AONS mechanism resulting from the K236A mutant suggest that such studies would be helpful to understanding the function of this protein.

Although mutation of the lysine residue seems to have a profound effect on the chemistry involved at the active site of AONS, mutation of the H133 residue has a far more dramatic effect on the binding of the PLP cofactor. A substitution of this basic residue for a non-polar residue results in such weak binding of the cofactor, that the enzyme is no longer able to retain the cofactor within its active site. Spectral analysis of the enzyme on addition of PLP indicates that the cofactor is present in the aldehyde form, suggesting that misalignment of PLP results in a loss of ability of the lysine residue to covalently bind to the cofactor.

It has already been noted that the H133 residue swings through 180° on addition of PLP in order to lie in parallel with the pyridine ring of the cofactor (37). The loss of positive charge on this residue may inhibit this realignment and subsequently sterically hinder correct configuration of the cofactor for formation of the aldimine linkage. Higher concentrations of L-alanine restore external aldimine formation, suggesting that PLP acts in a similar manner to the free molecule. The observation of kinetic activity indicates abstraction of the C_α proton and subsequent nucleophilic attack of the pimeloyl-CoA thioester bond, leading to the release of free CoASH.

There have been few studies into the effect of mutation of this conserved histidine residue. Alteration of this base in sheep liver cytosolic serine hydroxymethyltransferase (137) resulted in an enzyme with very little bound PLP. The H167R mutant of *E.coli* glutamate decarboxylase, shows a tighter binding of PLP (138). However, an absence of PLP binding was noted for this enzyme on mutation of the residue corresponding to the H207 residue in *E.coli*, suggesting cofactor binding may occur in a different manner in this enzyme.

Observation of similar activity for both mutants suggests that catalytic efficiency is reduced to the same degree on alteration of either residue and indicates that other residues in the active site are capable of a certain amount of compensation of function. Specificity for the second substrate is affected the least by

these mutations and although data indicates release of CoASH, further steps in the catalysis reaction cannot be monitored and thus it is possible that full catalysis may cease at a later stage. Results gained from observation of the activity of the histidine mutant would suggest that remote hydrogen bonding is necessary to anchor the PLP cofactor, and elimination of the lysine residue may inactivate the enzyme.

A section of this work is incorporated into the publication that forms appendix II. Permission to include this paper was granted from the relevant authors.

Chapter 4
Introduction to Thermophiles

4.1 Extremophiles

In the last few decades, microorganisms have been isolated from extreme locations, which were once thought to be incapable of sustaining life. These so-called extremophiles were initially assigned to a separate bacterial kingdom, the Archaebacteria. More recently, however, Eubacteria native to extreme environments have been isolated. Organsims found in such surroundings are generally classified into six groups as shown in table 4.1.

Table 4.1

Subgroup classification of extremophiles identified to date. (Adapted from 139)

Extremophile	Location	Optimum growth
Barophiles	Deep sea vents	High pressures
Halophiles	Salt lakes	High salt concentrations
Thermophiles	Geothermal locations	Temperatures above 50°C
Psycrophiles	Arctic waters	Temperatures below 0°C
Acidophiles	Acidic, sulphurous springs	Acidic conditions
Alkalophiles	Alkaline lakes	Alkaline conditions

Extremophiles are chemolithoautotrophs and utilize inorganic redox reactions to convert carbon and nitrogen compounds in their environment into energy sources. It is now widely accepted that life on earth was initiated in such hostile environments by these organisms (140).

The protein catalysts of extremophiles are unique in that they are able to withstand the various pressures of their environment, and thus the term "extremozymes" has been coined to define them.

4.1.1 Thermophiles

The largest class of extremophiles, containing to date twenty-seven genera of Archaea and three Eubacterial genera (*Thermotoga*, *Hydrogenobacter* and *Aquifex*), are thermophiles. Thermophiles grow at an optimal temperature above 50°C, although some of these organisms belong to a thermophilic subgroup of hyperthermophiles (141), where growth conditions of these latter organisms are generally between 80-106°C. The most heat stable of all organisms found to date is *Pyrolobus fumarii* which grows optimally at 113°C (142).

The universal phylogenetic tree separates the three main kingdoms of Archaea, Bacteria and Eukarya. Located about the root of the stem on the bacterial branch are the three hyperthermophilic genera *Thermatoga* (optimal growth temperature: 95°C), *Hydrogenobacter* (optimal growth temperature 90°C) and *Aquifex* (optimal growth temperature: 90°C) (fig 4.1.1). Stetter (143) suggests that the deeper along the branch the hyperthermophile lies, the hotter their optimum growth environment.

The lateral transfer of genes from Archaea to Bacteria has been suggested by Nelson on the basis of detailed investigation of the genome from *Thermotoga maritima*, a hyperthermophilic bacterium isolated from heated marine sediment from Vulcano, Italy (144). In *T.maritima*, 81 archeal like genes are clustered in 15 regions throughout the genome and 24% of the genome displays genes similar to archeal genes. A further 5% of the genes have analogues only in other thermophiles. Brown & Doolittle (145) also suggest this transfer on comparison of phylogenetic relationships.

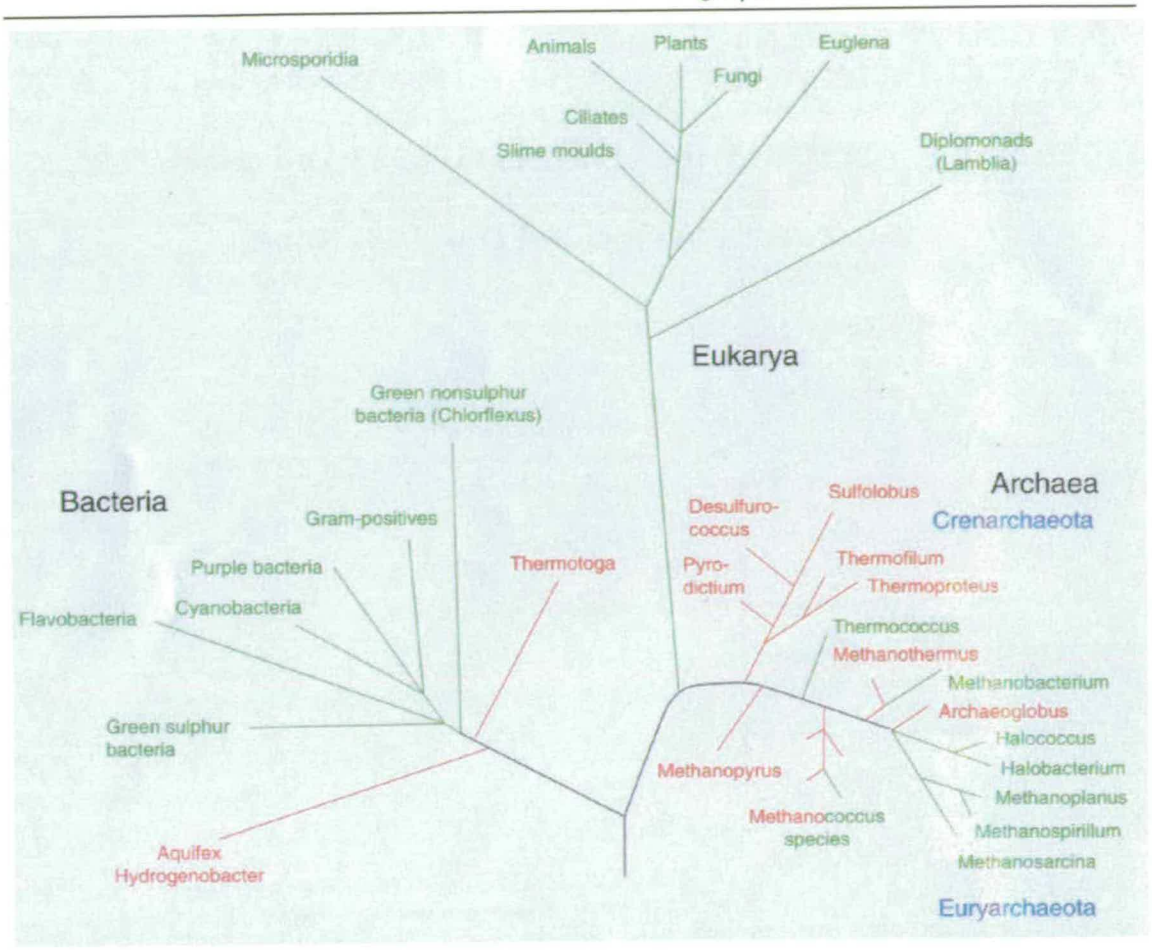

Figure 4.1.1

The universal phylogenetic tree of life. (Taken from 140).

To date, the majority of hyperthermophiles have been isolated from thermal vents at Yellowstone National Park, USA (146), which claims to house 80% of the world's geysers and 60% of its geothermal features. One organism, *Thermophilus aquaticus*, was isolated from Yellowstone in 1965. The purification of its DNA polymerase has proved catalytic in the progress of biotechnology. *T.aquaticus* DNA polymerase (Taq) is now the major enzyme used in the Polymerase Chain Reaction (PCR). Other extremozymes have made their way into industrial processes and many biotechnology companies are furthering this trend, over-expressing extremophilic proteins in *E.coli* or *Bacillus sp.* (147).

4.2 Protein Thermostabilty

Cell components of thermostable organisms must be able to withstand high temperatures, and research has shown that membranes of thermophiles are composed of novel ether lipids, dissimilar to the ester lipids common in mesophilic Eubacteria. A unique DNA type I topoisomerase has also been isolated from thermophiles (148). Reverse gyrase causes positive supertwists in the nucleotide molecule which are further stablised in Archaea by histones (149), similar to a feature mechanism utilised in eukaryotes. The role of heat shock proteins in thermophiles is still at an early stage of investigation (143).

Protein thermostability cannot be attributed to any single modification and it is not obvious from the secondary sequence how this is achieved. Comparison studies of thermophilic and mesophilic enzymes, however, has suggested possible mechanisms of heat stability (140) (150-153).

4.2.1 Amino acid composition

Hyperthermostable proteins are composed of the same 20 amino acids found in the composition of mesophilic and less thermostable proteins. At elevated temperatures, however, certain residues are more heat labile than others, and cysteine, asparagine and glutamine have the shortest half lives (151) as they tend to undergo deamidation or oxidation. It is therefore not suprising that there is a general decrease in the relative percentages of these amino acids within the primary structure of proteins from hyperthermophiles, which show an increase in percentage of the more robust, charged residues such as aspartate and glutamate.

Tighter amino acid packing is a feature of some hyperthermophilic proteins structures (152) (154-156). Higher levels of isoleucine and alanine have been suggested to allow this within the protein molecule (157). An increase in proline residues has also been suggested (158) to enhance loop

stability. This is demonstrated particularly well in thermostable aspartate aminotransferase (159) which displays an elevated proline content.

4.2.2 Hydrophobic packing

An efficiently packed hydrophobic core is a feature of most globular proteins, although this feature is generally observed in enzymes from organisms growing below 100°C (140) (160-162). Hydrophobic interactions are found at the subunit interface of glutamate dehydrogenase from *T.maritima* (163) although the same enzyme from *P.furiosus* (164) displays an intricate ion-pair network between subunits. Privalov & Gill (165) calculated Gibbs free energy values for hydrophobic interactions, but their results proved inconclusive, and it remains unclear whether such interactions are weakened at elevated temperatures.

4.2.3 Ionic Networks

Use of ion-pair networking within the macromolecule is a common strategy for stabilising heat stable proteins. Perutz &Raidt in 1975 (166) first proposed this on the basis of ferredoxin and haemoglobin studies, and an increase in charged residues is seen in many primary sequences of proteins from hyperthermophiles. Ionic interactions are more stable than the hydrophobic variety, and are not disrupted by alterations to the structure of water, which is compromised at higher temperatures. They are generally found on the surface, or solvent exposed parts of the molecule (140).

Ion-pair networks consisting of up to 18 residues (163) have been the most commonly observed difference between mesophilic and thermophilic protein structures. Comparisons of citrate synthase (154), glutamate dehydrogenase (163) and xylanase (156) from both thermophilic and mesophilic organisms has identified an increase in ion-pair networking within the heat stable molecules. The β-glycosidase from *S.solfataricus* (167) also displays an increase in these networks. Studies into other

proteins, however, have suggested that it is the position of certain bonds within the network, and not the network itself that is responsible for increased stability. Verification of this in both archea and bacteria is suggested by the results of mutagenesis studies of glutamate dehydrogenase from *Pyrococcus furiosus* (168), D-glyceraldehyde-3-phosphate dehydrogenase (169) and indole-3-glycerol phosphate synthase (170) both from *T. maritima.*

4.2.4 Subunit Association

Denaturing of the enzymes proceeds with unravelling of the monomeric subunit, thus proteins that function as oligomers must employ a strategy to retain the integrity of conformation. Ionic networks are increased at subunit interfaces and cavities are reduced in number in many of the proteins studied (163-164) (171). β-glycosidase displays an unusually large number of solvent molecules buried in hydrophilic cavities at the core of the protein (167). It has been suggested that these cavities aid the thermostability of the protein by resistance rather than rigidity. In the case of citrate synthase from *P.furiosus*, the carboxy terminus of one monomer interacts with the surface of the other monomer (140). This phenomenon is not found in the mesophilic enzyme from pig (154). The indole-3-glycerol phosphate dehydrogenase form *Sulfolobus solfactaricus* (172) is a monomer at 90°C. An increase in hydrophobic interactions within the molecule, coupled with an increase in helix capping have been observed to contribute to the stability of this protein. The enzymic structure is a TIM barrel and unlike its mesophilic *E.coli* counterpart which has one helix, the *S. solfactaricus* enzyme has two helices before the first β-strand. Both are bound by ionic interactions.

4.2.5 Structural Changes

Some proteins are observed to have minor structural changes compared to their mesophilic counterparts. The most common alteration is a reduction in the size of loops, resulting in closer packing of the protein (154) (171). Observations have also identified proteins with a reduced N-terminal helix (154) (164), although mesophilic citrate synthase enzymes also display a smaller N-terminal helix region, possibly suggesting that this may be a result of phylogenetic diversity (160) and not necessarily thermostability. Other enzymes may retain their N-terminal helix, but protect it from degradation by capping it with an acidic amino acid residue (see section 4.2.4).

In order to find a general strategy for protein thermostability, Szilágy & Závodszky (153) compared the 3D structures of 64 mesophilic and 29 thermophilic proteins, representing 25 different families. They discovered only one key element, common to all thermophiles, an increase in ion pairs. Other strategies were observed as trends, and the number of hydrogen bonds and buried cavities did not necessarily increase with increasing temperature. These findings conflict, however, with research conducted by Vogt *et al* (173), which suggests that hydrogen bonding may be responsible for the general stability of thermophilic proteins. Szilágy & Závodszky also observed that different protein families were also observed to employ different strategies for heat stability.

4.3 Activity in thermophiles

It has already been established that enzymes from hyperthermophiles are active at high temperatures, and indeed many show a denaturation half life of several hours at 100°C (142) (164) (174). There have, however, been far fewer kinetic characterisations of isolated thermostable enzymes to compare with their mesophilic counterparts. Sadly, many comparisons and conclusions have been made on the

basis of sequence homology rather than protein density. However, there are a few definitive studies which provide some data. In general, catalytic activity seems to increase with elevated temperatures. The activity of indole-3-glycerol phosphate synthase from *S.solfataricus* (172) is twenty-fold higher at 60°C than the rate observed at 25°C (170). This observation is reflected in the activity of indole-3-glycerol phosphate synthase from *T. maritima* which increases 3 fold on elevation of temperature from 25°C to 60°C. In contrast, the V_{max} values of citrate synthase are similar for the mesophilic enzyme in pig at 37°C (281±23); the thermophilic enzyme from *Thermoplasma acidophilum* at 60°C (100±14) and the hyperthermophilic enzyme of *P.furiosus* at 90°C (226±12) (154) (160) (175), suggesting there is a possible catalytic penalty to be paid for this enzyme.

4.4 Aims of this Project

The sequencing and subsequent annotation of the genome of *Aquifex aeolicus* (33) revealed the four conserved genes of the biotin biosynthetic pathway contained in this hyperthermophilic organism. In an attempt to further characterise the differences between mesophilic and hyperthermophilic enzymes, the *bio*F gene was cloned and the resulting protein AONS over-expressed.

Hyperthermophilic AONS from *A.aeolicus* is a 42,306 Da protein present in its active form as a dimer. The aim of this project was to obtain milligram quantities of AONS for characterisation by a number of chemical, biophysical and crystallisation techniques.

Chapter 5
Characterisation of AONS from *Aquifex aeolicus*

5.1 Isolation and Purification

The *A.aeolicus bio*F gene was successfully amplified from the *A.aeolicus* genomic DNA template by PCR using forward and reverse primers (see section 2.3.5). To facilitate cloning of the gene, the second amino acid codon was altered from the original serine encoding codon to a glycine in the forward primer, allowing incorporation of an *Nco*I site at the beginning of the gene. Initial cloning of the amplified fragment was achieved by ligation into a *Nco*I/*Bam*HI digest of pUC18. From this high copy number plasmid, designed to allow production of further quantities of the gene, the *bio*F fragment was excised at the *Nco*I/*Bam*HI sites at the 5' and 3' termini respectively and directionally sub-cloned into pET16b, an *E.coli* ampicillin resistant expression plasmid containing an IPTG inducible T7 promotor.

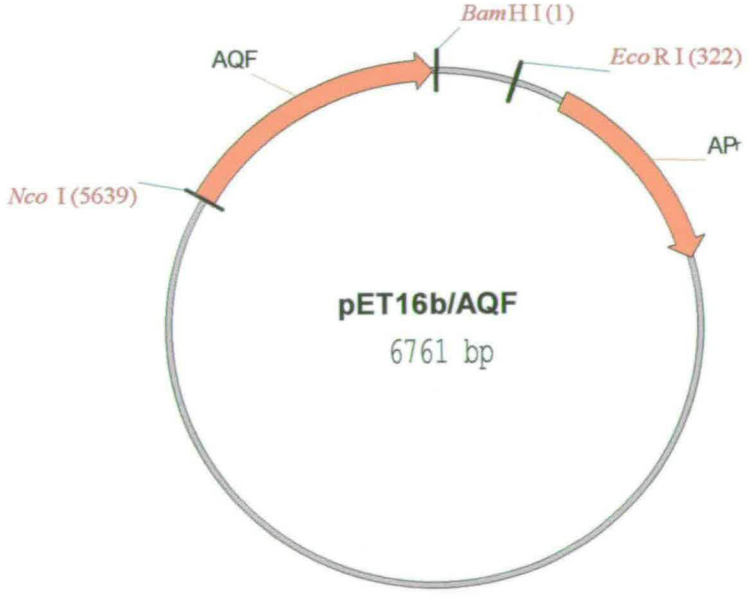

Figure 5.1.1

The initial clone of the *bio*F gene was sub-cloned into the ampicillin resistant expression vector pET16b using a *Nco*I/*Bam*HI digest of both plasmid and gene fragment. In pET16b, the gene is under the control of the powerful T7 IPTG-inducible promotor.

The pET16b/*bio*F plasmid was transformed into HMS174 (DE3) cells which were allowed to grow until approximate mid log phase, ($OD_{600} \approx 1$). Protein production was induced by addition of a final concentration of 1mM IPTG for three hours and cells were harvested (see section 2.2.2). Disruption of the cells removed cell debris and heat fractionation of the cell free extract resulted in precipitation of the majority of host *E.coli* proteins. An initial heat step fractionation was carried out at 60°C to allow precipitation of the most heat labile host proteins. After trials, a subsequent 80°C fractionation step was introduced to remove the more stable proteins from the extract. Heat fractionation was carried out in two stages to avoid a general precipitation of all proteins at the higher temperature, since initial studies indicated that a reduced yield of *A.aeolicus* AONS was obtained after only one temperature jump. Denaturing proteins in this manner also ensured that any AONS produced naturally by the *E.coli* host strain was removed from the solution as *E.coli* AONS does not survive temperatures greater than 60°C (36).

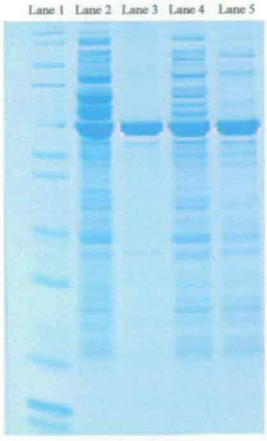

Figure 5.1.2

SDS PAGE gel (Invitrogen) of *A.aeolicus* AONS purification. Lane 1 - Standards; Lane 2 - Crude extract; Lane 3 - Anion exchange; Lane 4 - 60°C; Lane 5 - 80°C. Standards are: Myosin (200kDa); β galactosidase (116.3kDa); Phosphorylase b (97.4kDa); Bovine serum albumin (66.3kDa); Glutamic dehydrogenase (55.4kDa); Lactate dehydrogenase (36.5kDa); Carbonic anhydrase (31kDa); Trypsin inhibitor (21.5kDa); Lysozyme (14.4kDa); Aprotinin (6kDa); Insulin B chain (3.5kDa); Insulin A chain (2.5kDa)

The resulting heat treated fractions were passed down an anion exchange column and eluted using a linear gradient of 0-1M NaCl. Homogenous AONS was recovered at 260mM, the same salt concentration at which *E.coli* AONS is observed to elute, suggesting that both proteins have a similar affinity for the column and thus a similar ionic strength. This confirms the computational prediction of similar pI values for both proteins[4].

Table 5.1

Purification table of *A.aeolicus* AONS from expression in an *E.coli* host. Protein concentration was measured using the method of Bradford (120) and specific activities were measured in a coupled assay using 50mM L-alanine and 200μM pimeloyl-CoA. 1U AONS represents the transformation of 1μmol pimeloyl-CoA per minute at 30°C

Purification Step	Volume (ml)	Protein (mg/ml)	Specific activity (U/mg)	Total activity (U)	Yield (%)	Purification fold
Crude extract	40	75	--	--	--	--
60°C fraction	35	68	0.02	47.6	100	1
80°C fraction	33	39	0.03	38.6	81	1.5
Anion exchange	30	1.8	0.7	37.8	79	35

To ensure that the heat step did not result in modification of the enzyme, purification was also carried out using a protocol previously developed for *E.coli* AONS (36), involving ammonium sulphate fractionation followed by hydrophobic interaction and subsequent anion exchange chromatography. All purification steps were carried out at room temperature, as purification on ice or at 4°C resulted in denaturation of the *A.aeolicus* enzyme. There proved to be no noticeable difference in steady state kinetic activities or crystal

[4] Calculated values are 6.63 and 6.77 for the *E.coli* and *A.aeolicus* enzymes respectively.

growth between *A.aeolicus* protein purified by either method. As a consequence, the heat fractionation method was pursued, to allow faster and more efficient purification of the enzyme. This process yielded approximately 12mg/l protein of 95% purity as estimated by SDS PAGE. A typical preparation is summarised in table 3.1.

5.2 Physical Characterisation

5.2.1 Cofactor Binding

It was observed that dissociation of the PLP cofactor from *A.aeolicus* AONS during chromatography and prolonged dialysis was minimal. Freezing of the enzyme was not observed to disrupt the enzyme-PLP complex and the protein solution also remained yellow on thawing.

This contrasts to the behaviour of the *E.coli* enzyme, which loses most of its PLP during either freezing or dialysis. Initial observations of the UV/visible spectra of the AONS-PLP chromophore maxima indicated a wavelength of 430nm and it should be noted that this is slightly longer than the wavelength of 425nm displayed by the *E.coli* AONS chromophore. The absorbance coefficients of protein to internal cofactor aldimine complex were measured for both species of AONS by UV/visible spectrophotometry and they also show distinct differences. Measured $\varepsilon_{(\lambda=425nm)}$ for the native *E.coli* enzyme is 7,229 l mol^{-1} cm^{-1}, while $\varepsilon_{(\lambda=430nm)}$ for the *A.aeolicus* enzyme is 11,317 l mol^{-1} cm^{-1}. The higher value calculated for *A.aeolicus* AONS may indicate that there is increased cofactor binding for the PLP by the heat stable protein. However, the affinity of the proteins for their PLP cofactors could not be measured as size exclusion chromatography failed to separate the protein from the PLP molecule. Treatment of the enzyme with hydroxylamine reduced the amine bond and PLP could be removed. However, the enzyme was inactive.

5.2.2 Mass spectrometry

The mass of the native protein, measured using gel filtration against known standards indicated that the protein was isolated as a dimer.

Characterisation of *A.aeolicus* AONS by ESI mass spectrometry showed the monomer mass of the apoenzyme to be 42,306 Da (fig 5.2.1). This is 4 Daltons greater than the estimated value of 42,302 Da (PeptideMass (176)) and within the limits of experimental error. This mass indicates that the purified enzyme is post-translationally modified, with the loss of the N-terminal methionine. This modification is shared by *E.coli* AONS and occurred despite the artificial second residue introduced by the cloning procedure (see section 5.1). This characteristic has not been observed, however, by AONS purified from *B.sphaericus* (38). All three proteins have been over-expressed in *E.coli* host strains thus indicating that *E.coli* post-translational modification of *A.aeolicus* AONS occurs naturally and is not an artefact of the isolation procedure.

The second, smaller peak is not readily identifiable, but could represent ions present from the purification buffer, such as potassium, within the protein. Alternatively, the additional mass of approximately 130 Da may represent a further amino acid, such as leucine or aspartic acid attached to the molecule. This may have been acquired during cell growth and protein over-expression.

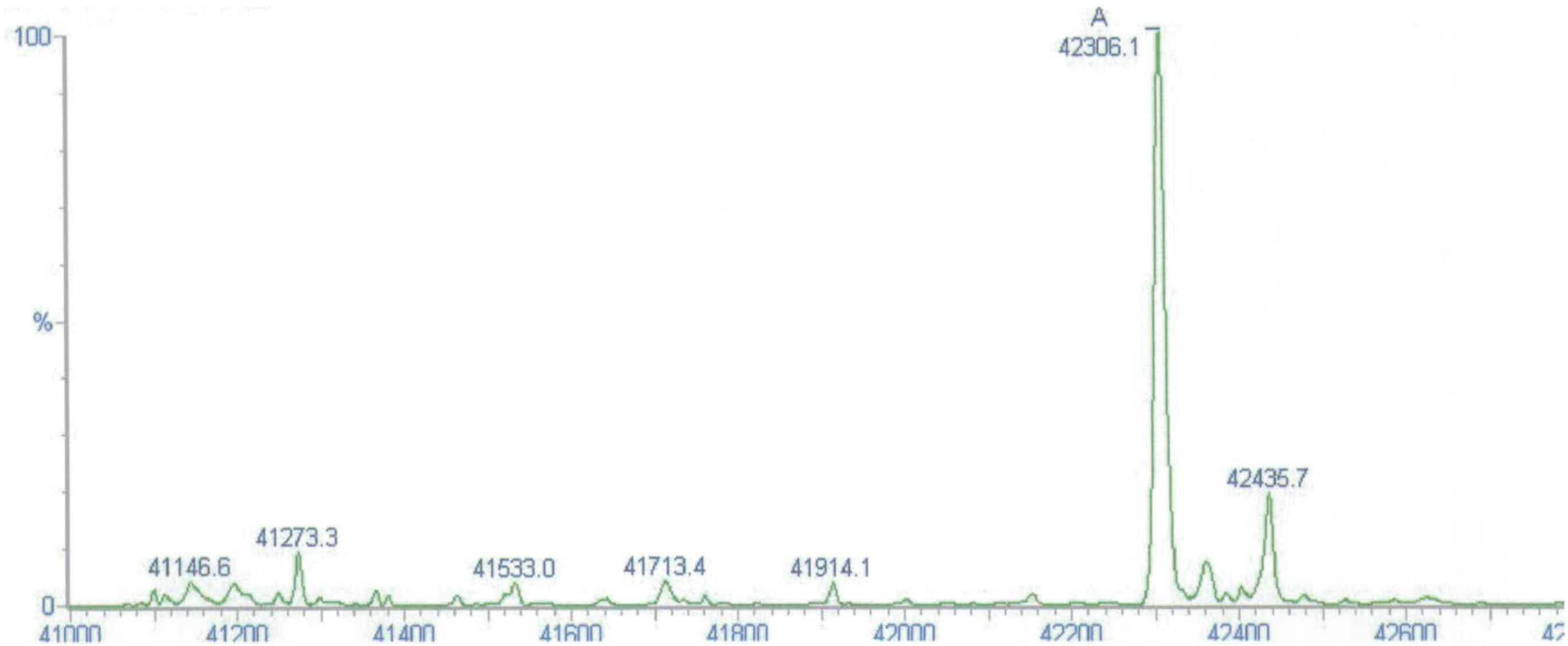

Figure 5.2.1

Mass spectrometry measurement of *A.aeolicus* AONS. The protein was separated from salts in the buffer by HPLC purification with H_2O/Acetonitrile containing 0.01% Trifluoroacetic acid as eluent on a C5 column. The calculated mass of the protein, excluding the N-terminal methionine residue, was 42,302 Da. Data was refined using MaxEnt software.

5.3 Absorbance Spectra

The UV-visible spectra of purified hyperthermostable *A.aeolicus* AONS can be seen to display peaks at 332nm and 430nm. These are characteristic of the internal enzyme-cofactor aldimine for a PLP containing protein, indicating the presence of the ketimine, protonated at C_4 of the PLP, and aldimine respectively (130). On addition of L-alanine, the peak at 430nm becomes more defined and a strong band appears at 490nm. The 490nm absorbance maximum has been assigned to the first quinonoid intermediate in the reaction catalysed by AONS (36). However, this species is seen in the corresponding *E.coli* enzyme only upon addition of the second substrate, pimeloyl-CoA. The AONS quinonoid intermediate is very stable and decays slowly over a period of 12 hours at room temperature.

L-alanine was titrated into the protein solution (fig 5.3.1) and the dissociation constant for the substrate calculated by fitting the 490nm absorbance at each L-alanine concentration to a hyperbolic saturation curve in equation 2. A dissociation constant of 20μM (±4μM) was calculated for the quinonoid (fig 5.3.2).

$$\Delta A_{max} = \frac{\Delta A_{max}[L-alanine]}{K_{\bar{d}} + [L-alanine]} \quad \text{.....Equation 2}$$

This compares to a calculated dissociation constant for L-alanine in *E.coli* AONS of 900mM, suggesting a much greater efficiency of substrate binding is demonstrated in the *A.aeolicus* enzyme. On addition of L-alanine, the characteristic peaks at 332nm and 430nm can still be observed and do not increase significantly as the peak at 490nm increases, suggesting that the major species obtained on addition of L-alanine is the quinonoid.

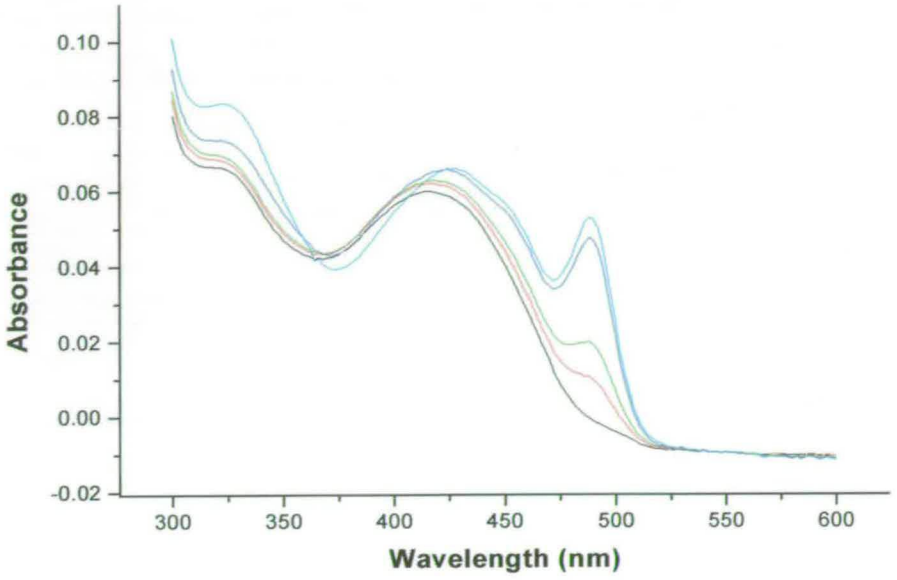

Figure 5.3.1

Titration of 8μM AONS with 1μM-1mM L-alanine. AONS was mixed with the substrate in 200mM potassium phosphate buffer, pH 7.5, and left to equilibrate for 30 minutes at 30°C. Acquisition of the spectra was at 30°C and pH 7.5. Concentrations from the top (cyan line) to the bottom (black line) - 1mM, 100μM, 10μM, 5μM, 1μM

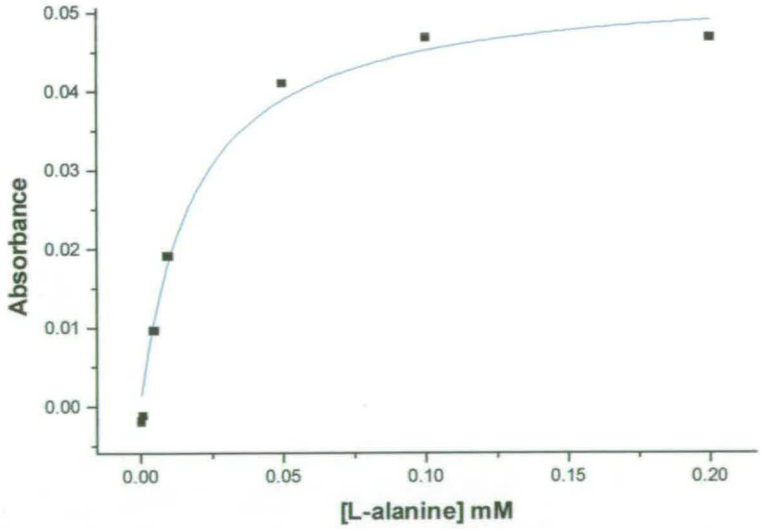

Figure 5.3.2

Saturation curve plotted by absorbance at 490nm *vs* L-alanine concentration. The dissociation constant was calculated using equation 1 above.

In contrast, at higher temperatures, a peak at 490nm is not seen after incubation for 20 minutes with concentrations of L-alanine greater than 5μM. If left overnight, the incubated enzyme-substrate complex was seen to precipitate. No enzyme precipitation was observed, however, in the presence of L-alanine and the second substrate, pimeloyl-CoA.

The spectrum of the enzyme-cofactor complex was investigated in different ionic conditions. There was no change observed in the spectra on addition of monovalent (Na^+, K^+, Cs^+) cations, or alteration of pH values in the range 6.5-8.5. The observed spectral changes on reaction of the protein with L-alanine under these conditions was not altered.

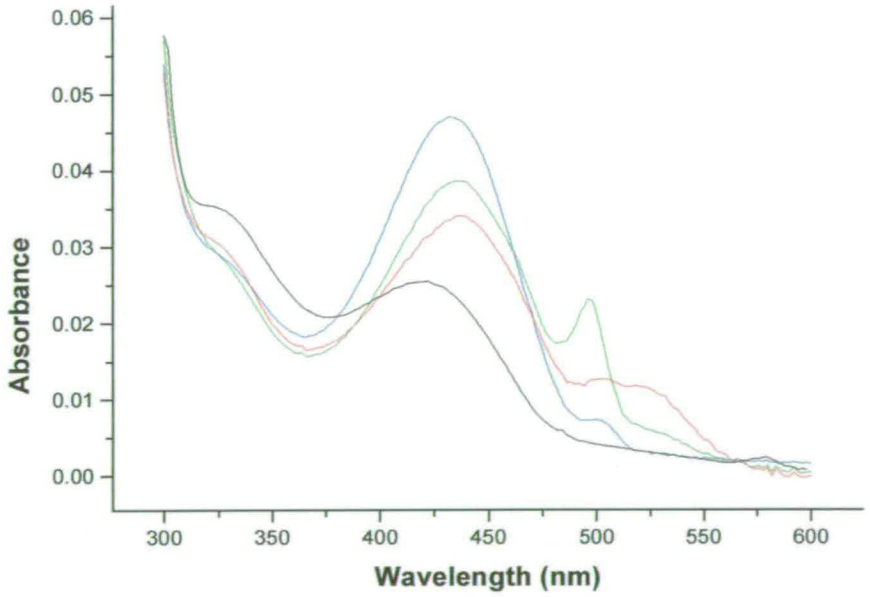

Figure 5.3.3

Change in the cofactor absorption spectra of *A.aeolicus* AONS on addition of substrates and product. Spectra were acquired at 30°C and pH 7.5.The PLP-AONS (5μM) spectrum is shown in black; in the presence of: 1mM L-alanine (blue); 1mM L-alanine and 100μM pimeloyl-CoA (green); 2mM AONS (red)

Formation of a substrate quinonoid, however, is inhibited by high concentrations (200mM) of divalent cations (Mg^{2+}, Ca^{2+}) as evinced from the absence of the 490nm peak. This inhibition is mimicked by *E.coli* AONS. In the absence of divalent cations, the peak at 490nm is greatly enhanced upon the addition of the second substrate. Under these conditions, a reduction in the absorbance of the peak at 430nm can also be observed. Incubation of the AONS-PLP complex with the product AON at 30°C allows observation of an absorbance maximum at 510nm. This corresponds to the characteristic product quinonoid peak of the AONS-AON exhibited by the *E.coli* enzyme (36).

5.4 Steady State Kinetics

The coupled assay to measure kinetic activity uses the release of CoASH, a result of thioester cleavage by the Cα carbanion (see section 1.2.1). This is a substrate for the second reaction catalysed by α-ketoglutarate decarboxylase, releasing NADH. The production of this molecule was followed by observing an increase at 340nm. The conversion of the observed velocity to concentration of pimeloyl-CoA used up in the reaction was calculated using an absorbance extinction coefficient for NADH of 6300 $l\ mol^{-1}\ cm^{-1}$.

Initially, temperature stability of AONS was measured by incubating the enzyme at a range of temperatures between 0°C-100°C prior to steady state assay at 30°C. This assay was carried out with excess substrate of 50mM L-alanine and 200μM pimeloyl-CoA. The enzyme was active after prolonged incubation at all temperatures in this range.

To establish the nature of thermostable activity, a single assay was carried out at defined temperatures in the range 0°C to 100°C using L-alanine and pimeloyl-CoA together with AONS present in 10mM potassium phosphate buffer, pH 7.5. The reaction was quenched after 10 minutes and coupled to the α-ketoglutarate dehydrogenase reaction at 30°C. The resulting rate of reaction was plotted against the temperature (fig 5.4.1) and an increase in rate almost proportional to an increase in temperature was observed. This relationship was halted at 80°C, where maximum activity was observed and the rate of reaction subsequently dropped off as the temperature approached 100°C.

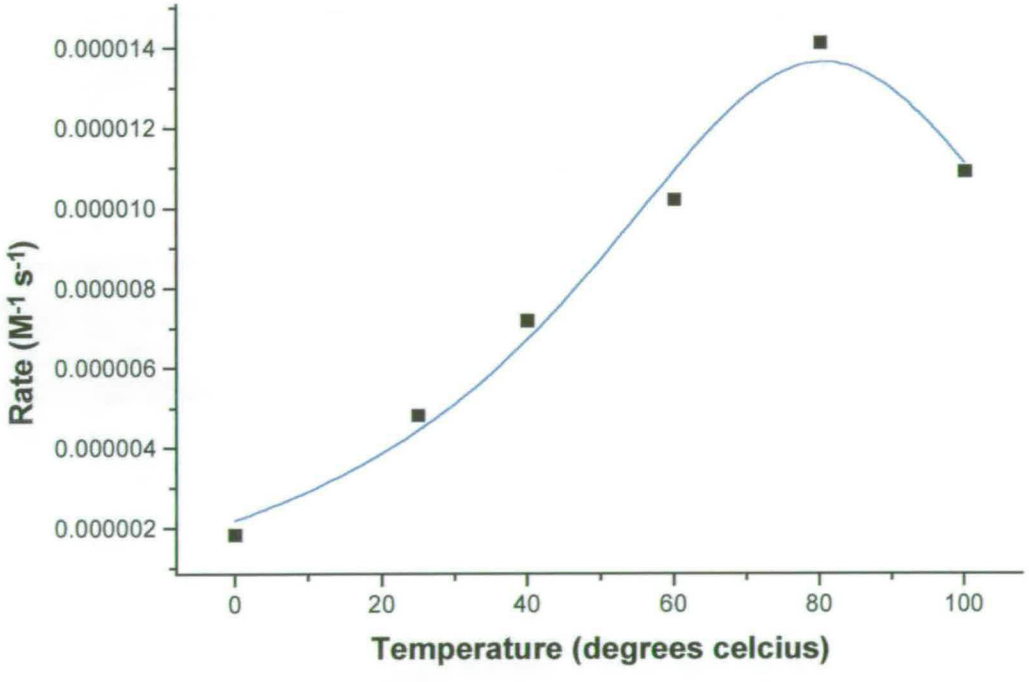

Figure 5.4.1

Temperature activity curve for *A.aeolicus* AONS. 2μM AONS was incubated for ten minutes at 0°C, 20°C, 40°C, 60°C, 80°C and 100°C in 10mM potassium phosphate buffer, pH 7.5, and 10mM L-alanine and 100μM pimeloyl-CoA. 50μl of the quenched reaction was added to the components for the coupled assay to a volume of 1ml, and increase in absorbance at 340nm was recorded. The rate of pimeloyl-CoA used in the reaction was plotted against temperature.

The temperature activity curve would suggest that the optimum activity for the enzyme lies at approximately 80°C. The drop off in activity as the temperature rises towards 100°C could be due to micro-precipitation of the protein solution. It may be that this does not correspond to the situation *in vivo*, where the protein may be stabilised by other cellular components.

Table 5.2

Steady state kinetic constants for AONS of *A.aeolicus*, *E.coli*, *B.sphaericus*. Steady-state kinetic constants for *A.aeolicus* AONS were measured at 30°C and pH 7.5 and fitted to equation 2 using Origin (Microcal) software. They are comparable to the values observed for *E.coli* and *B.sphaericus* AONS. The table is adapted with kind permission from Webster (36).

		pimeloyl-CoA		L-alanine	
AONS	k_{cat} (s^{-1})	K_m (μM)	k_{cat}/K_m ($s^{-1}M^{-1}$)	K_m (mM)	k_{cat}/K_m ($s^{-1}M^{-1}$)
E. coli	0.06(0.01)	25(2)	2400(430)	0.50(0.04)	120(21)
A. aeolicus	0.05(0.01)	15.5(1.4)	3226(645)	3.4 (0.3)	15(3)
*B. sphaericus**	0.3	1.5	$2x10^5$	2.5	120

* B.sphaericus data was collected at 25°C by O.Ploux (39) (*pers. commun.* with Scott Webster)

Steady state assays were conducted for the enzyme at 30°C and data was fitted to Michaelis-Menton saturation curves calculated by equation 1 (see section 2.4.1) from which kinetic constants were obtained.

The low temperature was chosen to enable comparisons of the final constants with those of other α-oxoamine synthases, in particular AONS from other species (Table 5.2).

Both Michaelis constants for *A.aeolicus* AONS are similar to those of other α-oxoamine synthases, where the typical values are in the millimolar range for the amino acid substrate, and in the micromolar range for the acyl CoA (36) (38-39) (45) (177).

The largest differences in the constants calculated from each AONS species is observed for the *B.sphaericus* enzyme. This assay was performed independently by Marquet's group in France and did not use a coupled assay, relying instead on measurement of an absorbance decrease at 230nm, indicating cleavage of the pimeloyl-CoA thioester bond. The assays were also conducted at 25°C. For these reasons, although the relative concentration ranges of the constants for each substrate are similar, it is not known whether the larger discrepancies, particularly in the turnover number, could be attributed to differences in the activity of the enzyme, or in the assay method. Attempts to duplicate their assay proved unsuccessful for measurement of *E.coli* (36) and *A.aeolicus* AONS kinetics.

The k_{cat} of the *A.aeolicus* AONS reaction is 0.05 sec^{-1} at 30°C. This is similar to the *E.coli* enzyme and would indicate a similar rate of turnover. The *A.aeolicus* enzyme, however, functions best at temperatures of 80°C and it would thus seem obvious that the kinetic constants at higher temperature would be consistent with an elevated rate of reaction. Steady state kinetics were therefore also carried out at 60°C and 80°C in the form of a quenched assay (Table 5.3).

The increase in temperature manifests itself as a 25-fold increase in turnover of the *A.aeolicus* AONS enzyme at 80°C in comparison with its catalysis rate at 30°C. An activation energy for the protein can be calculated using equation 4, and E_a = 53 kJ mol^{-1}. This corresponds to the activation energy of 50 kJ mol^{-1} seen over a 10°C - 40°C temperature range for mesophilic proteins (178).

$$\log \frac{k_2}{k_1} = \frac{Ea}{2.3R}\left(\frac{T_2 - T_1}{T_2 T_1}\right) \quad \text{.....Equation 4}$$

Table 5.3

Steady state kinetic constants for AONS of *A.aeolicus*, at 60°C and 80°C

		pimeloyl-CoA		L-alanine	
Assay temperature	k_{cat} (s^{-1})	K_m (μM)	k_{cat}/K_m ($s^{-1}M^{-1}$)	K_m (μM)	k_{cat}/K_m ($s^{-1}M^{-1}$)
60°C	0.45 (0.02)	18 (1)	25,000 (1125)	203 (34)	2,217 (277)
80°C	1.25 (0.1)	22 (3)	56,818 (6136)	52 (19)	24,000 (636)

There is very little difference in the apparent K_m values for the second substrate, pimeloyl-CoA across all three temperatures, although the specificity of the enzyme for this substrate does increase, as evinced by the k_{cat}/K_m values. There is, however, a visible reduction in the K_m for L-alanine on elevation of temperature, such that the constant value at 80°C decreases 65 fold on the value observed at 30°C. The binding specificity of *A.aeolicus* AONS for L-alanine rises significantly with each increase in temperature, suggesting a possible alteration in conformation of the protein molecule.

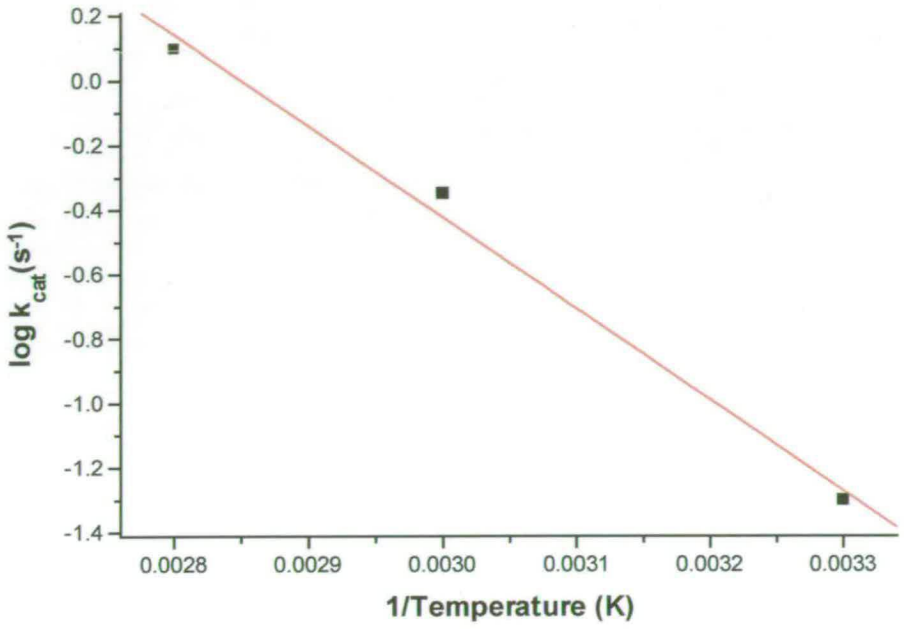

Figure 5.4.2

Plot of log k_{cat} *versus* 1/T for *A.aeolicus* AONS at fixed temperatures of 30°C, 60°C and 80°C. Turnover was measured using the quenched assay.

5.5 Sequence alignment

There are currently 12 fully annotated AONS sequences in the SwissProt database (23) (26) (31) (33) (179-185) together with 5 translated sequences in TrEMBL (186-189). Sequences of AONS from a further three species can be found at Genbank (190-192). Of these sequences, 18 are independent. Only one of the sequences represents AONS from an archae bacterium (see section 1.2.2), *Methanococcus jannaschii*.

Residues already recorded as being essential for cofactor and substrate binding in PLP dependent enzymes are strictly conserved. However, two specific active site residues in *E.coli*, glutamate 175 and tyrosine 264, a residue contributing to the active site from the opposite monomer, are not always conserved. They may become aspartate and phenylalanine respectively in several species, although there is not necessarily a correlation between either residue to suggest that they are present together in the active site. Exceptions to this change are the AONS proteins of *Chlamydia sp. Chlamydia trachiomatis* has a leucine residue in the position where a tyrosine or phenylalanine is usually found, and *Chlamydia pneumoniae* (*bio*F 1) has a serine residue instead of the more usual aspartate or glutamate residue. The initial glutamate/tyrosine combination can be found in the active site of *E.coli* AONS, whilst these residues are replaced by aspartate and phenylalanine in the *A.aeolicus* and *B.sphaericus* proteins. Two asparagine residues found in the active site of the *E.coli* protein (N47; N112) are conserved in all species. It is already accepted that asparagine is one of the residues generally replaced by a polar residue in heat stable enzymes. Thus this conservation suggest that both residues are vital for enzyme function.

A.aeolicus AONS displays other differences in its sequence compared with the *E.coli* sequence. The initial N-terminal α-helix seen in *E.coli* seems to be smaller in its thermophilic counterpart, although residues towards the C-terminal end of the protein show a high degree of conservation. The sequence of the hyperthermophilic enzyme also displays an increased percentage of ionic residues – in particular lysine and glutamic acid residues, and a distinct reduction in the number of alanine and glutamine residues. One third of the *A.aeolicus* gene is composed of charged residues. This compares to 20% for the *E.coli* and 27% for the *B.sphaericus* enzymes. The *A.aeolicus* enzyme sequence is closer to the *B.sphaericus* enzyme, sharing 40% sequence identity, compared with 36% identity to *E.coli* AONS.

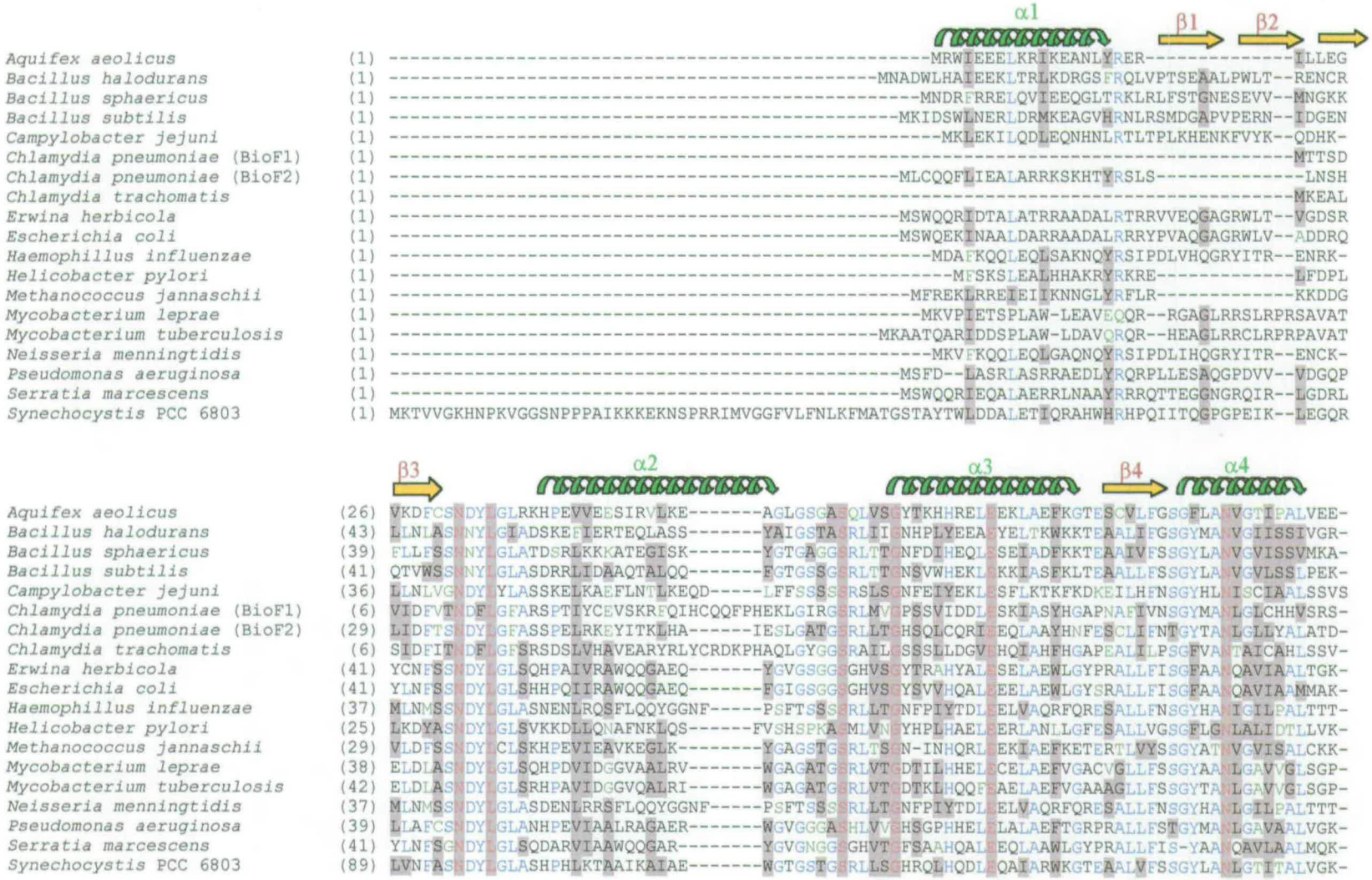
α1
β1
β2
Aquifex aeolicus (1) ----------MRWIEEELKRIKEANLYRER----------ILLEG
Bacillus halodurans (1) ----------MNADWLHAIEEKLTRLKDRGSFRQLVPTSEAALPWLT--RENCR
Bacillus sphaericus (1) ----------MNDRFRRELQVIEEQGLTRKLRLFSTGNESEVV--MNGKK
Bacillus subtilis (1) ----------MKIDSWLNERLDRMKEAGVHRNLRSMDGAPVPERN--IDGEN
Campylobacter jejuni (1) ----------MKLEKILQDLEQNHNLRTLTPLKHENKFVYK--QDHK-
Chlamydia pneumoniae (BioF1) (1) ----------MTTSD
Chlamydia pneumoniae (BioF2) (1) ----------MLCQQFLIEALARRKSKHTYRSLS----------LNSH
Chlamydia trachomatis (1) ----------MKEAL
Erwina herbicola (1) ----------MSWQQRIDTALATRRAADALRTRRVVEQGAGRWLT--VGDSR
Escherichia coli (1) ----------MSWQEKINAALDARRAADALRRRYPVAQGAGRWLV--ADDRQ
Haemophillus influenzae (1) ----------MDAFKQQLEQLSAKNQYRSIPDLVHQGRYITR--ENRK-
Helicobacter pylori (1) ----------MFSKSLEALHHAKRYRKRE----------LFDPL
Methanococcus jannaschii (1) ----------MFREKLRREIEIIKNNGLYRFLR----------KKDDG
Mycobacterium leprae (1) ----------MKVPIETSPLAW-LEAVEQQR--RGAGLRRSLRPRSAVAT
Mycobacterium tuberculosis (1) ----------MKAATQARIDDSPLAW-LDAVQRQR--HEAGLRRCLRPRPAVAT
Neisseria menningtidis (1) ----------MKVFKQQLEQLGAQNQYRSIPDLIHQGRYITR--ENCK-
Pseudomonas aeruginosa (1) ----------MSFD--LASRLASRRAEDLYRQRPLLESAQGPDVV--VDGQP
Serratia marcescens (1) ----------MSWQQRIEQALAERRLNAAYRRRQTTEGGNGRQIR--LGDRL
Synechocystis PCC 6803 (1) MKTVVGKHNPKVGGSNPPPAIKKKEKNSPRRIMVGGFVLFNLKFMATGSTAYTWLDDALETIQRAHWHRHPQIITQGPGPEIK--LEGQR
β3
α2
α3
β4
α4
Aquifex aeolicus (26) VKDFCSNDYLGLRKHPEVVEESIRVLKE-------AGLGSGASQLVSGYTKHHRELEEKLAEFKGTESCVLFGSGFLANVGTIPALVEE-
Bacillus halodurans (43) LLNLASNNYLGIADSKEFIERTEQLASS-------YAIGSTASRLIIGNHPLYEEAEYELTKWKKTEAALIFGSGYMANVGIISSIVGR-
Bacillus sphaericus (39) FLLFSSNNYLGLATDSRLKKKATEGISK-------YGTGAGGSRLTTGNFDIHEQLESEIADFKKTEAAIVFSSGYLANVGVISSVMKA-
Bacillus subtilis (41) QTVWSSNNYLGLASDRRLIDAAQTALQQ-------FGTGSSGSRLTTGNSVWHEKLEKKIASFKLTEAALLFSSGYLANVGVLSSLPEK-
Campylobacter jejuni (36) LLNLVGNDYLYLASSKELKAEFLNTLKEQD-----LFFSSSSSRSLSGNFEIYEKLESFLKTKFKDKEILHFNSGYHLNISCIAALSSVS
Chlamydia pneumoniae (BioF1) (6) VIDFVTNDFLGFARSPTIYCEVSKRFQIHCQQFPHEKLGIRGSRLMVGPSSVIDDLESKIASYHGAPNAFIVNSGYMANLGLCHHVSRS-
Chlamydia pneumoniae (BioF2) (29) LIDFTSNDYLGFASSPELRKEYITKLHA------IESLGATGSRLLTGHSQLCQRIEQLAAYHNFESCLIFNTGYTANLGLLYALATD-
Chlamydia trachomatis (6) SIDFITNDFLGFSRSDSLVHAVEARYRLYCRDKPHAQLGYGGSRAILGSSSLLDGVGHQIAHFHGAPEALILPSGFVANTAICAHLSSV-
Erwina herbicola (41) YCNFSSNDYLGLSQHPAIVRAWQQGAEQ-------YGVGSGGSGHVSGYTRAHYALESELAEWLGYPRALLFISGFAANQAVIAALTGK-
Escherichia coli (41) YLNFSSNDYLGLSHHPQIIRAWQQGAEQ-------FGIGSGGSGHVSGYSVVHQALEEELAEWLGYSRALLFISGFAANQAVIAAMMAK-
Haemophillus influenzae (37) MLNMSSNDYLGLASNENLRQSFLQQYGGNF-----PSFTSSSSRLLTGNFPIYTDLELVAQRFQRESALLFNSGYHANIGILPALTTT-
Helicobacter pylori (25) LKDYASNDYLGLSVKKDLLQNAFNKLQS------FVSHSPKASMLVNGYHPLHAELERLANLLGFESALLVGSGFLGNLALIDTLLVK-
Methanococcus jannaschii (29) VLDFSSNDYLCLSKHPEVIEAVKEGLK--------YGAGSTGSRLTSGN-INHQRLEEKIAEFKETERTLVYSSGYATNVGVISALCKK-
Mycobacterium leprae (38) ELDLASNDYLGLSQHPDVIDGGVAALRV-------WGAGATGSRLVTGDTILHHELECELAEFVGACVGLLFSSGYAANLGAVVGLSGP-
Mycobacterium tuberculosis (42) ELDLASNDYLGLSRHPAVIDGGVQALRI-------WGAGATGSRLVTGDTKLHQQFEAELAEFVGAAAGLLFSSGYTANLGAVVGLSGP-
Neisseria menningtidis (37) MLNMSSNDYLGLASDENLRRSFLQQYGGNF-----PSFTSSSSRLLTGNFPIYTDLELVAQRFQRESALLFNSGYHANLGILPALTTT-
Pseudomonas aeruginosa (39) LLAFCSNDYLGLANHPEVIAALRAGAER-------WGVGGGASHLVVGHSGPHHELELALAEFTGRPRALLFSTGYMANLGAVAALVGK-
Serratia marcescens (41) YLNFSGNDYLGLSQDARVIAAWQQGAR--------YGVGNGGSGHVTGFSAAHQALEEQLAAWLGYPRALLFIS-YAANQAVLAALMQK-
Synechocystis PCC 6803 (89) LVNFASNDYLGLASHPHLKTAAIKAIAE-------WGTGSTGSRLLSGHRQLHQDLEQAIARWKGTEAALVFSSGYLANLGTITALVGK-

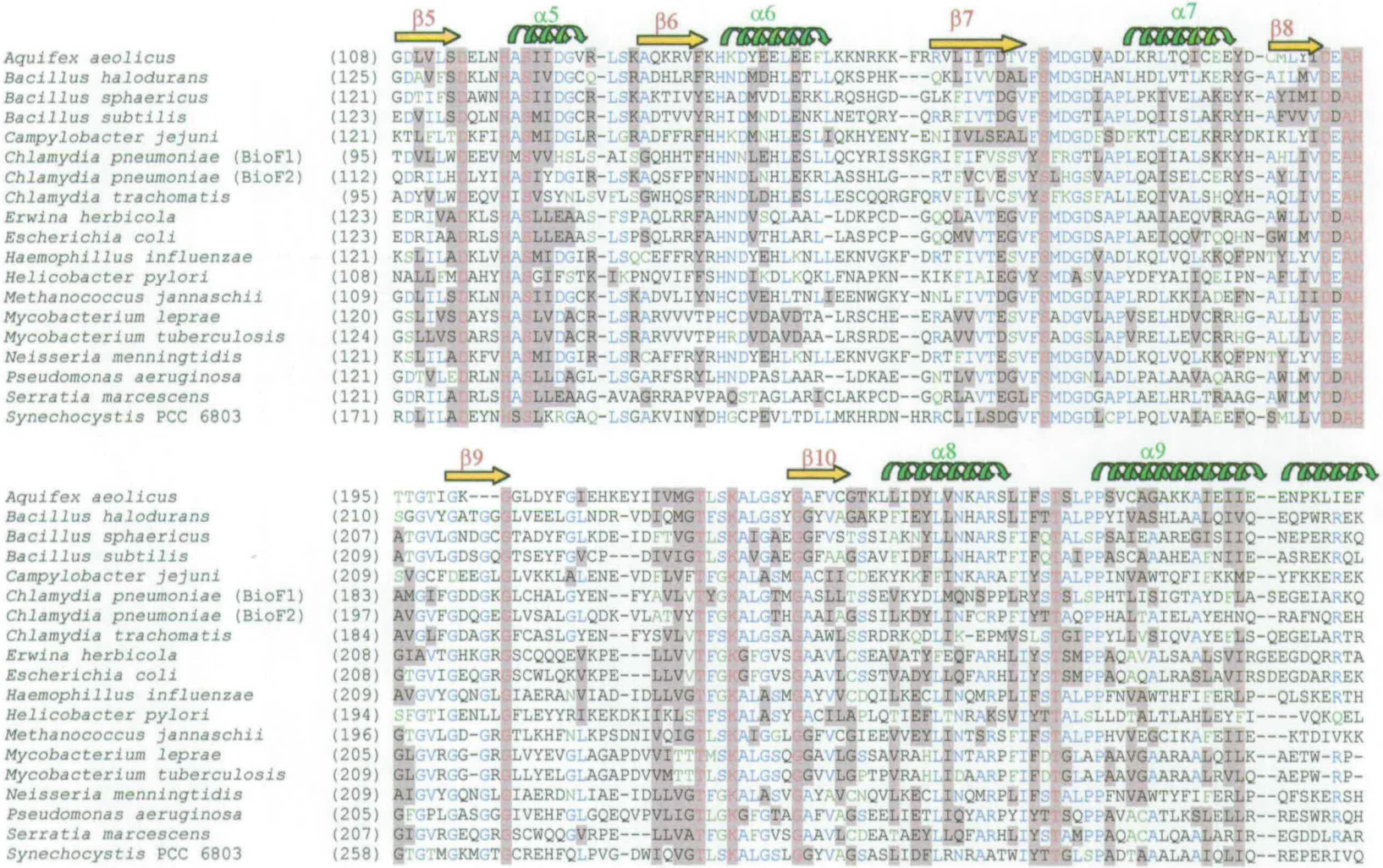
β5 α5 β6 α6 β7 α7 β8
Aquifex aeolicus (108) GDLVLSDELNHASIIDGVR-LSKAQKRVFKHKDYEELEEFLKKNRKK-FRRVLIITDTVFSMDGDVADLKRLTQICEEYD-GMDLYIDEAH
Bacillus halodurans (125) GDAVFSDKLNHASIVDGCQ-LSRADHLRFRHNDMDHLETLLQKSPHK---QKLIVVDALFSMDGDHANLHDLVTLKERYG-AILMVDEAH
Bacillus sphaericus (121) GDTIFSDAWNHASIIDGCR-LSKAKTIVYEHADMVDLERKLRQSHGD--GLKFIVTDGVFSMDGDIAPLPKIVELAKEYK-AYIMIDDAH
Bacillus subtilis (123) EDVILSDQLNHASMIDGCR-LSKADTVVYRHIDMNDLENKLNETQRY--QRRFIVTDGVFSMDGTIAPLDQIISLAKRYH-AFVVVDDAH
Campylobacter jejuni (121) KTLFLTDKFIHASMIDGLR-LGRADFFRFHHKDMNHLESLIQKHYENY-ENIIVLSEALFSMDGDFSDFKTLCELKRRYDKIKLYIDEAH
Chlamydia pneumoniae (BioF1) (95) TDVLLWDEEVMSVVHSLS-AISGQHHTFHHNNLEHLESLLQCYRISSKGRIFIFVSSVYSFRGTLAPLEQIIALSKKYH-AHLIVDEAH
Chlamydia pneumoniae (BioF2) (112) QDRILHDLYIHAGIYDGIR-LSKAQSFPFNHNDLNHLEKRLASSHLG---RTFVCVESVYSLHGSVAPLQAISELCERYS-AYLIVDEAH
Chlamydia trachomatis (95) ADYVLWDEQVHIGVSYNLSVFLSGWHQSFRHNDLDHLESLLESCQQRGFQRVFILVCSVYSFKGSFALLEQIVALSHQYH-AQLIVDEAH
Erwina herbicola (123) EDRIVADKLSHASLLEAAS-FSPAQLRRFAHNDVSQLAAL-LDKPCD--GQQLAVTEGVFSMDGDSAPLAAIAEQVRRAG-AWLLVDDAH
Escherichia coli (123) EDRIAADRLSHAGLLEAAS-LSPSQLRRFAHNDVTHLARL-LASPCP--GQQMVVTEGVFSMDGDSAPLAEIQQVTQQHN-GWLMVDDAH
Haemophillus influenzae (121) KSLILADKLVHAGMIDGIR-LSQCEFFRYRHNDYEHLKNLLEKNVGKF-DRTFIVTESVFSMDGDVADLKQLVQLKKQFPNTYLYVDEAH
Helicobacter pylori (108) NALLFMDAHYHAGIFSTK-IKPNQVIFFSHNDIKDLKQKLFNAPKN--KIKFIAIEGVYSMDASVAPYDFYAIIQEIPN-AFLIVDEAH
Methanococcus jannaschii (109) GDLILSDKLNHASIIDGCK-LSKADVLIYNHCDVEHLTNLIEENWGKY-NNLFIVTDGVFSMDGDIAPLRDLKKIADEFN-AILIIDDAH
Mycobacterium leprae (120) GSLIVSDAYSHAGLVDACR-LSRARVVVTPHCDVDAVDTA-LRSCHE--ERAVVVTESVFSADGVLAPVSELHDVCRRHG-ALLLVDEAH
Mycobacterium tuberculosis (124) GSLLVSDARSHAGLVDACR-LSRARVVVTPHRDVDAVDAA-LRSRDE--QRAVVVTDSVFSADGSLAPVRELLEVCRRHG-ALLLVDEAH
Neisseria menningtidis (121) KSLILADKFVHAGMIDGIR-LSRCAFFRYRHNDYEHLKNLLEKNVGKF-DRTFIVTESVFSMDGDVADLKQLVQLKKQFPNTYLYVDEAH
Pseudomonas aeruginosa (121) GDTVLEDRLNHAGLLDAGL-LSGARFSRYLHNDPASLAAR--LDKAE--GNTLVVTDGVFSMDGNLADLPALAAVAQARG-AWLMVDDAH
Serratia marcescens (121) GDRILADRLSHAGLLEAAG-AVAGRRAPVPAQSTAGLARICLAKPCD--GQRLAVTEGLFSMDGDGAPLAELHRLTRAAG-AWLMVDDAH
Synechocystis PCC 6803 (171) RDLILADEYNHSGLKRGAQ-LSGAKVINYDHGCPEVLTDLLMKHRDN-HRRCLILSDGVFSMDGDLCPLPQLVAIAEEFQ-SMLLVDDAH
β9 β10 α8 α9
Aquifex aeolicus (195) TTGTIGK---GGLDYFGIEHKEYIIVMGTLSKALGSYGAFVCGTKLLIDYLVNKARSLIFSTSLPPSVCAGAKKAIEIIE--ENPKLIEF
Bacillus halodurans (210) SGGVYGATGGGLVEELGLNDR-VDIQMGTFSKALGSYGGYVAGAKPFIEYLLNHARSLIFTTALPPYIVASHLAALQIVQ--EQPWRREK
Bacillus sphaericus (207) ATGVLGNDGCGTADYFGLKDE-IDFTVGTLSKAIGAEGGFVSTSSIAKNYLLNNARSFIFCTALSPSAIEAAREGISIIQ--NEPERRKQ
Bacillus subtilis (209) ATGVLGDSGQGTSEYFGVCP---DIVIGTLSKAVGAEGGFAAGSAVFIDFLLNHARTFIFCTAIPPASCAAAHEAFNIIE--ASREKRQL
Campylobacter jejuni (209) SVGCFDEEGLGLVKKLALENE-VDFLVFTFGKALASMGACIICDEKYKKFFINKARAFIYSTALPPINVAWTQFIFKKMP--YFKKEREK
Chlamydia pneumoniae (BioF1) (183) AMGIFGDDGKGLCHALGYEN--FYAVLVTYGKALGTMGASLLTSSEVKYDLMQNSPPLRYSTSLSPHTLISIGTAYDFLA-SEGEIARKQ
Chlamydia pneumoniae (BioF2) (197) AVGVFGDQGEGLVSALGLQDK-VLATVYTFGKALGTHGAAIAGSSILKDYLINFCRPFIYTTAQPPHALTAIELAYEHNQ--RAFNQREH
Chlamydia trachomatis (184) AVGLFGDAGKGFCASLGYEN--FYSVLVTFSKALGSAGAAWLSSRDRKQDLIK-EPMVSLSTGIPPYLLVSIQVAYEFLS-QEGELARTR
Erwina herbicola (208) GIAVTGHKGRGSCQQQEVKPE---LLVVTFGKGFGVSGAAVLCSEAVATYFEQFARHLIYSTSMPPAQAVALSAALSVIRGEEGDQRRTA
Escherichia coli (208) GTGVIGEQGRGSCWLQKVKPE---LLVVTFGKGFGVSGAAVLCSSTVADYLLQFARHLIYSTSMPPAQAQALRASLAVIRSDEGDARREK
Haemophillus influenzae (209) AVGVYGQNGLGIAERANVIAD-IDLLVGTFGKALASMGAYVVCDQILKECLINQMRPLIFSTALPPFNVAWTHFIFERLP--QLSKERTH
Helicobacter pylori (194) SFGTIGENLLGFLEYYRIKEKDKIIKLSTFSKALASYGACILAPLQTIEFLTNRAKSVIYTTALSLLDTALTLAHLEYFI----VQKQEL
Methanococcus jannaschii (196) GTGVLGD-GRGTLKHFNLKPSDNIVQIGTLSKAIGGLGGFVCGIEEVVEYLINTSRSFIFSTALPPHVVEGCIKAFEIIE---KTDIVKK
Mycobacterium leprae (205) GLGVRGG-GRGLVYEVGLAGAPDVVITTTMSKALGSQGAVLGSSAVRAHLINTARPFIFDTGLAPAAVGAARAALQILK--AETW-RP-
Mycobacterium tuberculosis (209) GLGVRGG-GRGLLYELGLAGAPDVVMTTTLSKALGSQGVVLGPTPVRAHLIDAARPFIFDTGLAPAAVGAARAALRVLQ--AEPW-RP-
Neisseria menningtidis (209) AIGVYGQNGLGIAERDNLIAE-IDLLVGTFGKALASVGAYAVCNQVLKECLINQMRPLIFSTALPPFNVAWTYFIFERLP--QFSKERSH
Pseudomonas aeruginosa (205) GFGPLGASGGGIVEHFGLGQEQVPVLIGTLGKGFGTAGAFVAGSEELIETLIQYARPYIYTTSQPPAVACATLKSLELLR--RESWRRQH
Serratia marcescens (207) GIGVRGEQGRGSCWQQGVRPE---LLVATFGKAFGVSGAAVLCDEATAEYLLQFARHLIYSTAMPPAQACALQAALARIR--EGDDLRAR
Synechocystis PCC 6803 (258) GTGTMGKMGTGCREHFQLPVG-DWIQVGTLSKALGSLGGYVAGSASLIDFLRNRAATWIYTTGLSPADTAAALAAIQLIQ--REPERIVQ

Figure 5.5.1

Sequence alignment of the twenty known sequences of 8-amino-7-oxononanoate synthase. The conserved residues are shaded red and similar residues are boxed in grey. Blue denotes identity over at least 12 sequences. The secondary structure of the E.coli enzyme is overlaid across the top of the sequence, identifying residues involved in α-helix and β-sheet formation. Sequencing was carried out using Clustal W on the EBI server. The default blosum matrix was chosen. The sequences were formatted using ESPript (www-pgm1.ipbs.fr:8080/ESPript). The accession numbers of all sequences from top to bottom are: O25320; Q9ZLN3; P44422; NC002203; Q9PIJ3; P22806; P53556; O58694; O66875; P74770; P12998; Q47829; P36570; NC002516; P45487; O06621; NC002570; O84782; Q9Z6Y3; Q9Z6L

5.6 Mutagenesis of *A.aeolicus* AONS

The conserved histidine residue, found to lie in parallel with the pyridine ring of the cofactor was mutated in *E.coli* AONS to a phenylalanine residue, resulting in reversible loss of cofactor binding. It has already been observed that PLP binding in *A.aeolicus* AONS is greater than in the *E.coli* enzyme, thus the corresponding mutation (H118F) was created in the heat stable protein to investigate this observation. Mutagenesis was carried out using the megaprimer method as for the *E.coli* mutants (see section 2.3.5) and the mutated gene cloned into pUC18 at the *Nco*I/*Bam*HI sites. It was subsequently sub-cloned, using the same digest, into the pET16b over-expression plasmid.

5.7 Isolation and purification of H118F

Over-expression and purification of H118F was carried out according to the protocol developed for wild type *A.aeolicus* AONS. The mutant protein eluted from the anion exchange column at 140mM NaCl.

The yield of 10mg/l was similar to that obtained for the wild type enzyme, and purity was >95% as judged by SDS PAGE of protein with specific activity 0.1U. A small amount of PLP cofactor remained bound to the mutant protein throughout the purification and freezing process, suggesting that, unlike its mesophilic counterpart, the PLP binding within the active site is not totally lost.

Table 5.4

Purification table of *A.aeolicus* H118F/AONS from expression in an *E.coli* host. Protein concentration was measured using the method of Bradford and specific activity was measured in a coupled assay using 50mM L-alanine and 200μM pimeloyl-CoA. 1U AONS represents the transformation of 1μmol pimeloyl-CoA by 1mg enzyme per minute at 30°C

Purification Step	Volume (ml)	Protein (mg/ml)	Specific activity (U/mg)	Total activity (U)	Yield (%)	Purification fold
Crude extract	41	16.4	--	--	--	--
60°C fraction	36	10	0.007	2.52	100	1
80°C fraction	32	8.6	0.009	2.47	98	1.3
Anion exchange	20	1.1	0.1	2.2	88	14

5.8 Physical Characterisation of H118F

Dialysis against potassium phosphate buffer, containing 100μM PLP followed by exhaustive washing showed that PLP remained bound within the enzyme. The measured coefficient for cofactor binding at 395nm is ε=1673 l mol^{-1} cm^{-1}. This is a seven-fold reduction from the chromophore binding observed in the wild type enzyme (see section 5.2), and the shorter wavelength would suggest that the orientation of the imine bond of the internal aldimine within the active site has been altered. The fact that the total PLP did not disappear after exhaustive washing indicates that the cofactor is actually held within the active site.

An approximate size was estimated for the mutant proteins by SDS PAGE analysis, using wild type AONS as a reference and was necessary during the purification process. As expected, the mutant protein

band ran concurrent with the wild type band. The predicted mass of the H118F mutant enzyme has been identified by ESI mass spectrometry. The predicted mass of the protein is 42,542.16 Da and the calculated mass 42,544 Da.

5.9 UV/visible Characterisation of H118F

The absorbance spectrum of the mutant displays the characteristic peak at 324nm and a further peak at 395nm.

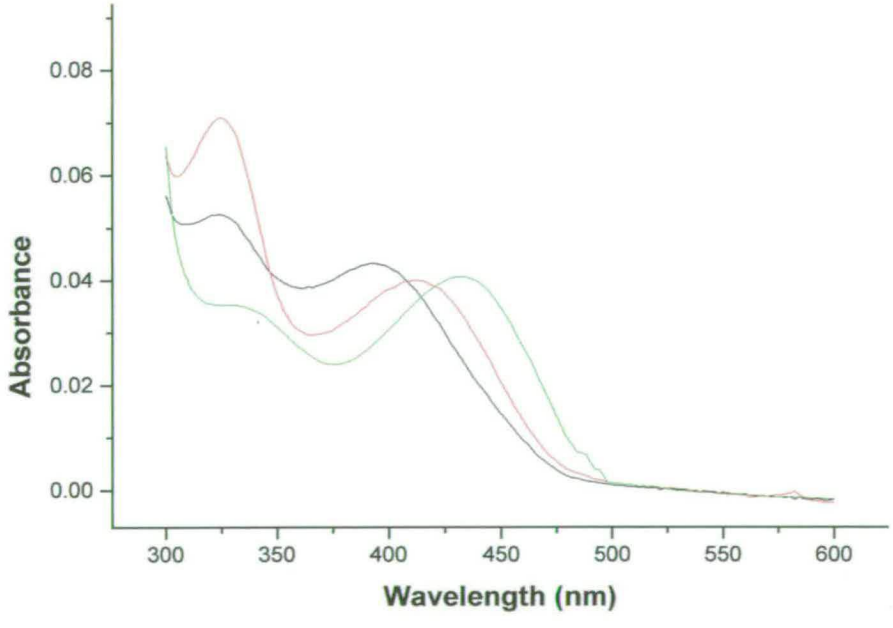

Figure 5.9.1

Change in the cofactor absorption spectra of *A.aeolicus* AONS for wild type and mutant protein. Spectra were acquired at 30°C and pH 7.5. H118F/AONS holoenzyme (black); in the presence of 50mM L-alanine (red); wild type AONS holoenzyme (green).

These are defined as the protonated and non-protonated forms of the internal aldimine respectively. The shorter wavelengths indicate that the normal orientation of the cofactor is perturbed. On addition of the first substrate, L-alanine, no quinonoid peak is observed. There is also no increase in the wavelength at 490nm on addition of saturating concentrations of the second substrate

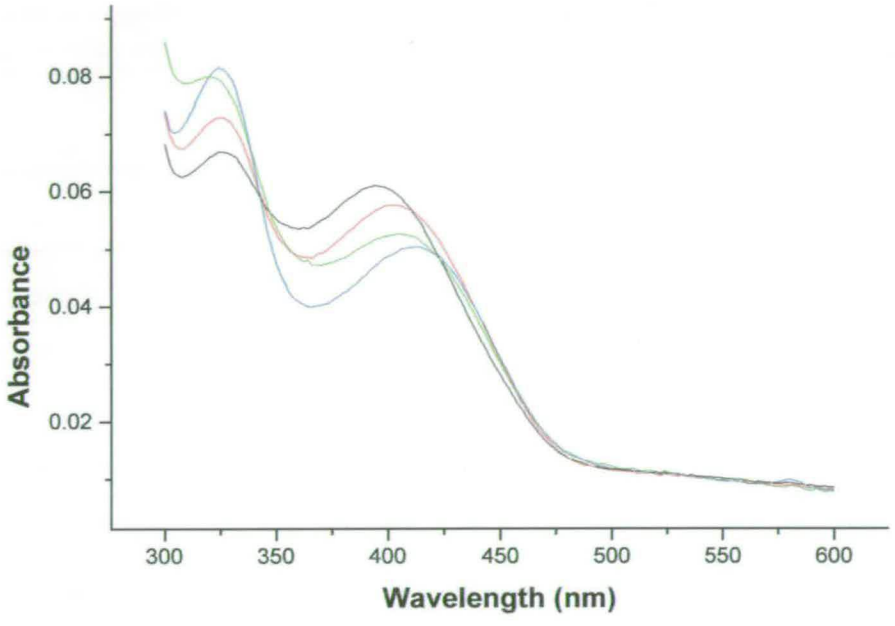

Figure 5.9.2

Titration of 8μM H118F/AONS with 1μM-1mM L-alanine. AONS was mixed with the substrate in 200mM potassium phosphate buffer, pH 7.5, and left to equilibrate for 30 minutes at 30°C. Acquisition of the spectra was at 30°C and pH 7.5. Concentrations are: 1mM (black); 10mM (red); 20mM (green); 50mM (blue).

The kinetic activity is evidence that the reaction proceeds, so a lack of visible quinonoid would suggest active site dynamics created by the mutant which do not favour the stability of this intermediate.

Although the absorbance maximum of the internal aldimine is shorter than wild type, it remained distinguishable from the absorbance peak of the free PLP molecule at 390nm. The wavelength for the aldimine peak increases on addition of L-alanine, but remains shorter than the wavelength assigned to the enzyme-cofactor aldimine of the wild type protein.

The mutant protein was titrated with increasing L-alanine concentrations and a slow shift in wavelength could be observed as the concentration increased. An isosbestic point is indicated at 330nm, suggesting equilibrium between the protonated and unprotonated species .

5.10 Steady state kinetics on H118F/AONS

The steady state kinetic parameters for the mutant enzyme were calculated using constants obtained from the activity of the protein in the coupled assay at 30°C, pH 7.5 (table 5.5).

Table 5.5

Steady state kinetic constants for AONS of *A.aeolicus*, wild type and H118F mutant. Steady-state kinetic constants for each substrate were measured at 30°C, pH 7.5 in the presence of the other substrate and data fitted to Michaelis-Menton saturation curves. Protein concentration used in the assay was 1μM.

		pimeloyl-CoA		**L-alanine**	
AONS	k_{cat} (s^{-1})	K_m (μM)	k_{cat}/K_m ($s^{-1}M^{-1}$)	K_m (mM)	k_{cat}/K_m ($s^{-1}M^{-1}$)
Wild type	0.05(0.01)	15.5(1.4)	3226(645)	3.4 (0.3)	15(3)
H118F	0.006 (0.0005)	55 (7)	109 (21)	8.2 (2.6)	0.7 (0.1)

The results suggest that the phenylalanine mutation reduces the turnover rate of the reaction to *ca.* 10% of the wild type activity. The binding efficiency of both substrates is also reduced, and this, together with the changes in λmax of the aldimine indicate a possible incorrect orientation for the pyridine ring of the cofactor within the active site.

There is a twenty-fold reduction in formation of the external aldimine and consequently the reaction of the amino acid substrate with pimeloyl-CoA is lowered to almost thirty-fold below the wild type activity, suggesting that once L-alanine is bound, the reaction with pimeloyl-CoA proceeds at *ca.* 10% wild type rate.

5.11 Crystallisation of *A.aeolicus* AONS

Protein fractions containing 95% pure AONS were pooled and loaded onto a Superdex 75 gel filtration column for buffer exchange from 20mM potassium phosphate, pH 7.5 to 10mM bis-tris propane, pH 7.5. This exchange was originally carried out in order to reproduce the conditions which led to the crystallisation of *E.coli* AONS (37). Subsequent light scattering experiments carried out on *A.aeolicus* AONS indcated that a low salt buffer such as bis-tris propane was necessary to reduce aggregation of the protein, thus confirming the choice of buffer. A further indicator was the crystallisation itself. As a control, crystal trials were conducted with 20mM potassium phosphate buffer, pH 7.5 but, as expected, the buffer contributed to aggregation of the protein and a solid precipitate formed throughout the droplet.

Initial crystal trials were conducted at varying pH values with ammonium sulphate as the precipitant; emulating the conditions under which the *E.coli* AONS crystals were produced. These trials were conducted in Linbro® 24 multi-well plates in the hanging drop version of the vapour diffusion technique. Initial trials with commercial Structure Screens I and II were also set up as sitting droplets

within the well solution. Protein set in trials containing polyethylene glycol (PEG) did not form crystals at any concentration of either protein or PEG.

Crystals were only produced in those drops containing unbuffered $(NH_4)_2SO_4$ at pH 5.5. Further trials were set up to define the optimum protein and precipitant concentration. The protein solution was concentrated to 10mg/ml and crystallised just as well between 1.6M-2.5M $(NH_4)_2SO_4$.

Yellow trapezial crystals were produced and crystals grew at temperatures of 17°C, 37°C and 60°C. Coloration was due to the presence of the PLP cofactor which was not lost during either the crystallisation or the freezing process. This contrasts to the behaviour of the *E.coli* protein, which loses its cofactor under these conditions. Growth was slower at the lower temperatures and at 17°C it took 14 days for crystals to reach an average size of 0.5mm x 0.2mm. Much of the protein had aggregated and many crystals grew through a layer of precipitate in the droplet. Such aggregation would suggest a protein concentration higher than necessary, but reducing this concentration resulted in no crystal formation at all. At the slightly higher temperature of 37°C, crystal growth was slower and the average crystal size after 4 weeks was 0.3mm x 0.2mm x 0.2mm. Crystals grew at concentrations between 0.5M-0.7M $(NH_4)_2SO_4$ and there was no precipitate observed in these wells. At 60°C, crystals grew under the same precipitant conditions observed at 17°C and attained the same average size after only 7 days.

All crystals were grown by the vapour diffusion method and trials at 17°C were conducted using the hanging drop technique. The sitting drop version was employed for trials at 37°C and 60°C, as this method offers better retention of the well solution at higher temperatures, and avoids drying of the droplets.

Crystals were mounted on cryoloops and frozen in liquid nitrogen after protecting them from freezing damage with Paraton N oil. This was found to preserve the crystals, which dissolved slowly on contact with a more traditional cryoprotectant made by addition of glycerol to the mother liquor.

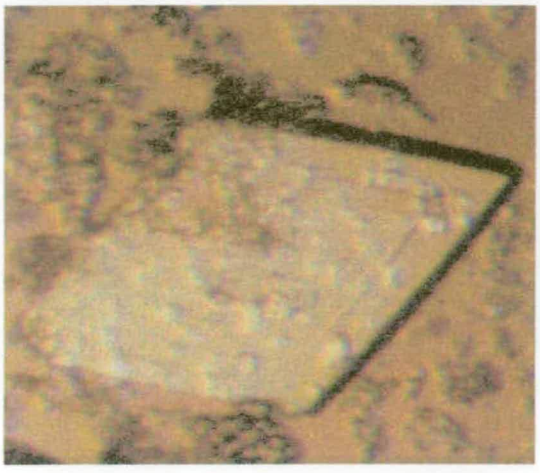

Figure 5.11.1

Crystal grown at 60°C. Rhombic crystals were grown by the sitting drop method and achieved a maximum size of 0.5mm x 0.2mm within 7 days.

5.12 Data Collection

An initial study of the viability of a crystal for X-ray diffraction was conducted at the Structural Biology on-site facility in Edinburgh. Data was collected over an exposure time of 30 minutes at 100K using a MAR research 345mm image plate at a distance of 300mm from the crystal. Most of the crystals were twinned, but a single crystal grown at 60°C diffracted to a maximum resolution of 4.6Å and was taken forward to SRS CLRC Daresbury Laboratory, Warrington, UK for data collection.

X-ray diffraction data was collected at station 7.2 at 100K using a MAR research 345mm image plate at a crystal-to-detector distance of 300mm for 181.6° at an oscillation angle of 0.8°. The wavelength was

λ = 1.488Å. High resolution data was collected over an 18 hour period in the range 20Å-2.94Å. The image plate was set at a distance of 300mm. A second pass of 180° with an oscillation angle of 3° and detector set at 500mm provided low resolution data between 30Å-4.6Å. Data was processed and scaled using DENZO/SCALEPACK software (124).

Crystallographic data was consistent with the space group; $P2_12_12$. The unit cell was relatively large with dimensions of a = 159.93, b = 188.16, c = 95.13 and unit angles $\alpha=\beta=\gamma=90°$.

Table 5.7

Crystal diffraction parameters. Data was collected in two passes, reflecting high and low resolution data sets. These were processed and scaled using DENZO/SCALEPACK. Values in parentheses are for the high resolution shell 3.36Å-2.94Å

	AONS holoenzyme
Space group	$p2_12_12$
Unit cell dimensions (Å)	a = 159.93, b = 188.16, c = 95.13
Unit cell volume ($Å^3$)	2.8 x 10^6
Completeness (%)	99.6 (98.8)
$I > 3\sigma(I)$ (%)	32.8 (66.2)
R_{merge} (%)	11.1 (49.9)
Unique reflections	55,562
Multiplicity	7.9 (6.0)

The space group indicates a primitive lattice arrangement, indicating that there is one lattice point per unit cell, with no recurring points on the face or centre of the cell.

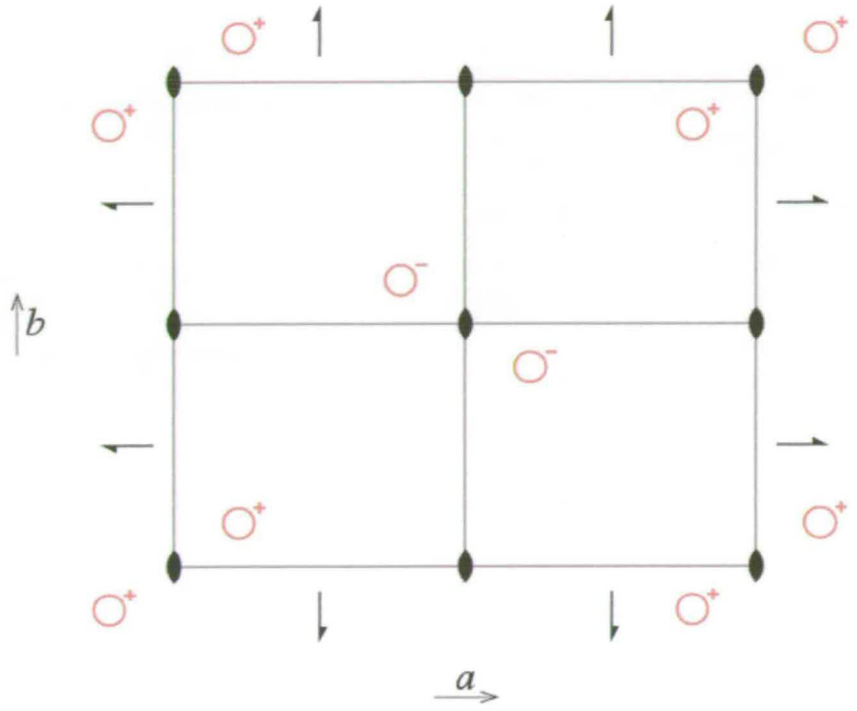

Figure 5.12.1

Space group $P2_12_12$. The origin is in the plane of the paper, and black shaded areas indicate the two-fold dyad axis parallel to the *c* axis through the plane of the paper. O^+ indicates a molecule above the plane of the paper, and O^- indicates one below this plane. The half arrows represent the positions of the two-fold screw axes.

The space group also displays perpendicular screw axes parallel to *a* and *b* and a single two-fold rotation axis parallel to the *c* axis. This space group also indicates the relationship between the four asymmetric units located within the cell: x,y,z; ½ + x, ½ + y, -z; ½ - x, ½ + y, z; -x, -y, z. Any atom is present in four copies at each of these positions in the cell.

5.13 Data Resolution

The temperature factor of the data was elevated, at 60.2Å^2, as estimated from the Wilson Plot.

Patterson maps were calculated using diffraction data in the resolution range 30Å-2.94Å. A large translation peak was observed at fractional co-ordinates of 0.243 x 0.500 x 0.500, the height of which was one third of an arbitrary origin. The co-ordinates of the translation peak define the non-crystallographic translational symmetry operators, which will be used to find the arrangement of molecules within the unit cell.

The phase problem was much simplified as the structure of *E.coli* AONS had already been solved (37), and can be used as a model for the molecular replacement method (126). The crystallographic were space group $P2_12_12$ was confirmed by molecular replacement, which was most successful using this space group.

Due to the large volume of the unit cell, there was some doubt over the number of protein molecules within the asymmetric unit of the cell. The *E.coli* enzyme exists as a dimer, and gel filtration studies have indicated that the same is true for the *A.aeolicus* enzyme (see section 5.2). The Matthew's coefficient (Vm) can be calculated using equation 3 and defines the crystal volume per unit of protein molecular weight (193).

$$Vm = \frac{V}{M.Z} \quad \text{.....Equation 3}$$

where V(Å^3) is cell volume; M (Da) is relative molecular weight; Z is the number of molecules in the unit cell

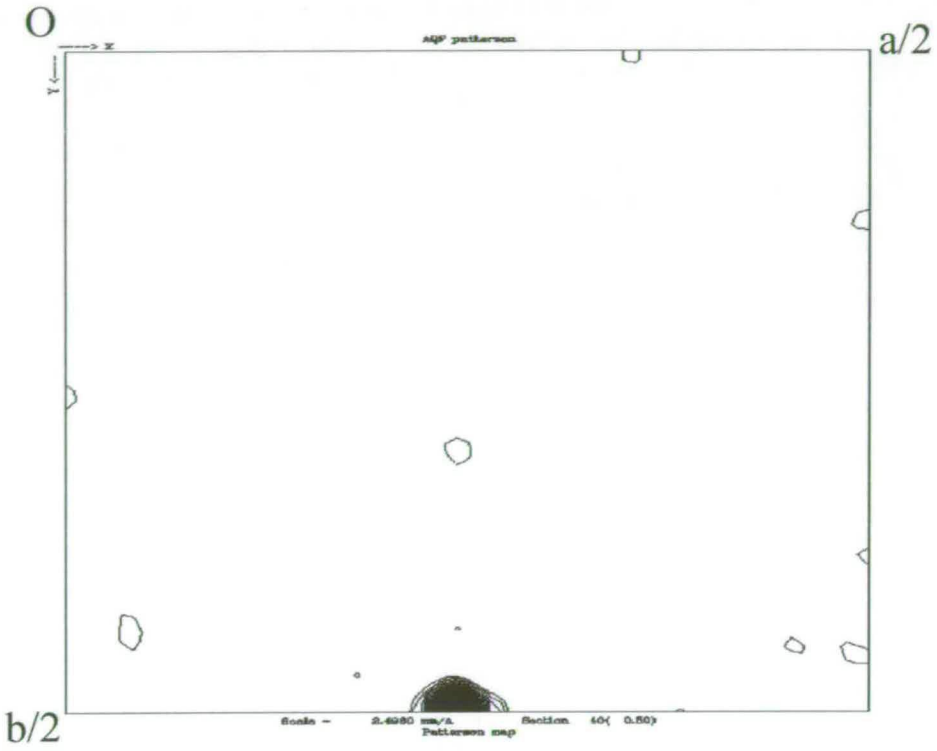

Figure 5.13.1

Patterson Map. The map was calculated using the CCP4 suite of programs and shows a single large translation peak at 0.243x0.500x0.500.

The CCP4 program Matthews was used to calculate Matthews' coefficients. The mass of each subunit is 42,306 Da (see section 3.2) and a $P2_12_12$ space group allows four possible asymmetric units within the unit cell (see section 5.12). Thus Vm = 8.27 $Å^3Da^{-1}$ for one dimer and 2.76 $Å^3Da^{-1}$ for three dimers, or six subunits. The most commonly observed coefficient is approximately 2.15 $Å^3Da^{-1}$ (193), thus up to fours dimers in the asymmetric unit would not be impossible.

Using the AONS structure from *E.coli* as the molecular replacement model, the dimer did not produce an interpretable rotation function. With the monomer, however, the two best solutions showed the monomeric protein arranged in a dimeric conformation similar to that already established for the *E.coli* enzyme. This dimer was used as the new search model for molecular replacement and two further dimers were identified.

AONS from *B.sphaericus*[5] has a higher sequence identity to *A.aeolicus* AONS (see section 5.5) and molecular replacement studies were repeated using the *B.sphaericus* dimer rather than the *E.coli* monomer as the model (table 5.8). This not only confirmed the solutions previously identified with *E.coli*, but provided a significant improvement of the molecular replacement solutions found.

Three Rf peaks were superior to the subsequent solutions, which displayed Rf values of 4.54σ and below. Each rotation function solution was used to search for an appropriate translation function, which would specify the location of the dimer in the asymmetric unit. As each dimer was added to the model, the correlation factor increased to a final value of 0.362 for the six subunit solution with an R factor of 52.6% (Table 5.9).

Table 5.8

Molecular Replacement solutions for *A.aeolicus* AONS. The *B.sphaericus* AONS dimer was used as the model molecule.

Solution	α (alpha)	β (beta)	γ (gamma)	θ (theta)	ϕ (phi)	χ (chi)	Rf	Rf/σ (sigma)
1	71.32	74.53	47.07	41.53	102.12	131.9	$0.4072E^{-5}$	13.36
2	83.78	44.41	137.8	156.41	-117.01	141.63	$0.2144E^{-5}$	7.04
3	165.16	27.2	147.71	28.52	-131.27	59.01	$0.2122E^{-5}$	6.96

[5] The co-ordinates for this macromolecule were communicated to D. Alexeev from C. Cambillau, France

The NCS dyad axis relating the two monomers of the dimeric molecular replacement model is parallel to *y* for the first Rf solution. This gives a translation function peak consistent with the observed translation function peak in the Patterson map.

Table 5.9

Translation search for each of the three rotation function solutions. These were calculated using the three dimeric rotation functions. R factors and correlation coefficients are the result of a cumulative effect for all subunits.

Rotation solution	α (alpha)	β (beta)	γ (gamma)	xfrac	yfrac	zfrac	R factor	Correlation
1	71.32	74.53	47.07	0.412	0.472	0.088	0.565	0.295
2	83.78	44.41	137.8	0.238	0.978	0.426	0.538	0.302
3	165.16	27.2	241.71	0.670	0.066	0.422	0.526	0.362

The dimer clustering observed in the graphical representation of the unit cell suggested room for a fourth dimer within the asymmetric unit, although there was no molecular replacement solution to reinforce this observation.

5.14 Structure Refinement

Based on the sequence alignment of *A.aeolicus* and *B.sphaericus* AONS, the amino acid residues of the latter were replaced with those of the heat stable protein. The resulting model was displayed over the average electron density map, which was calculated using CNS suite of programs (128) and averaged using the CCP4 suite of programs. All graphical data was viewed in O on a Silicon Graphics workstation.

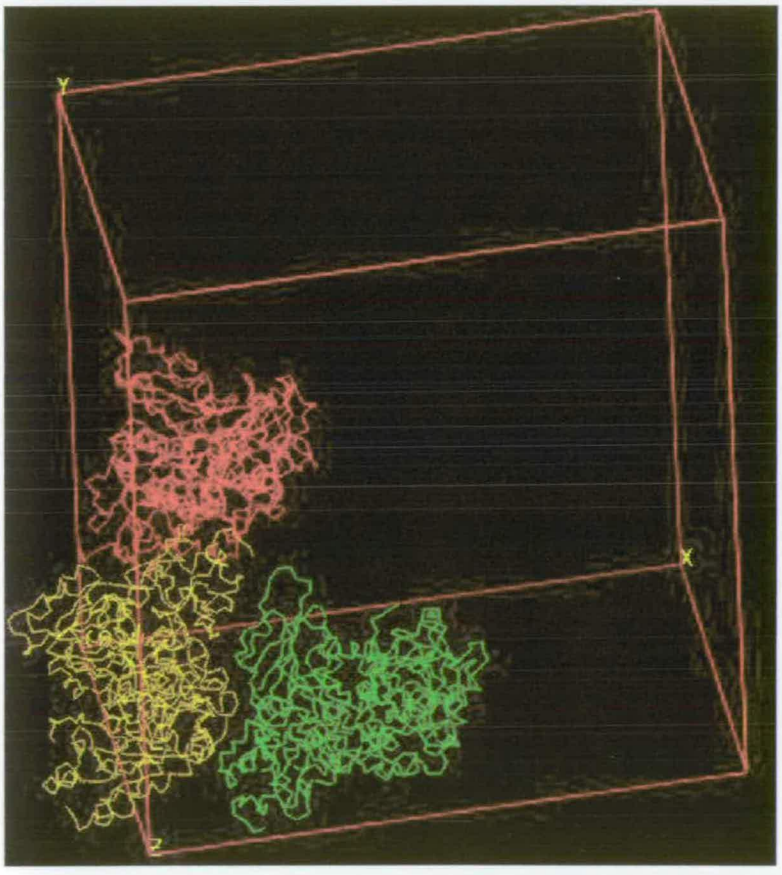

Figure 5.14.1

Probable unit cell make-up using dimeric *B.sphaericus* AONS molecules fitted to the *A.aeolicus* AONS X-ray data. Clustering of the subunits suggests room for a fourth dimer. The diagram was created in O.

The molecular model was manipulated to fit the electron density maps $2F_o$-F_c and F_o-F_c, and the maps recalculated. The initial refinement factor (R factor) of the data to the electron density maps was 52%. Manual adjustment of the residues in the map was carried out many times, but the R factor did not go below 49%, suggesting a possible error in the initial data. As the majority of crystals tested were twinned, and the spot pattern from the processed data set far from perfect, it is possible that the quality of this crystal was not good enough for structural studies. Further refinement of this data is thus now beyond the realms of this project.

Discussion

Over-expression of the hyperthermostable protein in a functional form was achieved in *E.coli* at 37°C, indicating that a high temperature is not required for correct folding of the enzyme. Post-translational modification of *A.aeolicus* AONS, in the form of loss of the N-terminal methionine, was also observed, despite the presence of a mutated second residue. Correct folding of the enzyme at temperatures well below its native surroundings suggest that the conformational fold of the protein is stable over a wide temperature range. Other recombinant proteins of a thermophilic origin expressed in a mesophilic host generally have the same properties as their mesophilic counterparts, indicating that thermostability is an intrinsic property (140). *A.aeolicus* AONS becomes unstable, however, when purification takes place at 4°C. This is consistent with observations by Jaenicke and Böhm (152) on refolding of the heat stable protein, glyceraldehyde 3-phosphate dehydrodgenase (GAPDH). This enzyme folded incorrectly at temperatures below 10°C. Conclusions as to why this might be the case are, as yet, unclear, but the inefficient packing of hydrophobic core may form part of the cause. Hydrophobic packing is prevalent in hyperthermophilic globular proteins (162), in particular those with an optimum activity below 100°C (160) (161). It has been suggested (165) that hydrophobic interactions may become weaker below room temperature and specific hydrophobic states, which may be critical for subunit assembly of the dimer are not attained (194).

Initial kinetic studies of *A.aeolicus* AONS suggest that the catalytic mechanism for this hyperthermostable enzyme is similar to the *E.coli* enzyme, which has been suggested to follow an ordered bi bi pathway (36) (178). The hyperthermostable protein is active both at low and also very high temperatures, indicating a flexible active site. Activity at 30°C is comparable to the mesophilic *E.coli* and *B.sphaericus* enzymes, an observation consistent with the activity of thermophilic aspartate aminotransferase from *Thermus thermophilus* (195) which displays a similar activity at lower

temperatures to its mesophilic counterpart. As activity is seen to increase at higher temperatures, this kinetic observation would suggest that catalysis is less than optimal at 30°C, and indeed, a higher turnover is observed at temperatures up to 80°C. Activity was observed to decrease slowly between 80°C and 100°C, possible due to microprecipitation of the protein. This observation is consistent with enzyme activity within a bacterium surviving at 89°C and is comparable to other heat stable enzymes studied (161) (174) (196). Assays at 60°C and 80°C indicate that specificity of the enzyme for L-alanine is enhanced at elevated temperatures, suggesting a conformational change in the protein may occur.

Although the turnover of *A.aeolicus* AONS approximates that of the *E.coli* enzyme at 30°C, both proteins are active at one fifth of the rate reported for the *B.sphaericus* enzyme. It should be noted here, however, that the assay methods were different. Sequencing has shown that the majority of active site residues are conserved throughout all AONS sequences, but it is possible that the aspartate/phenylalanine couple in both *A.aeolicus* and *B.sphaericus* enzymes has an influence on the rate of reaction, and thus the turnover.

On addition of the first substrate of the reaction, L-alanine, an intermediate is observed with a wavelength at 490nm. This has been assigned to the formation of the first reaction quinonoid and is seen in *E.coli* AONS only after addition of the second substrate, pimeloyl-CoA (36). The quinonoid is the result of abstraction of the C_2 proton (197) (39) and modelling has suggested this intermediate may be stabilised by a strictly conserved active site asparagine (N47 in *E.coli* AONS). In the *E.coli* enzyme, Webster *et al* (36) demonstrate that there is a time lag on addition of pimeloyl-CoA and suggest that it is necessary to confer a rotation about the Cα-N bond in order to place the C_2 proton closer to the critical PLP binding lysine, allowing proton abstraction by the base and thus the quinonoid is not seen on addition of L-alanine alone. Ploux *et al* (39) also suggest that the presence of both substrates is necessary to optimise heterolytic cleavage of the C_2-H bond, as rupturing of this bond is slow. However, a stereospecific exchange of the C_2 proton by an active site base has also been observed in the *B.sphaericus*

enzyme in the absence of pimeloyl-CoA. This may suggest that proton abstraction occurs as a result of binding of the amino acid substrate, but the formation of the quinonoid intermediate proceeds too fast in *E.coli* to allow the quinonoid to be visible by UV/visible spectroscopy. The lag that is observed in this enzyme upon pimeloyl-CoA binding may be as a result of the conformational shift around the C_α-COO^- bond, placing it orthogonal to the pyridine ring of the cofactor ready for decarboxylation. Thus it may be postulated that slowing the reaction of L-alanine with the cofactor by incubation of the heat stable *A.aeolicus* enzyme at 30°C allows observation of the quinonoid. This phenomenon is also seen in the ALAS enzyme of *Rhodobacter sphaeroides* (49) in the form of a peak at 510nm, which is observed on addition of glycine. Analogous to *A.aeolicus* AONS, the peak is enhanced on titration of the amino acid substrate. This peak has, however, not been observed in the erythroid form of ALAS (50) (177), which has been well characterised. Comparison of the protein sequence of the *R.sphaeroides* enzyme (198) with that of mouse erythroid ALAS (SwissProt accession number: P08680) and the AONS enzymes of *A.aeolicus* and *E.coli* suggest no obvious change in the active site that would enhance quinonoid formation to a degree that it is visible by UV/visible spectroscopy. Measurement of the equilibrium dissociation constant for L-alanine in the micromolar range would also suggest that the quinonoid equilibrium is more favourable than internal/external aldimine formation. This would confirm the theory that the quinonoid generally is in fast equilibrium with its precursor aldimine, an observation substantiated by the activity of *A.aeolicus* AONS at high temperature, which fails to display a visible quinonoid with larger concentrations of L-alanine.

The absence of a visible quinonoid after titration of the mutant protein H118F/AONS with L-alanine would suggest that removal of the histidine residue reduces the thermodynamic favourability of quinonoid formation. However, kinetic assays confirm that C_2 proton abstraction and thioester bond cleavage must occur within the active site as an activity can be measured for the mutant enzyme. This activity is reduced, however, and possible misalignment of the cofactor, which hinders displacement of

the active site lysine residue by the incoming amino acid substrate, may be the cause. Subsequent reaction with the second substrate is thus also reduced.

The increased affinity of *A.aeolicus* AONS for its cofactor already suggests a change in the configuration of the active site to favour retention of PLP. A serine residue is apparent at position 222 in the sequence. The corresponding residue in *E.coli* is glycine 235 and it has already been established that PLP binding to this enzyme is much weaker than its thermophilic counterpart. Comparison of cofactor binding observed in the HF mutants of both *E.coli* and *A.aeolicus* enzymes would also suggest a further stabilising factor present in the active site of the heat stable protein. Sequence alignment suggests that this residue may be either a glycine or a serine. Both are aliphatic residues, but serine contains a hydroxyl group. As this residue is adjacent to the crucial lysine residue responsible for cofactor binding (see section 1.2.1), it is possible that it forms an hydrogen bond with the phosphate of the PLP cofactor, thus stabilising it further in the active site. Comparison of all AONS sequences known with established evolutionary patterns (199) would suggest that the serine/phenylalanine/aspartate active site, as seen in *A.aeolicus* and Methanococcus *jannaschii*, combination evolved first. The initial change to this group was possibly the phenylalanine/tyrosine switch in the contributory opposite monomer. The greatest flexibility is indicated for the acidic residues aspartate and glutamate, although it is unclear when these changes occurred. However, the serine/aspartate and glycine/glutamate combinations seem to be favoured (see Appendix I). The C-terminal region, corresponding to the area of conformational change observed in *E.coli* AONS on binding of the product (AON) to the cofactor, is well conserved throughout all species.

Many extremophiles belong to Archea (143) (199) and only a few to the genera of Eubacteria. *A.aeolicus* is only the second genome of an eubacterial hyperthermophile to be completely sequenced (www.ebi.ac.uk/genomes/). To date there have been few studies on hyperthemophilic PLP dependent enzymes from Eubacteria. Initial observations of the *A.aeolicus* enzyme have indicated that the catalytic

mechanism is similar to that previously established, but the real difference lies in the ability of the enzyme to function at 80°C, although how this is achieved is still unclear. A strategy common to temperature stability in proteins is an increase in ion pair networks (152) (173) and the fact that one third of the *A.aeolicus* AONS enzyme sequence, (compared to one fifth in the *E.coli* protein) is composed of charged residues suggests this may be a strategy for temperature stability in this protein. The unrefined structure already suggests tighter packing of some α-helices within the protein, and a reduced N-terminal region compared to *E.coli* and *B.sphaericus* proteins. It is already established that glutamine and asparagine residues are replaced by glutamate and aspartate residues in heat stable proteins. The conservation of both asparagine residues within the active site of AONS suggests that they are vital for activity of the enzyme. Modelling in the *E.coli* enzyme (36) has already indicated that N47 is necessary for stabilising the first quinonoid intermediate, thus it may not be unreasonable to suggest that the second asparagine residue (N112 in *E.coli*) is also involved in the thermodynamic stability of AONS catalysis. Further comparison must await final refinement of the *A.aeolicus* structure.

A section of this chapter has been submitted to Acta Crystallographica, Section D.

Chapter 6
References

6.1 References

1. Dakshinamurti, K., and Chauhan, J. (1988) *Ann. Rev. Nutr.* **8,** 211-233
2. Samolo, D., Thornton, C. G., Murtif, V. L., Kumar, G. K., Haase, F. C., and Wood, H. G. (1988) *J. Biol. Chem.* **263**(14), 6461-6464
3. Knowles, J. (1989) *Ann. Rev. Biochem.* **58,** 195-221
4. Trotter, J., and Hamilton, J. A. (1966) *Biochem.* **5**(2), 713-714
5. Goodall, G. J., Prager, R., Wallace, J. C., and Keech, D. B. (1983) *FEBS Letts* **163**(1), 6-9
6. Alban, C., Job, D., and Douce, R. (2000) *Ann. Rev. Plant Physiol. and Plant Mol. Biol.* **51,** 17-47
7. Sweetman, L., and Nyhan, W. L. (1986) *Ann. Rev. Nutr.* **6,** 317-343
8. Speck, D., Ohsawa, I., Gloeckler, R., Zinsius, Z., Bernard, S., Ledoux, C., Kisou, T., Kamogawa, K., and Lemoine, Y. (1991) *Gene* **106,** 39-45
9. Wilchek, M., and Bayer, E. A. (1988) *Anal. Biochem.* **171,** 1-32
10. Green, N. M. (1963) *Biochem. J.* **89,** 599
11. Hillier, Y., Gershoni, J. M., Bayer, E. A., and Wilchek, M. (1987) *Biochem. J.* **248,** 167-171
12. Lindqvist, Y., and Schneider, G. (1996) *Curr. Opinion in Struct. Biol.* **6,** 798-803
13. Eisenberg, M. A. (1966) *Biochem. J.* **101,** 598-606
14. Eisenberg, M. A. (1975) *Metabolic Pathways*, 27, Academic Press, New York
15. Neidhardt, F. C. (ed) (1996) *Escherichia coli and Salmonella typhimurium: cellular and molecular biology*, 2nd Ed., ASM Press, Washington D.C.
16. Baldet, P., Gerbling, H., Axiotis, S., and Douce, R. (1993a) *Eur. J. Biochem.* **217,** 479-485
17. Baldet, P., Alban, C., and Douce, R. (1997) *FEBS Letts* **419,** 206-210
18. Cleary, P. P., and Campbell, A. (1972) *J. Baceriolt.* **112,** 830-839
19. Baldet, P., Alban, C., Axiotis, S., and Douce, R. (1993b) *Arch. Biochem. Biophys.* **303,** 67-73
20. Rolfe, B., and Eisenberg, M. A. (1968) *J. Bacteriol.* **96,** 515-524

21. Cleary, P. P., Campbell, A., and Chang, R. (1972) *Proc. Nat. Acad. Sci.* **69**(8), 2219-2223

22. Schwartz, M. (1966) *J. Bacteriol.* **92,** 1083-1089

23. Otsuka, A. J., Buonovistiani, M. R., Howard, P. K., Flamm, J., Johnson, C., Yamamoto, R., Uchida, K., Cook, C., Ruppert, J., and Matsuzaki, J. (1988) *J. Biol. Chem.* **263,** 19577-19585

24. Guha, A. (1971) *J. Mol. Biol* **56,** 53-62

25. Otsuka, A. J., and J., A. (1978) *Nature* **276,** 689-693

26. Wu, C.-H., Chen, H.-Y., and Shiuan, D. (1996) *Gene* **174,** 251-258

27. Sakurai, N., Imai, Y., Masuda, M., Komatsubara, S., and Tosa, T. (1993) *Appl. Environ. Microbiol.* **59**(9), 2857-2863

28. Shiuan, D., and Campbell, A. (1988) *Gene* **67,** 203-211

29. Simpson, A. J. G., Reinach, F. C., Arruda, P., Abreu, F. A., Acencio, M., Alvarenga, R., Alves, L. M. C., Araya, J. E., Baia, G. S., Baptista, C. S., Barros, M. H., Bonaccorsi, E. D., Bordin, S., Bove, J. M., Briones, M. R. S., Bueno, M. R. P., Camargo, A. A., Camargo, L. E. A., Carraro, D. M., Carrer, H., Colauto, N. B., Colombo, C., Costa, F. F., Costa, M. C. R., Costa-Neto, C. M., Coutinho, L. L., Cristofani, M., Dias-Neto, E., Docena, C., El-Dorry, H., Facincani, A. P., Ferreira, A. J. S., Ferreira, V. C. A., Ferro, J. A., Fraga, J. S., Franca, S. C., Franco, M. C., Frohme, M., Furlan, L. R., Garnier, M., Goldman, G. H., Goldman, M. H. S., Gomes, S. L., Gruber, A., Ho, P. L., Hoheisel, J. D., Junqueira, M. L., Kemper, E. L., Kitajima, J. P., Krieger, J. E., Kuramae, E. E., Laigret, F., Lambais, M. R., Leite, L. C. C., Lemos, E. G. M., Lemos, M. V. F., Lopes, S. A., Lopes, C. R., Machado, J. A., Machado, M. A., Madeira, A. M. B. N., Madeira, H. M. F., Marino, C. L., Marques, M. V., Martins, E. A. L., Martins, E. M. F., Matsukuma, A. Y., Menck, C. F. M., Miracca, E. C., Miyaki, C. Y., Monteiro-Vitorello, C. B., Moon, D. H., Nagai, M. A., Nascimento, A. L. T. O., Netto L.E.S., Nhani, A., Nobrega, F. G., Nunes, L. R., Oliveira, M. A., de Oliveira, M. C., de Oliveira, R. C., Palmieri, D. A., Paris, A., Peixoto, B. R., Pereira, G. A. G., Pereira, H. A., Pesquero, J. B., Quaggio, R. B., Roberto, P. G., Rodrigues, V., Rosa, A. J. D., de

Rosa, V. E., de Sa, R. G., Santelli, R. V., Sawasaki, H. E., da Silva, A. C. R., da Silva, A. M., da Silva, F. R., Silva, W. A., da Silveira, J. F., et al. (2000) *Nature* **406**(6792), 151-157

30. Perkins, J. B., Bower, S., Howitt, C. L., Rogers Yocum, R., and Pero, J. (1996) *J. Bact.* **178**(21), 6361-6365

31. Gloeckler, R., Ohsawa, I., Speck, D., Ledoux, C., Bernard, S., Zinsius, M., Villeval, D., Kisou, T., Kamogawa, K., and Lemoine, Y. (1990) *Gene* **87**, 63-70

32. Hatakeyama, K., Kohama, K., Verteo, A. A., Kobayashi, H., Kurusu, Y., and Yukawa, H. (1993) *DNA seq.* **4**, 177-184

33. Deckert, G., Warren P.V., Gaasterland T., Young W.G., Lenox A.L., Graham D.E., Overbeek R., Snead M.A., Keller M., Aujay M., Huber R., Feldman R.A., Short J.M., Olsen G.J., and Swanson R.V. (1998) *Nature* **392**, 353-358

34. Levy-Schil, S., Debussche, L., Rigault, S., Soubrier, F., Baccetta, F., Lagneaux, D., Schleuniger, J., Blanche, F., Crouzet, J., and Mayaux, J.-F. (1993) *Appl. Microbiol. Biotech.* **38**(755-762)

35. Izumi, Y., Morita, H., Tani, Y., and Ogata, K. (1972) *Agr. Biol. Chem.* **36**(3), 519-520

36. Webster, S. P., Alexeev, D., Campopiano, D. J., Watt, R. M., Alexeeva, M., Sawyer, L., and Baxter, R. L. (2000) *Biochem.* **39**, 516-528

37. Alexeev, D., Alexeeva, M., Baxter, R. L., Campopiano, D. J., Webster, S. P., and Sawyer, L. (1998a) *J. Mol. Biol.* **284**, 401-419

38. Ploux, O., and Marquet, A. (1992) *Biochem. J.* **283**, 327-331

39. Ploux, O., and Marquet, A. (1996) *Eur. J. Biochem.* **236**, 301-308

40. Alexander, F. W., Sandmeier, E., Mehta, P. K., and Christen, P. (1994) *Eur. J. Biochem.* **219**, 953-960

41. Zaman, Z., Jordan, P. M., and Akhtar, M. (1973) *Biochem. J.* **135**, 257-263

42. Jordan, P. M. (1991) in *Biosynthesis of Tetrapyroles* (Jordan, P. M., ed), pp. 1-66, Elsevier Science, Amsterdam

43. Merrill, A. H., and Jones, D. D. (1990) *Biochim. Biophys. Acta* **1044**(1), 1-12

44. Mukherjee, J. J., and Dekker, E. E. (1987) *J. Biol. Chem.* **262**(30), 14441-14447

45. Gong, J., Kay, C. J., Barber, M. J., and Ferreira, G. C. (1996) *Biochem.* **35,** 14109-14117

46. Gong, J., Hunter, G. A., and Ferreira, G. C. (1998) *Biochem.* **37,** 3509-3517

47. Hunter, G. A., and Ferreira, G. C. (1995) *Anal. Biochem.* **226,** 221-224

48. Hunter, G. A., and Ferreira, G. C. (1999) *Biochem.* **38,** 3711-3718

49. Nandii, D. L. (1978) *J. Biol. Chem.* **253**(24), 8872-8877

50. Tan, D., and Ferreira, G. C. (1996) *Biochem.* **35,** 8934-8941

51. Tan, D., Harrison, T., Hunter, G. A., and Ferreira, G. C. (1998a) *Biochem* **37,** 1478-1484

52. Tan, D., Barber, M. J., and Ferreira, G. C. (1998b) *Prot. Sci.* **7,** 1208-1213

53. Gable, K., Slife, H., Bacikova, D., Monaghan, E., and Dunn, T. M. (2000) *J. Biol. Chem.* **275**(11), 7597-7603

54. Mehta, P. K., and Christen, P. (1994) *Biochem. Biophys. Res. Comm.* **198**(1), 138-143

55. Toney, M. D., Hohenester, E., Keller, J. W., and Jansonius, J. N. (1995) *J. Mol. Biol.* **245**(2), 151-179

56. Grishin, N. V., Phillips, M. A., and Goldsmith, E. J. (1995) *Prot. Sci.* **4**(7), 1291-1304

57. Stoner, G. L., and Eisenberg, M. A. (1975*b*) *J. Biol. Chem.* **250,** 4037-4043

58. Stoner, G. L., and Eisenberg, M. A. (1975*a*) *J. Biol. Chem.* **250**(11), 4029-4036

59. Kaeck, H., Sandmark, J., Gibson, K., Schneider, G., „ and Lindqvist, Y. (1999) *J. Mol. Biol.* **291,** 857-876

60. Ford, G. C., Eichele, G., and Jansonius, J. (1980) *Proc. Natl. Acad. Sci. USA* **77,** 2559-2563

61. Mehta, P., Hale, T. I., and Christen, P. (1993) *Eur. J. Biochem.* **214**(2), 549-561

62. Shah, S. A., Shew, B. W., and Brunger, A. T. (1997) *Structure* **5**(8), 1067-1075

63. Eisenberg, M. A., and Krell, K. (eds) (1979) *Dethiobiotin Synthetase* Vol. 62. Methods in Enzymology

64. Alexeev, D., Baxter, R. L., and Sawyer, L. (1994b) *Structure* **2,** 1061-1072

65. Schneider, G., and Lindqvist, Y. (1997) *Meth. Enzymol.* **279,** 376-385

66. Krell, K., and Eisenberg, M. A. (1970) *J. Biol. Chem.* **245**(24), 6558-6566

67. Baxter, R. L., Ramsey, A. J., McIver, L. A., and Baxter, H. C. (1994a) *J. Chem. Soc. Chem. Commun.* 559-560

68. Gibson, K. J., Lorimer, G. H., Rendina, A. R., Taylor, W. S., Cohen, G., Gatenby, A. A., Payne, W. G., Roe, D. C., Lockett, B. A., Nudelman, A., Marcovici, D., Nachun, A., Wexler, B. A., Marsili, E. L., Turner, I. M., Howe, L. D., Kalbach, C. E., and Chi, H. (1995) *Biochem.* **34,** 10976-10984

69. Huang, W., Jia, J., Gibson, K. J., Taylor, W. S., Rendina, A. R., Schneider, G., and Lindqvist, Y. (1995) *Biochem.* **34,** 10985-10995

70. Alexeev, D., Baxter, R. L., Smekal, O., and Sawyer, L. (1995) *Structure* **3**(11), 1207-1215

71. Baxter, R. L., and Baxter, H. C. (1994b) *J. Chem. Soc. Chem. Commun.* 759-760

72. Gibson, K. J. (1997) *Biochem.* **36,** 8474-8478

73. Alexeev, D., Bury, S. M., Boys, C. W. G., Turner, M. A., Sawyer, L., Ramsey, A. J., Baxter, H. C., and Baxter, R. L. (1994a) *J. Mol. Biol.* **235,** 774-776

74. Huang, W., Lindqvist, Y., Schneider, G., Gibson, K., Flint, D., and Lorimer, G. (1994) *Structure* **2,** 407-414

75. Ifuku, O., Kishimoto, J., Haze, S., Yanagi, M., and Fukushima, S. (1992) *Biosci. Biotech. Biochem.* **56,** 1780-1785

76. Even, L., Florentin, D., and Marquet, A. (1990) *Bull. Soc. Chem. Fr.* **127,** 758-768

77. Sanyal, I., Lee, S., and Flint, D. (1994) *J. Am. Chem. Soc.* **116,** 2637-2638

78. Birch, O. M., Fuhrmann, M., and Shaw, N. M. (1995) *J. Biol. Chem.* **270,** 19158-19165

79. Weaver, L. M., Yu, F., Wurtele, E. S., and Nikolau, B. J. (1996) *Plant Physiol.* **110,** 1021-1028

80. Birch, O. M., Hewitson, K. S., Fuhrmann, M., Burgdorf, K., Baldwin, J. E., Roach, P. L., and Shaw, N. M. (2000) *J. Biol. Chem.* **275**(41), 32277-32280

81. Duin, E. C., Lafferty, M. E., Crouse, B. R., Allen, R. M., Sanyal, I., Flint, D. H., and Johnson, M. K. (1997) *Biochem.* **36,** 11811-11820

82. Tse Sum Bui, B., Florentin, D., Marquet, A., Benda, R., and Trautwein, A. X. (1999) *FEBS Letts* **459,** 411-414

83. Mulliez, E., Fontecave, M., Gaillard, J., and Reichard, P. (1993) *J. Biol. Chem.* **268**(4), 2296-2299

84. Moss, M. L., and Frey, P. A. (1990) *J. Biol. Chem.* **265**(30), 18112-18115

85. Knappe, J., Elbert, S., Frey, M., and Wagner, A. F. V. (1993) *Biochem. Soc. Trans.* **21**(3), 731-734

86. Guianvarc'h, D., Florentin, D., Tse Sum Bui, B., Nunzi, F., and Marquet, A. (1997) *Biochem. Biophys. Res.Comm.* **236,** 402-406

87. Tse Sum Bui, B., Florentin, D., Fournier, F., Ploux, O., Mejean, A., and Marquet, A. (1998) *FEBS Letts* **440,** 226-230

88. Tse Sum Bui, B., Escalettes, F., Chottard, G., Florentin, D., and Marquet, A. (2000) *Eur. J., Biochem.* **267,** 2688-2694

89. Kiyasu, T., Asakura, A., Nagahashi, Y., and Hoshino, T. (2000) *J. Bact.* **182**(10), 2879-2885

90. Zheng, L., White, R. H., Cash, V., and Dean, D. (1994) *Biochem.* **33,** 4714-4720

91. Florentin, D., Bui, B., Marquet, A., Ohshiro, T., and Izumi, Y. (1994) *C R Acad. Sci.* **317,** 485-488

92. Hewitson, K. S., Baldwin, J. E., Shaw, N. M., and Roach, P. L. (2000) *FEBS Letts* **466,** 372-376

93. McIver, L., Leadbeater, C., Campopiano, D. J., Baxter, R. L., Daff, S., Chapman, S. K., and Munro, A. W. (1998) *Eur. J. Biochem.* **257,** 577-585

94. Koga, N., Kishimoto, J., Haze, S., and Ifuku, O. (1996) *J. Ferm. Bioeng.* **81,** 482-487

95. Cronan, J. E. (1989) *Cell* **58,** 427-429

96. Xu, Y., and Beckett, D. (1997) *Meth. Enzym.* **279,** 405-421

97. Eisenberg, M. A. (1984) *Ann. N.Y. Acad. Sci.* **447,** 335-349

98. Barker, D. F., and Campbell, A. M. (1980) *J. Bact.* **143,** 789-800

99. Abbott, J., and Beckett, D. (1993) *Biochem.* **32,** 9649-9656

100. Beckett, D., and Matthews, B. W. (1997) *Meth. Enzym.* **279,** 362-377

101. Bower, S., Perkins, J., Rogers Yocum, R., Serror, P., Sorokin, A., Rahaim, P., Howitt, C. L., Prasad, N., Ehrlich, S. D., and Pero, J. (1995) *J.. Bact.* **177**(9), 2572-2575

84. Moss, M. L., and Frey, P. A. (1990) *J. Biol. Chem.* **265**(30), 18112-18115

85. Knappe, J., Elbert, S., Frey, M., and Wagner, A. F. V. (1993) *Biochem. Soc. Trans.* **21**(3), 731-734

86. Guianvarc'h, D., Florentin, D., Tse Sum Bui, B., Nunzi, F., and Marquet, A. (1997) *Biochem. Biophys. Res.Comm.* **236,** 402-406

87. Tse Sum Bui, B., Florentin, D., Fournier, F., Ploux, O., Mejean, A., and Marquet, A. (1998) *FEBS Letts* **440,** 226-230

88. Tse Sum Bui, B., Escalettes, F., Chottard, G., Florentin, D., and Marquet, A. (2000) *Eur. J., Biochem.* **267,** 2688-2694

89. Kiyasu, T., Asakura, A., Nagahashi, Y., and Hoshino, T. (2000) *J. Bact.* **182**(10), 2879-2885

90. Zheng, L., White, R. H., Cash, V., and Dean, D. (1994) *Biochem.* **33,** 4714-4720

91. Florentin, D., Bui, B., Marquet, A., Ohshiro, T., and Izumi, Y. (1994) *C R Acad. Sci.* **317,** 485-488

92. Hewitson, K. S., Baldwin, J. E., Shaw, N. M., and Roach, P. L. (2000) *FEBS Letts* **466,** 372-376

93. McIver, L., Leadbeater, C., Campopiano, D. J., Baxter, R. L., Daff, S., Chapman, S. K., and Munro, A. W. (1998) *Eur. J. Biochem.* **257,** 577-585

94. Koga, N., Kishimoto, J., Haze, S., and Ifuku, O. (1996) *J. Ferm. Bioeng.* **81,** 482-487

95. Cronan, J. E. (1989) *Cell* **58,** 427-429

96. Xu, Y., and Beckett, D. (1997) *Meth. Enzym.* **279,** 405-421

97. Eisenberg, M. A. (1984) *Ann. N.Y. Acad. Sci.* **447,** 335-349

98. Barker, D. F., and Campbell, A. M. (1980) *J. Bact.* **143,** 789-800

99. Abbott, J., and Beckett, D. (1993) *Biochem.* **32,** 9649-9656

100. Beckett, D., and Matthews, B. W. (1997) *Meth. Enzym.* **279,** 362-377

101. Bower, S., Perkins, J., Rogers Yocum, R., Serror, P., Sorokin, A., Rahaim, P., Howitt, C. L., Prasad, N., Ehrlich, S. D., and Pero, J. (1995) *J.. Bact.* **177**(9), 2572-2575

102. Tissot, G., Pepin, R., Job, D., Douce, R., and Alban, C. (1996) *Eur. J. Biochem.* **258,** 586-96

103. Metzler, D. E., Ikawa, M., and Snell, E. E. (1953) *The Clayton Foundation for Research*

104. Hayashi, H. (1995) *J. Biochem.* **118,** 463-473

105. Metzler, D. E. (1977) *Biochemistry*, Academic Press

106. Ahmed, S. A., McPhie, P., and Miles, E. W. (1996) *J. Biol. Chem.* **271**(15), 8612-8617

107. John, R. A. (1995) *Biochim. Biophys. Acta* **1248,** 81-96

108. Dunathan, H. C. (1966) *Proc. Natl. Acad. Sci. USA* **55,** 712-716

109. Dunathan, H. C., and Voegt, J. C. (1974) *Proc. Natl. Acad. Sci. USA* **71**(10), 3888-3891

110. Jencks, W. (1975) *Adv. Enzymol.* **43,** 219-410

111. Jansonius, J. N. (1998) *Curr. Opin. Struct. Biol.* **8**(6), 759-769

112. Denessiouk, K., Denesyuk, A., L.,, Lehtonen, J. V., Korpele, T., and Johnson, M. S. (1999) *Proteins* **35,** 250-261

113. Sun, S., and Toney, M. D. (1999) *Biochem.* **38,** 4058-4065

114. Yanisch-Perron, C., Viera, J., and Messing, J. (1985) *Gene* **33,** 103-108

115. Grant, S. G. N. (1990) *Proc. Natl. Acad Sci* USA **87,** 4645 - 4649

116. Phillips, T. A., Van Bogelen, R. A., and Neidhardt, F. C. (1984) *J.Bacteriol.* **159,** 283-287

117. Maniatis, T., Fritsch, E. F., and Sambrook, J. (1982) Molecular Cloning

118. Laemmeli, U. K. (1970) *Nature* **227,** 680-685

119. Deutscher, e. a. (1990) *Guide to Protein Purification.* Methods in Enzymology (Deutscher, M. P., Ed.), 182, Academic Press Inc.

120. Bradford, M. M. (1976) *Anal. Biochem.* **72**(248-254)

121. Sarker, G., and Sommers, S. S. (1990) *BioTechniques* **8,** 404-407

122. Sanger, F., Nicklen, S., and Coulson, A. R. (1977) *Proc. Natl. Acad. Sci. USA* **74,** 5463-5467

123. Rossmann, M. G., and van Beek, C. G. (1999) *Acta Cryst. Sect. D* **55**(10), 1631-1640

124. Otwinowski, Z. (1993) in *CCP4 Study Weekend* (Sawyer, L., Isaacs, N., and Bailey, S., eds), pp. 56-62, Daresbury Laboratory, Warrington, England

125. Bailey, S. (1994) *Acta Cryst. Sect. D* **50**(5), 760-763

126. Vagin, A., and Teplyakov, A. (1997) *J. App. Cryst.* **30**(6), 1022-1025

127. Jones, T. A., Zou, J. Y., Cowan, S. W., and Kjeldgaard, M. (1991) *Acta Ctyst. Sect. A* **47**(Pt2), 110-119

128. Brunger, A. T., Adams, P. D., Clore, C. D., Delano, W. L., Gros, P., Grosse-Kunstleve, R. W., Jiang, J.-S., Kuszemski, J., Nilges, N., Pannu, N. S., Reed, R. J., Rice, L. M., Simonson, T., and Warren, G. L. (1998) *Acta Cryst.* **D54,** 905-921

129. Metzler, C. M., Harris, A. G., and Metzler, D. E. (1988) *Biochem.* **27** 4923-4933

130. Toney, M. D., and Kirsch, J. F. (1993) *Biochem.* **32,** 1471-1479

131. Rege, V. D., Kredich, N. M., Tai, C.-H., Karsten, W. E., Schnackerz, K. D., and Cook, P. F. (1996) *Biochem.* **35,** 13485-13493

132. Schirch, D., Delle Fratte, S., Iurescia, S., Angelaccio, S., Contestabile, R., Bossa, F., and Scirch, V. (1993) *J. Biol. Chem.* **268**(31), 23132-23138

133. Watanabe, A., Kurokawa, Y., Yoshimura, T., Kurihara, T., Soda, K., and Esaki, N. (1999) *J. Biol. Chem.* **274**(7), 4189-4194

134. White M.F., Vasquez, J., Yang, S., and Kirsch, J. F. (1994) *Biochem.* **91,** 12428-12432

135. Burkhard, P., Tai, C.-H., Ristroph, C. M., Cook, P. F., and Jansonius, J. N. (1999) *J. Mol. Biol.* **291,** 941-953

136. Szebenyi, D. M. E., Liu, X., Kriksunov, I. A., Stover, P. J., and Thiel, D. J. (2000) *Biochem.* **39,** 13313-13323

137. Jagath, J. R., Sharma, B., Rao, N. A., and Savithri, H. S. (1997) *J. Biol. Chem.* **272** (39), 24355-24362

138. Tramonti, A., De Biase, D., Giartosio, A., Bossa, F., and John, R. A. (1998) *J. Biol. Chem.* **279**(4), 1939-1945

139. Persidis, A. (1998) *Nature Biotech.* **16**(6), 593-594

140. Danson, M. J., and Hough, D. W. (1998) *TIMS* **6**(8), 307-314

141. Adams, M. W. W. (1994) *FEMS Microbiol. Rev.* **15**(2), 261-277

142. Blöchl, E., Rachel, R., Burggraf, S., Hafenbradl, D., Jannasch, H. W., and Stetter, K. O. (1997) *Extremophiles* **1**(1), 14-21

143. Stetter, K. O. (1999) *FEBS letts.* **452,** 22-25

144. Nelson, K. E., Clayton, R. A., Gill, S. R., Gwinn, M. L., Dodson, R. J., Haft, D. H., Hickey, E. K., Peterson, J. D., Nelson, W. C., Ketchum, K. A., McDonald, L., Utterback, T. R., Malek, J. A., Linher, K. D., Garrett, M. M., Stewart, A., M.,, Cotton, M. D., Pratt, M. S., Phillips, C. A., Richardson, D., Heidelberg, J., Sutton, G. G., Fleischmann, R. D., White, O., Salzberg, S. L., Smith, H. O., Venter, J. C., and Fraser, C. M. (1999) *Nature* **399**(6734), 323-329

145. Brown, J. R., and Doolittle, W. F. (1997) *Microbiol. Mol. Biol. Rev.* **61,** 456-502

146. Hoyle, R. (1998) *Nature Biotech.* **16**(4), 312

147. Pennisi, E. (1997) *Science* **276**(5313), 705-706

148. Krah, R., Kozyavkin , S., Slesarev, A. I., and Gellert, M. (1996) *Proc. Natl. Acad. Sci. USA* **93**(1), 106-110

149. Sandman, K., Krzycki, J. A., Dobrinski, B., Lurz, R., and Reeve, J. N. (1990) *Proc. Natl. Acad. Sci. USA* **87**(15), 5788-5791

150. Scandurra, R., Consalvi, V., Chiaraluce, R., Politi, L., and Engle, P. C. (1998) *Biochimie* **80**(11), 933-941

151. Jaenicke, R. (1991) *CIBA Foundation Symposia* **161,** 206-221

152. Jaenicke, R., and Boehm, G. (1998) *Curr. Opin. Struct. Biol.* **8,** 738-748

153. Szilagy, A., and Zavodszky, P. (2000) *Structure.* **8,** 493-504

154. Russell, R. J. M., Ferguson, J. M. C., Hough, D. W., Danson, M. J., and Tayloer, G. L. (1997) *Biochem.* **36,** 9983-9984

155. Lim, J.-H., Yu Y.G., Han Y.S., Cho S-J., Ahn B-Y., Kim S-H., and Y., C. (1997) *J. Mol. Biol.* **270,** 259-274

156. Leggio, L. L., Kalogiannis, S., Bhat, M. K., and Pickersgill, R. W. (1999) *Proteins* **36,** 295-306

157. Shortle, D., Stites, W. E., and Meeker, A. K. (1990) *Biochem.* **39,** 8033-8041

158. Watanabe, E. K., Kitmura K., Hata, Y., Katsube, Y., and Suzuki, Y. (1991) *FEBS Letts* **290,** 221-223

159. Nakai, T., Okada, K., Akutsu, S., Miyahara, I., Kawaguchi, S.-i., Katoa, R., Kuramitsu, S., and Hirotsu, K. (1999) *Biochem.* **38,** 2413-2424

160. Russell, R. J. M., Hough, D. W., Danson, M. J., and Taylor, G. L. (1994) *Structure.* **2,** 1157-1167

161. Jaenicke, R. (1996) *FASEB J.* **10,** 84-92

162. Robb, F. T., and Clark, D. S. (1999) *J. Mol. Microbiol. Biotechnol.* **1,** 101-105

163. Knapp, S., de Vos, W. M., Rice, D., and Ladenstein, R. (1997) *J. Mol. Biol.* **267,** 916-932

164. Yip, K. S. P., Stilllman, T. J., Britton, K. L., Artymiuk, P. J., Baker, P. J., Sedelnikova, S. E., Engel, P. C., Pasquo, A., Chiaraluce, R., Consalvi, V., Scandurra, R., and Rice, D. W. (1995) *Structure* **3,** 1147-1158

165. Privalov, P. L., and Gill, S. J. (1988) *Adv. Prot. Chem* **39,** 191-234

166. Perutz, M. F., and Raidt, H. (1975) *Nature* **255,** 256-259

167. Aguilar, C. F., Sanderson, I., Moracci, M., Ciaramella, M., Nucci, R., Rossi, M., and Pearl, L. H. (1997) *J. Mol. Biol.* **271,** 789-802

168. Pappenberger, G., Schurig, H., and Jaenicke, R. (1997) *J. Mol. Biol.* **274,** 676-683

169. Tomschy, A., Boehm, G., and Jaenicke, R. (1994) *Prot. Eng.* **7,** 1471-1478

170. Merz, A., Knoechel, T., Jansonius, J., and Kirschner, K. (1999) *J. Mol. Biol.* **288,** 753-763

171. Chang, C., Park, B. C., Lee, D.-S., and Suh, S. W. (1999) *J. Mol. Biol.* **288,** 623-634

172. Hennig, M., Darimont, B., Sterner, R., Kirschner, K., and Jansonius, J. (1995) *Structure* **3,** 1295-1306

173. Vogt, G., Woell S., and P. A. (1997) *J. Mol. Biol.* **269,** 631-643

174. Choi, I.-G., Bang, W.-G., Kim, S.-H., and Yu Y.G. (1999) *J. Biol. Chem.* **274**(2), 881-888

175. Remington, S., Wiegand, G., and Huber, R. (1982) *J. Mol. Biol.* **158,** 111-152

176. Wilkins, M. R., Lindskog, I., Gasteiger, E., Bairoch, A., Sanchez, J.-C., Hochstrasser, D. F., and Appel, R. D. (1997) *Electrophoresis* **18**(3-4), 403-408

177. Ferreira, G. C., and Dailey, H. A. (1993) *J. Biol. Chem.* **268**(1), 584-590

178. Segel, I. H. (1975) *Enzyme Kinetics*, John Wiley & Son, New York

179. Bower, S., Pero, J., Perkins, J. B., Rogers Yocum, R., Howitt, C. L., and Rahaim, R. (1996) *J. Bact.* **178**(14), 4122-4130

180. Bult, C. J., White, O., Olsen, G. J., Zhou, L. X., Fleischmann, R. D., Sutton, G. G., Blake, J. A., FitzGerald, L. M., Clayton, R. A., Gocayne, J. D., Kerlavage, A. R., Dougherty, B. A., Tomb, J. F., Adams, M. D., Reich, C. I., Overbeek, R., Kirkness, E. F., Weinstock, K. G., Merrick, J. M., Glodek, A., Scott, J. L., Goeghagen, N. S. M., Weidman, J. F., Fuhrmann, J. L., Nguyen, D., Utterback, T. R., Kelley, J. M., Peterson, J. D., Sadow, P. W., Hanna, M. C., Cotton, M. D., Roberts, K. M., Hurst, M. A., Kaine, B. P., Borodovsky, M., Klenk, H. P., Fraser, C. M., Smith, H. O., Woese, C. R., and Venter, J. C. (1996) *Science* **273**(5278), 1058-1073

181. Cole, S. T., Brosch, R., Parkhill, J., Garnier, T., Churcher, C., Harris, D., Gordon, S. V., Eiglmeier, K., Gas, D., Barry, C. E., Tekaia, F., Badcock, K., Basham, D., Brown, D., Chillingworth, T., Connor, R., Davies, R., Devlin, K., Feltell, T., Gentles, S., Hamlin, N., Holroyd, S., Hornby, T., Jagels, K., Krogh, A., McLean, J., Moule, S., Murphy, L., Oliver, K., Osborne, J., Quail, M. A., Rajandream, M. A., Rogers, J., Rutter, S., Seeger, K., Skelton, J., Squares, R., Squares, S., Sulston, J. E., Taylor, K., Whitehead, S., and Barrell, B. G. (1998) *Nature* **393**(6685), 537-560

182. Fleischmann, R. D., Adams, M. D., White, O., Clayton, R. A., Kirkness, E. F., Kerlavage, A. R., Bult, C. J., Tomb, J. F., Dougherty, B. A., Merrick, J. M., McKenney, K., Sutton, G., Fitzhugh, W., Fields, C., Gocayne, J. D., Scott, J., Shirley, R., Lui, L., Glodek, A., Kelley, J. M., Weidman, J. F., Phillips, C. A., Spriggs, T., Hedblom, E., Cotton, M. D., Utterback, T. R., Hanna, M. C., Nguyen, D. T., Saudek, D. M., Brandon, R. C., Fine, L. D., Fritchman, J. L., Fuhrman, J. L., Geoghagen, N. S. M., Gnehm, C. L., McDonald, L. A., Small, K. V., Fraser, C. M., Smith, H. O., and Venter, J. C. (1995) *Science* **269**(5223), 496-512

183. Smith, D. R., and Robison, K. (1994) *Submitted (MAR-1994) to the EMBL/GenBank/DDBJ databases*

184. Stephens, R. S., Kalman, S., Lammel, C., fan, J., Marathe, R., Aravind, L., Mitchell, W., Olinger, L., Tatusov, R. L., Zhao, Q. X., Koonin, E. V., and Davis, R. W. (1998) *Science* **282**(5389), 754-759

185. Tomb, J. F., White, O., Kerlavage, A. R., Clayton, R. A., Sutton, G. G., Fleischmann, R. D., Ketchum, K. A., Klenk, H. P., Gill, S., Dougherty, B. A., Nelson, K., Quackenbush, J., Zhou, L. X., Kirkness, E. F., Peterson, S., Loftus, B., Richardson, D., Dodson, R., Khalak, H. G., Glodek, A., McKenney, K., Fitzgerald, L. M., Lee, N., Adams, M. D., Hickey, E. K., Berg, D. E., Gocayne, J. D., Utterback, T. R., Peterson, J. D., Kelley, J. M., Cotton, M. D., Weldman, J. M., Fuji, C., Borodovsky, M., Karp, P. D., Smith, H. O., Fraser, C. M., and Venter, J. C. (1997) *Nature* **388**(6642), 539-547

186. Kalman, S., Mitchell, W., Marathe, R., Lammel, C., Fan, L., Hyman, R. W., Olinger, L., Grimwood, L., Davis, R. W., and Stephens, R. S. (1999) *Nat. Genet.* **21**(4), 385-389

187. Kaneko, T., Tanaka, A., Sato, S., Kotani, H., Sazuka, T., Miyajima, N., Sugiura, M., and Tabata, S. (1995) *DNA Res.* **2**, 153-166

188. Parkhill, J., Wren, B. W., Mungall, K., Ketley, J. M., Churcher, C., Basham, D., Chillingworth, T., Davies, R. M., Feltwell, T., Holroyd, S., Jagels, K., Karleyshev, A., Moule, S., Pallen, M. J., Penn, C. W., Quail, M. A., Rajandream, M. A., Rutherford, K. M., van Vliet, A. H. M., Whitehead, S., and Barrell, B. G. (2000a) *Nature* **403**, 665-668

189. Sakurai, N., Akatsuka, H., Kawai, E., Imai, Y., and Komatsubara, S. (1996) *Microbiol.* **142**, 3295-3303

190. Parkhill, J., Achtman, M., James, K. D., Bentley, S. D., Churcher, C., Klee, S. R., Morelli, G., Basham, D., Brown, D., Chillingworth, T., Davies, R. M., Davis, P., Devlin, K., Feltwell, T., Hamlin, N., Holroyd, S., Jagels, K., Leather, S., Moule, S., Mungall, K., Quail, M. A., Rajandream, M. A., Rutherford, K. M., Simmonds, M., Skelton, J., Whitehead, S., Spratt, B. G., and Barrell, B. G. (2000b) *Nature* **404**(6777), 502-506

191. Stover, C. K., Pham, X.-Q. T., Erwin, A. L., Mizoguchi, S. D., Warrener, P., Hickey, M. J., Brinkman, F. S. L., Hufnagle, W. O., Kowalik, D. J., Lagrou, M., Garber, R. L., Goltry, L., Tolentino, E., Westbrook-Wadman, S., Yuan, Y., Brody, L. L., Coulter, S. N., Folger, K.

R., Kas, A., Larbig, K., Lim, R. M., Smith, K. A., Spencer, D. H., Wong, G. K.-S., Wu, Z., Paulsen, I. T., Reizer, J., Saier, M. H., Hancock, R. E. W., Lory, S., and Olson, M. V. (2000) *Nature* **406,** 959-964

192. Takami, H., Nakasone, K., Hirama, C., Takaki, Y., Masui, N., Fuji, F., Nakamura, Y., and Inoue, A. (1999) *Extremophiles* **3,** 21-28

193. Matthews, B. W. (1968) *J. Mol. Biol.* **33,** 491-497

194. Diruggiero, J., and Robb, F. T. (1996) *Adv. Prot. Chem.* **48,** 311-339

195. Okamoto, A., Kato, R., Masui, R., Yamagishi, A., Oshima, T., and Kuramitsu, S. (1996) *J. Biochem* **119,** 135-144

196. Nobe, Y., Kawaguchi, S.-i., Ura, H., Nakai, T., Hirotsu, K., Kato, R., and Kuramtsu, S. (1998) *J. Biol. Chem.* **273**(45), 29554-29564

197. Laghai, A., and Jordan, P. M. (1977) *Biochem. Soc. Trans.* **5,** 299-300

198. Neidle, E. L., and Kaplan, S. (1993) *J. Bact.* **175**(8), 2292-2303

199. Olsen, G. J., Woese C.R., and Overbeek R. (1994) *J. Bact.* **176**(1), 1-6

Appendices

Appendix I

Evolutionary relationships between AONS proteins

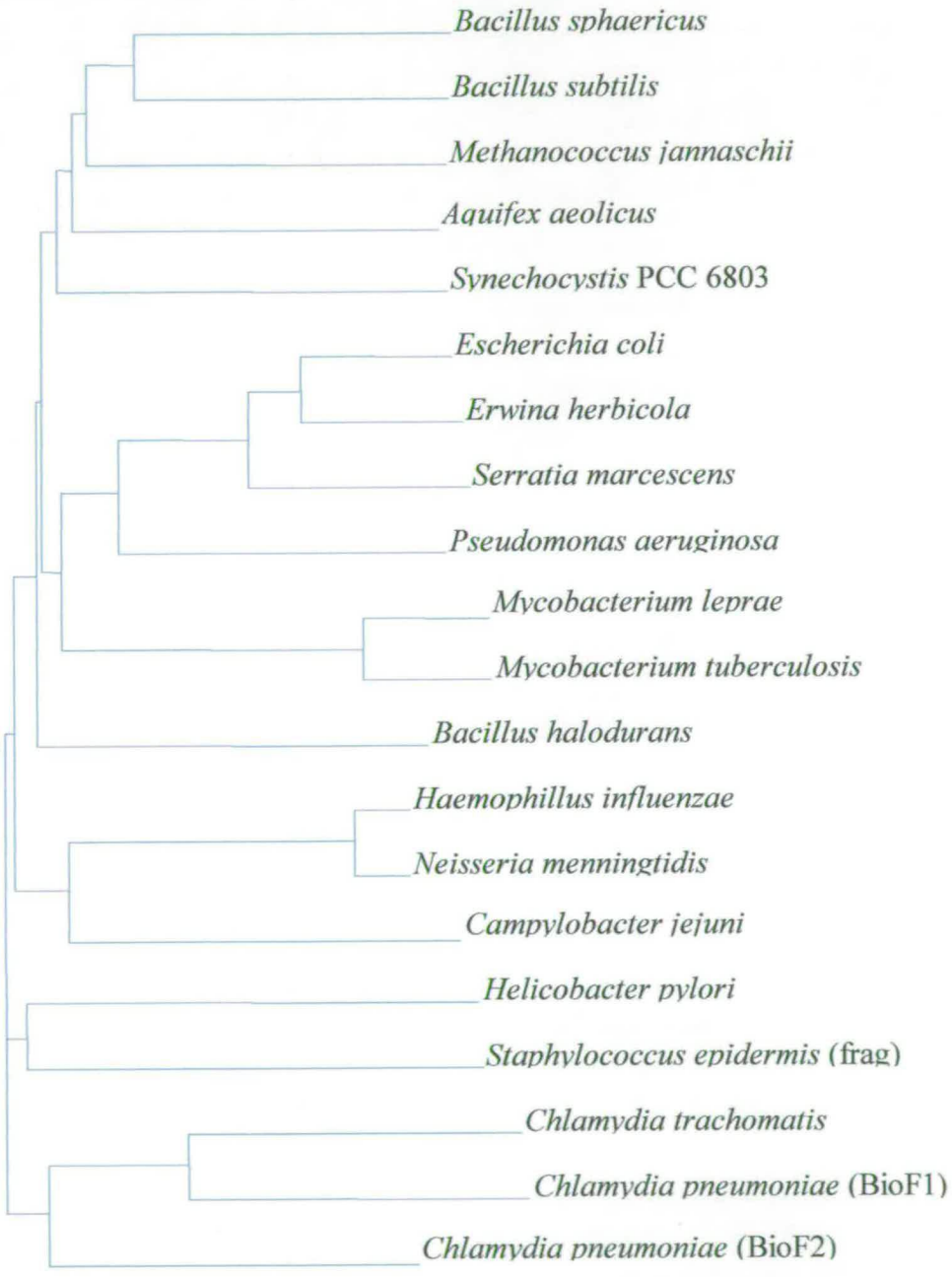

Evolutionary relationships between AONS proteins – amino acid count

	Aae	Bhalo	Bsp	Bsu	Cje	Cpn1	Cpn2	Ctr	Eco	Ehe	Hin	Hpy	Mja	Mle	Mtu	Nme	Paer	Sep	Sma	Sy
Alanine	21	35	31	35	23	24	35	38	53	58	27	32	16	57	66	28	60	4	62	43
Asparagine	9	14	14	15	19	12	17	10	8	5	20	20	22	3	4	19	8	13	9	16
Cysteine	6	3	2	3	6	9	9	6	5	5	5	1	8	11	6	7	2	1	6	4
Glutamine	5	14	10	13	9	11	21	21	27	24	25	11	3	7	10	23	13	13	27	18
Glycine	26	33	36	31	15	23	21	26	32	35	19	17	29	38	38	22	44	5	38	39
Isoleucine	29	25	35	32	26	22	25	18	16	15	21	25	40	10	6	21	12	12	13	26
Leucine	46	51	34	34	54	39	53	45	44	41	47	59	35	48	50	47	58	10	52	52
Methionine	5	6	11	9	6	8	2	3	8	3	9	4	3	2	4	9	7	2	5	11
Phenylalanine	15	11	18	16	31	20	16	20	11	11	20	26	18	6	7	22	12	9	8	12
Proline	9	15	9	13	7	13	9	10	14	14	15	12	9	16	19	15	18	3	14	24
Serine	20	27	32	32	27	35	32	39	29	29	25	31	21	28	23	25	27	11	17	27
Threonine	17	18	22	22	14	17	21	14	14	18	21	16	16	19	17	20	15	2	15	25
Tryptophan	1	5	1	3	1	2	0	4	7	6	1	0	1	3	3	1	4	0	6	7
Tyrosine	16	12	9	9	13	14	16	14	7	8	15	14	12	4	3	17	7	10	8	10
Valine	23	24	21	25	11	28	15	30	25	26	21	14	24	47	42	19	26	8	18	22
Aspartic acid	17	20	21	25	18	14	14	16	20	17	18	14	22	20	22	16	19	8	21	20
Glutamic acid	42	28	28	19	32	22	21	20	17	20	22	22	32	19	16	20	24	6	15	18
Arginine	21	25	18	21	12	13	20	18	28	31	22	9	15	30	37	25	29	2	38	24
Histidine	7	14	7	14	13	29	22	14	12	12	10	13	10	12	9	8	12	1	7	19
Lysine	38	15	30	18	43	15	13	11	7	7	17	33	36	5	4	16	4	6	3	20
TOTAL	373	395	389	389	380	370	382	377	384	385	380	373	372	385	386	380	401	126	382	437

Abbreviatons

Aae - Aquifex aeolicus
Bhaol - Bacillus halodurans
Bsp - Bacillus sphaericus
Bsu - Bacillus subtillis
Cje - Campylobacter jejuni
Cpn1 - Chlamydia pneumoniae bioF1
Cpn2 - Chlamydia pneumoniae bioF2
Ctr - Chlamydia trachomatis
Eco - Escherichia coli
Ehe - Erwinia herbicola
Hin - Haemophilus influenzae
Hpy - Helicobacter pylori
Mja - Methanococcus jannaschii
Mle - Mycobacterium leprae
Mtu - Mycobacterium tuberculosis
Nme - Neisseria menningtidis
Paer - Pseudomonas aeruginosa
Sma - Serratia marcescens
Sy - Synechocystis PCC 6803
Sep - Staphylococcus epidermis (frag)

Appendix II

Mechanistic Studies Of 8-Amino-7-Oxononanoate Synthase.

Scott P. Webster[1]*, Dmitriy Alexeev[2], Dominic J. Campopiano[1], Lisa J. Mullan[1], Lindsay Sawyer[2], Robert. L. Baxter[1].
[1]Edinburgh Centre for Protein Technology, Department of Chemistry, University of Edinburgh, West Mains Road, Edinburgh EH9 3JJ, UK and [2]Structural Biochemistry Group, University of Edinburgh, Swann Building, Mayfield Road, Edinburgh, EH9 3JR, UK.

Summary

8-amino-7-oxononanoate synthase is a pyridoxal 5'-phosphate-dependent enzyme which catalyses the decarboxylative condensation of L-alanine with pimeloyl-CoA to form 8-amino-7-oxononanoate. Individual steps in the reaction mechanism of *Escherichia coli* AONS have been probed by spectroscopy, pre-steady state kinetics and crystallography. Our results suggest that conformational transitions, induced by substrate and product binding, play an important role in catalysis.

Introduction.

The biotin biosynthetic pathway is an essential metabolic pathway found only in plants and microorganisms, making it an attractive target for herbicide and antibiotic development. In *Escherichia coli,* the first committed step in the biosynthesis of biotin is catalysed by the pyridoxal 5'-phosphate-dependent enzyme 8-amino-7-oxononanoate synthase (AONS) (1). This involves the decarboxylative condensation of pimeloyl-CoA and L-alanine to produce 8-amino-7-oxononanoate (AON), coenzyme A and carbon dioxide (Figure 1).

FIGURE 1. Reaction catalysed by AONS.

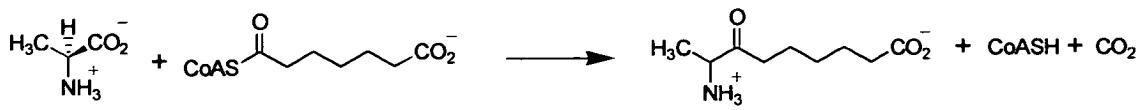

The structure and overall reaction mechanism of AONS places it in the α-family of PLP-dependent enzymes (2). Alignment of the amino acid sequence of AONS with the enzymes of the α-oxoamine synthase family - 5-aminolevulinate synthase, serine palmitoyltransferase and 2-amino-3-oxobutyrate CoA ligase - shows that almost all of the active site residues are conserved within this family of enzymes (3). The overall tertiary fold of AONS is closest to that of dialkylglycine decarboxylase although they have negligible amino acid sequence identity (4). The PLP cofactor is covalently bound to Lys236 through an imine linkage and interacts with two other basic residues, His133 and His207, which may play an important role in substrate binding and catalysis (3).

TABLE 1: Kinetic parameters for AONS.

pimeloyl-CoA			L-alanine		
k_{cat} (s^{-1})	K_m (μM)	k_{cat}/K_m ($M^{-1}s^{-1}$)	K_m (mM)	k_{cat}/K_m ($M^{-1}s^{-1}$)	k_1 ($M^{-1}s^{-1}$)
0.06(0.01)	25(2)	2400(430)	0.50(0.04)	120(21)	20000(6000)

The steady state kinetic parameters for AONS exhibit no metal ion dependence, and are comparable to those of other α-oxoamine synthases (Table 1) (5). Although the kinetic mechanism of AONS has not been investigated in detail, it is thought to adhere to an ordered bi-bi model in which L-alanine binds to the enzyme active site before pimeloyl-

CoA (6). In common with the mechanisms of other PLP-dependent enzymes, the initial step of the AONS catalysed reaction involves displacement of the internal aldimine complex by the incoming amino acid substrate to form an external aldimine. This is followed by heterolytic cleavage of the Cα–H bond of the amino acid leading to a resonance stabilised quinonoid intermediate (7). This quinonoid is thought to react subsequently with the other substrate, pimeloyl-CoA, in a Claisen-type condensation to form a putative β-ketoacid aldimine intermediate. Decarboxylation of the resultant β-ketoacid presumably occurs to generate a second quinonoid intermediate, which is then protonated at C8 to form a product external aldimine. Finally, product release leads to regeneration of the internal aldimine with Lys236.

Here we report a study of the interaction of AONS with its substrates and product, and suggest a mechanistic pathway in which conformational transitions of the enzyme play a critical catalytic role. This mechanism may prove to be common to all four enzymes of the α-oxoamine synthase family.

Materials and Methods

Protein characterisation. Purification of AONS and determination of steady state kinetic parameters were carried out as described previously (3).

Spectroscopic methods. All UV-visible spectra were recorded on a Hewlett-Packard 8452A diode array spectrophotometer. The AONS concentration in all analyses was 10μM in 20mM potassium phosphate (pH 7.5). Reference cuvettes contained all other components except AONS.

Pre-steady state kinetics. Transient absorption kinetics were determined under pseudo-first order conditions using an Applied Photophysics SX17 stopped-flow spectrophotometer, thermostatically controlled at 30°C. For the determination of rates of formation of external aldimine, syringes contained 20μM AONS and 0-100mM L- or D-alanine. Spectra were recorded at 425nm and fitted to single exponential saturation

curves. Rate constants were determined from the slope of a best-fit line produced from a plot of observed rate constant versus alanine concentration. For analysis of quinonoid formation, one syringe contained 25μM AONS pre-equilibrated with 10mM L-alanine and the other 0-300μM pimeloyl-CoA. Spectra were recorded at 486nm and the separate phases fitted to single exponential curves.

Determination of dissociation constants. Enzyme samples were dialysed overnight in 20mM potassium phosphate (pH 7.5) containing 100μM PLP. Non-enzyme bound PLP was removed by multiple washes with 20mM potassium phosphate through a Centrex UF2 concentrator (Schleicher & Schuell). Assays typically contained 10-50mM AONS in 20mM potassium phosphate (pH 7.5) with varying amounts of L- or D-alanine (0-80mM). Pimeloyl-CoA (143mM) was included where required. After addition of substrate, the reactants were mixed and allowed to equilibrate for 20mins at 30°C. Spectra were recorded and changes in absorbance at 425nm plotted against L- or D-alanine concentration. Data were fitted to a hyberbolic saturation curve using the equation, $\Delta A_{obs}=\Delta A_{max}.S/K_d+S$ where ΔA_{max} is the maximal absorbance change, S is the L- or D-alanine concentration, and K_d is the dissociation constant.

Crystallography. Crystals of AONS were grown as previously described (3). X-ray diffraction data of crystals containing AON was collected to a resolution of 2.0Å (D. Alexeev, personal communication).

Results and Discussion.

Substrate external aldimine formation. The absorbance spectrum of AONS holo-enzyme shows peaks at 334nm and 425nm which we assign to the non-coplanar and coplanar forms of the AONS-PLP internal aldimine (Figure 2). Addition of L- or D-alanine to AONS leads to an increase in the absorbance of the 425nm band indicating formation of an external aldimine. The pre-steady state rate constant, k_1, for L-alanine external aldimine formation is $2x10^4M^{-1}s^{-1}$ and $125M^{-1}s^{-1}$ for D-alanine, which is not a

substrate. If an ordered bi-bi mechanism is assumed we would expect k_1 to approximate k_{cat}/K_m for L-alanine (6). The fact that k_{cat}/K_m is less than k_1 for L-alanine suggests that there may be a slow step following external aldimine formation that is necessary for productive binding of pimeloyl-CoA.

FIGURE 2: Changes in cofactor absorbance spectra. (A) AONS (solid line), AONS + L-alanine (dashed line) and (B) AONS + pimeloyl-CoA (solid line), AONS +AON (dashed line).

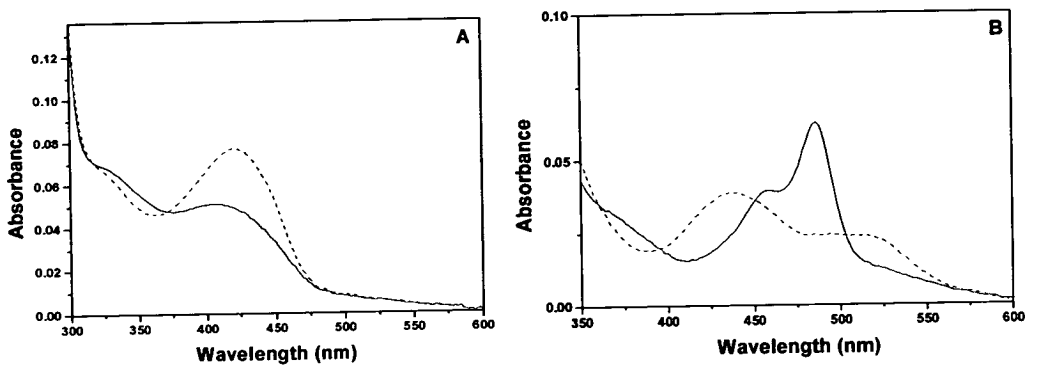

The equilibrium between internal and external aldimine forms of AONS is affected by the presence of pimeloyl-CoA. A plot of absorption increase at 425nm versus L-alanine concentration gives a curve with dissociation constant, K_d=0.9mM, while titration of AONS with D-alanine gives a K_d=9.8mM (Figure 3). In the presence of saturating amounts of pimeloyl-CoA, titration of AONS with D-alanine leads to a more than two-fold decrease in the dissociation constant (K_d=4.5mM). A decrease in the dissociation constant (K_d=0.3mM) of L-alanine in the presence of pimeloyl-CoA is also observed (data obtained from reciprocal plots of steady state kinetic data). Although we have no direct structural evidence, we speculate that the dissociation constant is reduced by binding of pimeloyl-CoA, which blocks the exit path of the amino acid substrate from the bottom of the binding site. Additionally, it is also conceivable that pimeloyl-CoA induces a conformational change which leads to a more tightly bound external aldimine species.

FIGURE 3: Binding of L-alanine to AONS. (A) Absorbance spectra in presence of L-alanine (from bottom to top 0, 0.1, 0.5, 1, 2, 5, 10, 15 and 20mM), (B) plot of absorbance versus titrant concentration.

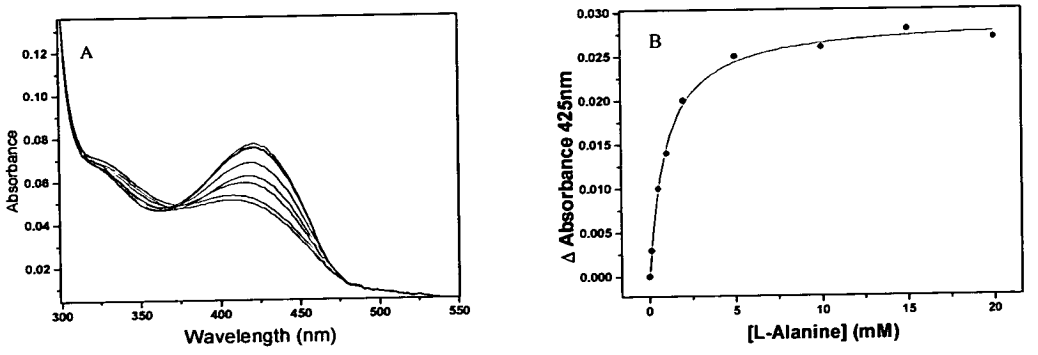

Addition of L- or D-alanine to AONS does not lead to quinonoid formation as indicated by the absence of a band at longer wavelength in the absorbance spectrum (Figure 2). It therefore seems likely that binding of L-alanine alone is insufficient to promote significant proton abstraction at Cα and leads to a benign form of the external aldimine-enzyme complex. The L-alanine external aldimine complex has not yet been crystallised, but has been modelled by analogy with the product aldimine structure (Figure 4). A probable interaction (analogous to the C7 carbonyl interaction in the product aldimine structure) between a carboxylate oxygen of the L-alanine-PLP complex and His133 places the Cα hydrogen away from the catalytic Lys236, making reaction with Lys236 unlikely. Proton abstraction would thus require a rotation around the N-Cα bond in the pyridine plane, which would direct the Cα hyrogen towards Lys236. Such a rotation would place the Cα carboxylate, previously interacting with His133, within hydrogen bonding distance of the side chain of Asn47, and thus generating a stable external aldimine complex.

Reaction with pimeloyl-CoA. In addition to enhancing the binding of L-alanine to AONS, addition of pimeloyl-CoA to the pre-formed external aldimine complex leads to formation of a quinonoid intermediate (Figure 2). Pre-steady state kinetic experiments revealed that the formation of this intermediate (k_{obs}=45s^{-1}) is preceded by a distinct lag

phase (~30ms). It is likely that this lag represents conformational transitions of the enzyme which place the Cα hydrogen of the L-alanine-PLP complex and the catalytic lysine in a favourable orientation for catalysis. Modelling suggests that docking of pimeloyl-CoA in the active site may lead to displacement of the carboxylate oxygen of L-alanine from His133 which then forms a hydrogen bond with Asn47. This new orientation of the external aldimine places the Cα proton close to Lys236 in a position perpendicular to the pyridine ring leading to cleavage of the Cα-H bond in accordance with Dunathan's hypothesis (8). Following this pimeloyl-CoA-induced Cα deprotonation, the quinonoid is free to attack the thioester carbonyl of pimeloyl-CoA liberating coenzymeA and producing a β-ketoacid-aldimine complex. At present, little is known about the mechanism of decarboxylation of the β-ketoacid, but our results suggest it is likely to lead to formation of a second quinonoid intermediate (Figure 2).

Interaction with AON. In solution, incubation of AONS holo-enzyme with the product of the reaction, AON, gives rise to a spectrum with maxima at 436nm and 520nm (Figure 2). It is likely that these bands reflect the equilibrium between the external aldimine and quinonoid forms of the product complex respectively. The quinonoid form has an absorption maximum at a substantially longer wavelength than the substrate-PLP quinonoid formed earlier in the catalytic pathway and probably arises from the decarboxylation of the putative β-ketoacid described above.

The structure of AONS incubated with its product, AON, has been determined to 2.0Å resolution. In contrast to the equilibrium between quinonoid and aldimine forms existing in solution, only the aldimine form is observed in the crystal. The N8=C4A double bond of the AON-PLP complex is coplanar with the pyridine ring while the C7 carbonyl oxygen of the complex is hydrogen bonded to His133. The carboxylate of AON is bound to Arg21 from the N-terminal domain and Arg349 from the C-terminal domain of the enzyme. A magnesium ion is coordinated to O3, N8, the hydroxyl of Ser179 and two water molecules. Since the enzymatic activity of AONS exhibits no magnesium

dependence it is unlikely that the ion plays a role in catalysis and may have arisen from trace ions present in the crystallisation buffer.

FIGURE 4: Cofactor binding site. PLP internal aldimine (left) and AON-PLP external aldimine (right).

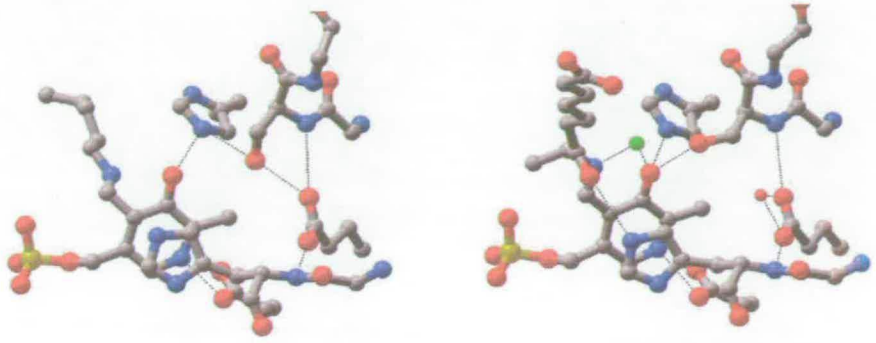

C-terminal domain movement. The overall refined protein structure of the AON-enzyme complex is close to that of the holo-enzyme. However, the β-sheet of the C-terminal domain undergoes a conformational transition whereby three β-strands of this flexible domain fold towards the active site of the AONS catalytic dimer (Figure 5). This movement narrows the access to the binding site and may be analogous to the apparent transition, which occurs upon binding of pimeloyl-CoA to the pre-formed substrate external aldimine complex. The release of this structural cap over the active site must be reversed upon product release and concomitant reformation of the internal aldimine. The energy barrier for this process is likely to be large and it may represent the rate determining step in the enzymatic reaction, since neither substrate external aldimine formation or quinonoid formation approximate k_{cat}.

FIGURE 5: Conformational changes in AONS structure.

Conclusion. These results suggest a mechanistically reasonable pathway for the catalytic action of AONS, which may prove common for other members of the α-oxoamine family of enzymes. Further studies will shed light on the role of active site residues in the catalytic reaction and may explain the involvement of conformational changes in the protein during catalysis.

References

1. Eisenberg, M. (1987) *Biosynthesis of biotin and lipoic acid*, Vol. 1, American Society of Microbiology, Washington DC.
2. Alexander, F. W., Sandmeier, E., Mehta, P. K., and Christen, P. (1994) *Eur. J. Biochem.* **219**, 953-960.

3. Alexeev, D., Alexeeva, M., Baxter, R. L., Campopiano, D. J., Webster, S. P., and Sawyer, L. (1998) *J. Mol. Biol.* **284**, 401-419.
4. Toney, M. D., Hohenester, E., Cowan, S. W., and Jansonius, J. N. (1993) *Science* **261**, 756-759.
5. Ferreira, G. C., and Dailey, H. A. (1993) *J. Biol. Chem.* **268**, 584-590.
6. Segel, I. H. (1975) *Enzyme Kinetics*, John Wiley & Sons, New York.
7. Ploux, O., and Marquet, A. (1996) *Eur. J. Biochem.* **236**, 301-308.
8. Dunathan, H. C. (1966) *Proc. Natl. Acad. Sci. U.S.A.* **55**, 712-716.

Acknowledgements.

We are grateful to the BBSRC for funding. Thanks also to Marina Alexeeva, Mhairi Brunton and Dr Rory M. Watt for technical assistance.

*Current address: PanTherix Ltd, Unit 6.03 Kelvin Campus, West of Scotland Science Park, Maryhill Road, Glasgow G20 0SP, United Kingdom. E-mail: scott.webster@pantherix.co.uk

Appendix III

Purification of E.coli AONS

The *E.coli* AONS protein, induced with 1mM IPTG, is easily distinguished from the background expression as a large band visible on an SDS polyacrylamide gel at 42kDa in figure III-1. The over-expression plasmid was pET16b/bioF transformed into *E.coli* HMS 174 cells.

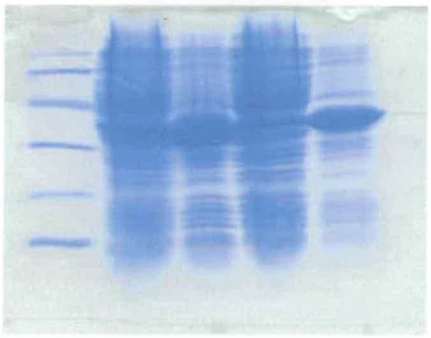

Figure III-1

Over-expression of *E.coli* AONS as seen after mini-induction (see section 2.2.1). Lane 1 – Standards; Lane 2 – Uninduced cells; Lane 3 – Induced cells; Lane 4 - Uninduced cells; Lane 5 – Induced cells. Standards are: Phosphorylase b (97kDA); Albumin (66kDa); Ovalbumin (45kDa); Carbonic anhydrase (30kDA); Trypsin inhibitor (20.1kDa); α-lactalbumin (14.4kDa)

The induced cell culture was harvested and after sonication and ammonium sulphate fractionation the protein solution was passed down a Phenyl sepharose column (see section 2.2). Fractions containing AONS eluted at 3% ammonium sulphate and were visible as large bands on an SDS polyacrylamide gel (see figure III-2).

Figure III-2

Elution of *E.coli* AONS after hydrophobic interaction chromatography (see section 2.2.5). Lane 1 – Standards; Lanes 3 –10 show fractions containing AONS. Standards are: Phosphorylase b (97kDA); Albumin (66kDa); Ovalbumin (45kDa); Carbonic anhydrase (30kDA); Trypsin inhibitor (20.1kDa); α-lactalbumin (14.4kDa)

The final step of purification involves anion exchange chromatography. The pooled AONS fractions from the previous chromatographic step are passed down a Q-sepharose column with a 0-1M NaCl linear gradient. Fractions containing AONS at up to 95% purity are visible on a SDS polyacrylamide gel.

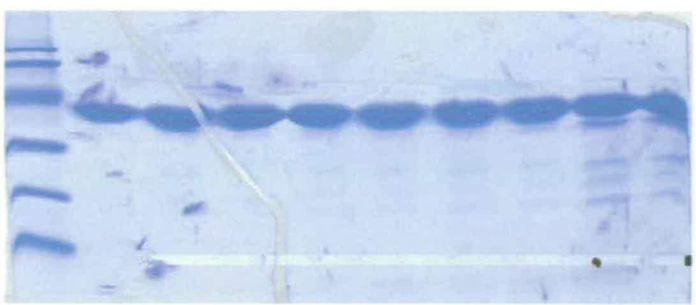

Figure III-3

Elution of *E.coli* AONS after hydrophobic interaction chromatography (see section 2.2.5). Lane 1 – Standards; Lanes 2 –8 show fractions containing AONS at 95% purity. Standards are: Phosphorylase b (97kDA); Albumin (66kDa); Ovalbumin (45kDa); Carbonic anhydrase (30kDA); Trypsin inhibitor (20.1kDa); α-lactalbumin (14.4kDa)

Appendix IV

Courses and conferences attended

1998

Radiation Protection Course

Departmental Postgraduates Lecture Series

27th Royal Society of Chemistry - Perkin Division (St. Andrews, 18.12.98)

NMR Lecture Series

Bio-inorganic Firbush Meeting (10-12.06.98)

665th Biochemical Society Meeting (Southampton, 31.03-03.04.98)

Walker Memorial Lecture

AMES Symposium

HGMP Introduction to Gene Identification

1999

Departmental Postgraduates Lecture Series. Oral presentation given

28th Royal Society of Chemistry - Perkin Division (Dundee, 18.12.99)

Royal Society of Chemistry Bio-organic meeting (London, 08.01.99); Oral presentation given, poster presented

Walker Memorial Lecture

AMES Symposium

Presentation Skills Workshop

Introduction to UNIX

Career Planning and Interview Skills